THE ENERGY BUDGET

OF THE

MIDDLE AND UPPER

STRATOSPHERE

by

WILLIAM RICHARD TAHNK

B.A., University of Minnesota

1967

SUBMITTED IN PARTIAL FULFILLMENT

OF THE REQUIREMENTS FOR THE

DEGREE OF MASTER OF

SCIENCE

at the

MASSACHUSETTS INSTITUTE OF

TECHNOLOGY

September, 1973

Signature of Author ....
Department of Meteorology,
August 10, 1973

Certified by ....
Thesis Supervisor

Accepted by ....
Chairman, Departmental Committee on Graduate Students

THE ENERGY BUDGET OF THE
MIDDLE AND UPPER STRATOSPHERE

by

WILLIAM RICHARD TAHNK

Submitted to the Department of Meteorology on August 10, 1973 in partial fulfillment of the requirements for the degree of Master of Science.

ABSTRACT

A weekly and monthly statistical analysis was made of the effects of large scale horizontal and vertical eddy transport processes on the zonal angular momentum, heat and total energy budget of the 10 to 2mb layer of the stratosphere. Geostrophic wind components were calculated based on 1972 data for the 100, 10, 5, and 2mb levels for use in determining the various quantities needed for the analysis. This represents a first attempt at describing the energetics of the upper stratosphere using hemispheric data on a time scale of a year.

It was determined that eddy processes in the stratosphere play a vital role in maintaining the energy budget of the middle and upper stratosphere. Eddy processes are also responsible for supplying energy to the stratosphere from the troposphere through the action of a vertical flux of energy.

The 10 to 2mb layer was found to resemble a heat engine in winter with an internal heat source and destruction of eddy available potential energy through radiational processes. In contrast, the summer stratosphere resembles a refrigerator, relying on an external heat source to maintain itself.

Thesis Supervisor: Reginald E. Newell

Title: Professor of Meteorology

TABLE OF CONTENTS

LIST OF TABLES

LIST OF TABLES - Continued

LIST OF FIGURES

LIST OF FIGURES - Continued

FIGURE NO. PAGE

I. INTRODUCTION

Over the past twenty years or so, there has been an extensive amount of work done in describing the energetics of the atmosphere. For the purpose of a long-term and complete study, though, investigators have been confined to the region of the atmosphere from the surface to 10 millibars (about 30 kilometers) which encompasses the troposphere, lower and middle stratosphere. Above the 10 millibar level, an overall lack of meteorological data on a hemispheric scale for extended periods of time (a year or so) has restricted the examination of the upper stratospheric energetics to discussions of various aspects of the total picture, such as studies of the energetics of upper stratospheric warmings (i.e., Miller, et. al., 1972). The purpose of this study is to examine the magnitude of large scale horizontal and vertical eddy processes as well as their effect on the monthly zonal momentum, heat and total energy budget of a closed region in the atmosphere. The closed region dealt with in this study is a North polar cap bounded by a vertical surface at 5° North latitude and by the 10 and 2 millibar surfaces. In addition, the 100 millibar surface was included in the calculations so as to examine the influence of processes in the lower stratosphere on those occurring in the upper stratosphere.

The equations which have been developed for use in a study of the energy budget of the atmosphere have been derived from the laws of conservation of mass, momentum, and energy. Using techniques of statistical averaging, as first formulated by Priestly (1949) and further refined and extensively used by Prof. V.P. Starr and his colleagues at M.I.T., in the general circulation project (i.e., Starr and White, 1952), one can examine distributions of meteorological variables such as wind, temperature, energy flux, etc., by first averaging them with respect to time and space, thereby reducing them from four-dimensional distributions (λ, ϕ, p, t) to two-dimensional variables in time and space. In this manner, one can get a better feel for the variation of a particular quantity and its overall effect on the energy budget.

In the process of deriving the energetics equations, one begins with an expression which describes the transport of a quantity B by a wind component A. The transport equation is derived through a consideration of time and space means as first introduced by Reynolds (1894) in which the quantities A and B can be expressed as follows:

$$A = \bar{A} + A' \tag{1.1}$$

$$B = \bar{B} + B' \tag{1.2}$$

where the bar denotes a time mean and the prime a deviation from that mean. One can further decompose the time means to obtain space averages as follows:

$$\bar{A} = [\bar{A}] + \bar{A}^* \tag{2.1}$$

$$\bar{B} = [\bar{B}] + \bar{B}^* \tag{2.2}$$

where the bracket denotes an average around a latitude circle and the star a deviation from that zonal mean. By combining (1.1) and (1.2) one obtains the following expression:

$$AB = \bar{A}\,\bar{B} + A'B' + \bar{A}B' + A'\bar{B} \tag{3}$$

which in turn leads to the following equation after taking a time mean of each quantity:

$$\overline{AB} = \bar{A}\,\bar{B} + \overline{A'B'} \tag{4}$$

where the product of the mean and deviation quantities have now vanished. Finally, the equation for transport of the quantity B is obtained by taking space averages of theterms in (4) using the relationship given in (2.1) and (2.2). This yields the expression

$$\left[\overline{AB}\right] = \left[\bar{A}\right]\left[\bar{B}\right] + \left[\bar{A}^{*}\bar{B}^{*}\right] + \left[\overline{A'B'}\right] \tag{5}$$

in which the three terms on the right hand side represent the total large-scale transport of B in the following manner: the first term represents transport by the mean motion; the second gives the standing eddy flux; and the third term the transient eddy flux of B. If B were to represent sensible heat or angular momentum, then, the terms on the right hand side of (5) provide a means of evaluating certain terms of the energy budget for a particular region.

In an examination of the role which the eddy fluxes play in transporting quantities such as angular momentum, the time period used for averaging becomes a significant consideration. For the transport of B by transient eddies, $\left[\overline{A'B'}\right]$, the bulk of this transport results from eddies or waves with periods of a minimum of one or two weeks. For the transport of B by standing or stationary waves, $\left[\bar{A}^*\bar{B}^*\right]$, the concept of stationary flow will depend on the period of averaging. On a time scale of one year, a wave may appear stationary, whereas in terms of a five year average it becomes transient. In terms of observational evidence, Richards (1967) found that monthly values of the standing eddy transport of angular momentum were at least equal to and often greater than the transient eddy transport values. Over a 60-month period of time, though, Starr et. al., (1970) found that the transient eddies play the dominant role in transporting momentum. So the role of the standing and transient eddies changes significantly, depending on the time period used for averaging.

This basic procedure has been used by a number of investigators to examine the energetics of different regions of the atmosphere. Their results have clearly shown that eddy fluxes play a vital role in the energy processes which control the circulation of the lower stratosphere, as indeed this study will also show for the upper stratosphere. Further, a good deal of evidence has been put forth which shows the lower stratosphere to be a region of forced motion, deriving its energy from the troposphere, as was originally suggested by Starr (1960). For the upper stratosphere, though, what has been lacking is observational evidence of the role that eddy fluxes play in the total energetics. Richards (1967) gave a fairly comprehensive outline of the work that had been done to date in atmospheric energetics as well as presenting his results of a study of the energy budget for the region from 100 to 10 millibars for 1965. The aim of this study is to do the same type of analysis as Richards did but for the region from 10 to 2 millibars, utilizing data that has been made available to me for all of 1972. Although there are certain limitations involved in the utilization of the raw data, this study nevertheless represents a first attempt at describing the energetics of the upper stratosphere on an extended time scale.

II. NOTATION AND DEFINITIONS

C_p = specific heat at constant pressure = 1.0046×10^7 erg gm^{-1} $^oK^{-1}$

R = gas constant for dry air = 2.8704×10^6 erg gm^{-1} $^oK^{-1}$

T = temperature in degrees Kelvin

θ = potential temperature in degrees Kelvin = $T \left(\frac{p_{oo}}{p}\right)^{\kappa}$

t = time

p_{oo} = 1000mb

p = pressure

$\kappa = \frac{R}{C_p}$ = 0.286 for dry air

a = radius of the earth = 6.371×10^8 cm

g = gravitational acceleration = 9.8062×10^2 cm sec^{-2}

ϕ = latitude, measured northward

λ = longitude, measured eastward

Ω = earth's angular velocity = 7.292×10^{-5} sec^{-1}

f = Coriolis parameter = $2\,\Omega \sin\phi$

H = geopotential height

u = west wind component (positive if from west) = $-\frac{g}{fa}\frac{\partial H}{\partial \phi}$

v = south wind component (positive if from south) = $g\,(fa\cos\phi)^{-1}\frac{\partial H}{\partial \lambda}$

ω = vertical velocity in pressure coordinates = $\frac{dp}{dt}$

w = vertical velocity in height coordinates = $\frac{dz}{dt}$

ρ = density

α = specific volume

Q = rate of non-adiabatic heating per unit mass

dM = increment of mass = $\rho dxdydz = a^2 \cos\phi\, d\phi d\lambda \left(-\frac{dp}{g}\right)$

$\gamma = \left(\frac{\tilde{\bar{T}}}{} - \frac{pC_p}{R}\frac{\partial\tilde{\bar{T}}}{\partial p}\right)^{-1}$	=	stability parameter.
A, B	=	dummy variables.
$\bar{A} = \frac{1}{\Delta t}\int_{t_1}^{t_2} A\,dt \simeq \frac{1}{N}\sum_{r=1}^{N} A_r$	=	the time averaged value of A at a given grid point and level where N is the number of days in a month.
$A' = A - \bar{A}$	=	deviation from the time average.
$\overline{AB} = \frac{1}{\Delta t}\int_{t_1}^{t_2} AB\,dt \simeq \frac{1}{N}\sum_{r=1}^{N} A_r B_r$	=	the time average of AB at a given grid point and level.
$\overline{A'B'} = \overline{AB} - \bar{A}\,\bar{B}$	=	the temporal covariance of A and B at a given grid point and level (Transient eddy covariance).
$\sigma(A) = \sqrt{\overline{A'^2}} = \sqrt{\overline{A^2} - \bar{A}^2}$	=	the time standard deviation of A at a given grid point and level.
$[A] = \frac{1}{2\pi}\int_0^{2\pi} A\,d\lambda \simeq \frac{1}{36}\sum_{r=1}^{36} A_r$	=	Zonal average of grid point values of A at a given latitude and level.
$A^* = A - [A]$	=	deviation from the zonal average at a given grid point and level.
$A^*B^* = (A - [A])(B - [B])$	=	spatial covariance of A and B at a given grid point and level (Standing eddy covariance).

$[\overline{A'B'}]$ = the zonal average at a given latitude and level of the temporal covariance of A and B.

$[\bar{A}^* \bar{B}^*]$ = the zonal average at a given latitude and level of the spatial covariance of the time averages of A and B.

$\sqrt{[\bar{A}^{*2}]} = \sqrt{[\bar{A}^2] - [\bar{A}]^2}$ = the space standard deviation of the time average of A at a given latitude and level.

$$\tilde{A} = \frac{1}{2\pi(1-\sin\phi_a)} \int_{\phi_a}^{\frac{\pi}{2}} \int_0^{2\pi} A \cos\phi \, d\lambda \, d\phi \approx \frac{\pi}{36(1-\sin\phi_a)} \left\{ \sum_{i=a+1}^{N} [A]_i \cos\phi_i + \frac{1}{2} [A]_a \cos\phi_a \right\}$$

= the area average of A at a given level North of latitude ϕ_a where N is the number of equally spaced latitude bands north of latitude ϕ_a.

$[A]'' = [A] - \tilde{A}$ = deviation of the area average from the zonal average at a given latitude and level.

$[\overline{AB}] = [\bar{A}][\bar{B}] + [\bar{A}^* \bar{B}^*] + [\overline{A'B'}]$ = resolution of the time and space mean of AB into the mean component ($[\bar{A}][\bar{B}]$) and the eddy components ($[\bar{A}^* \bar{B}^*] + [\overline{A'B'}]$).

THE EQUATIONS FOR ZONAL AND EDDY FORMS OF ENERGY AND FLUX COMPUTATIONS.

$A_Z = \frac{C_p}{2} \int \gamma [\bar{T}]''^2 \, dM$ = Zonal available potential energy integrated over the entire mass of the atmosphere in the region in question. [Lorenz approximation (Lorenz, 1955 and 1967)].

$$A_E = \frac{C_p}{2} \int \gamma \left[\overline{T}^{*2}\right] dM$$

= eddy available potential energy integrated over the entire mass of the region in question. [Lorenz approximation (Lorenz, 1955 and 1967)].

$$K_Z = \frac{1}{2} \int \left(\left[\overline{u}\right]^2 + \left[\overline{v}\right]^2\right) dM$$

= mean zonal kinetic energy integrated over the entire mass of the region in question.

$$K_E = \frac{1}{2} \int \left(\left[\overline{u}^{*2} + \overline{v}^{*2}\right] + \left[\overline{u'^2} + \overline{v'^2}\right]\right) dM$$

= eddy kinetic energy integrated over the entire mass of the region in question.

$$G_Z = \int \gamma \left[\overline{Q}\right]'' \left[\overline{T}\right]'' dM$$

= generation of zonal available potential energy integrated over the entire mass of the region in question. [Lorenz approximation (Lorenz, 1955 and 1967)].

$$G_E = \int \gamma \left[\overline{Q}^* \overline{T}^*\right] dM$$

= generation of eddy available potential energy integrated over the entire mass of the region in question. [Lorenz approximation (Lorenz, 1955 and 1967)].

$$\left[\overline{pw}\right] = \rho \left[\overline{u}\right] f \frac{\left[\overline{\theta}^* \overline{v}^*\right]}{\frac{\partial \left[\overline{\theta}\right]}{\partial Z}} = -\frac{f}{g} \left[\overline{u}\right] \frac{\left[\overline{\theta}^* \overline{v}^*\right]}{\frac{\partial \left[\overline{\theta}\right]}{\partial p}} =$$

vertical energy flux at a given latitude and level (positive flux upward). [Eliassen and Palm (1961) approximation].

$$\left[\overline{pv}\right] = -\rho \left[\overline{u}\right] \left[\overline{u}^* \overline{v}^*\right] = \frac{-p}{R\left[\overline{T}\right]} \left[\overline{u}\right] \left[\overline{u}^* \overline{v}^*\right]$$

= horizontal energy flux at a given latitude and level (positive flux northward). [Eliassen and Palm (1961) approximation]

CONVERSIONS BETWEEN EDDY AND ZONAL FORMS OF BOTH AVAILABLE POTENTIAL ENERGY AND KINETIC ENERGY

$C_A = A_Z \rightarrow A_E$	=	Rate of conversion of zonal available potential energy to eddy available potential energy.
$C_K = K_Z \rightarrow K_E$	=	Rate of conversion of zonal kinetic energy to eddy kinetic energy.
$C_E = A_E \rightarrow K_E$	=	Rate of conversion of eddy available potential energy to eddy kinetic energy.
$C_Z = A_Z \rightarrow K_Z$	=	Rate of conversion of zonal available potential energy to zonal kinetic energy.

III. DATA AND THEIR REDUCTION

The basic data used in this study are weekly and monthly grid point values of geopotential height and temperature at the 100, 10, 5, and 2 mb levels for all of 1972 which were provided in the original map form by various agencies of the National Oceanic and Atmospheric Administration of the Department of Commerce. Specifically, the 100 and 10 mb levels, which were obtained from the National Climatic Center at Asheville, North Carolina, consisted of once-weekly 1200 Z charts for the entire year as analyzed by computer at the National Meteorological Center (NMC). The maps for the 5 and 2 mb levels were obtained from the Upper Air Branch of the National Meteorological Center and consisted of: once-weekly maps for January-April and September-December; maps for the middle week only for months May, June and July; and maps for the middle and last week for the month of August. It should be pointed out that the maps at the 5 and 2 mb levels were hand drawn by the Upper Air Branch of NMC, based on both high-level rawindsonde and meteorological rocketsonde data at 5 mb and mainly rocketsonde data at the 2 mb level. The maps are just preliminary determinations of the wind field at those levels and represent a first effort by NMC to prepare constant-pressure charts for the upper stratosphere over the entire northern hemisphere. Methods of chart analysis, including station coverage and raw data interpretation, are detailed in other publications and will not be repeated here (see Finger, et al., 1965, and Staff, Upper Air Branch NMC, 1971).

The data as received on the NMC maps (NWAC No. 555, Scale 1:40,000,000) was reduced for use in this study as follows:

Grid values at all four levels were linearly interpolated from the maps to obtain the geopotential height (within 20 GPM) and the temperature (within 0.5°C) at every 10° latitude and longitude from 0° to 90°N. Weekly and mean monthly geostrophic wind components were then computed at 10° latitude and longitude increments from 5°N to 85°N and from 5°E to 5°W. Computation of the geostrophic wind components using finite difference approximations was as follows: (see Sect. II for motation)

$$u_{i,j} = -\frac{g}{fa}\left(\frac{H_{i+1,j} - H_{i-1,j}}{\phi_{i+1} - \phi_{i-1}}\right)$$

$$v_{i,j} = \frac{g}{fa\cos\phi_i}\left(\frac{H_{i,j+1} - H_{i,j-1}}{\lambda_{j+1} - \lambda_{j-1}}\right)$$

This allows computation of u at 5°N plus every 10° latitude to 85°N, at 0°E plus every 10° longitude. Similarly, v is computed at 5°E plus every 10° longitude to 5°W, at 0° latitude plus every 10° to 90°N (v=0 at 90°N). Then by averaging the values of u at 5°N 0°E with u at 5°N 10°E and so on around the latitude circles and averaging v at 5°E 0° latitude with v at 5°E 10°N and so on along the longitude circle, u and v were computed at a common point (i.e. 5°N 5°E, 15°N 5°E, 5°N, 15°E, etc).

It is important to keep in mind the limitations in such a method of computation of wind components for a northern hemispheric cap. Due to a lack of data and/or a lack of significant change of geopotential height and temperature at tropical latitudes (i.e. from 0° to say 20°N) there was normally little or no analysis on which to base my interpolation. I attempted to make reasonable estimates of the geopotential height and temperature based on the trend of the variables from high to low latitudes, which is particularly dangerous as gradients often change south of 20°N. It is possible, then, that where I extrapolated the temperature (or height) down to a minimum (or maximum) at the equator, it may in fact have reached its minimum (or maximum) value at, say, 5 or 10°N. In such a case, the u and v components could have an opposite sign from what I calculated and be quite different in magnitude. For that reason, I did not include computed quantities at 5° and/or 15°N in cases where the data were doubtful; even where I have included them, for cases where the pattern was apparently well behaved, one should exercise caution in utilizing them for anything beyond gross comparisons. One could, of course, make a better estimate of the geopotential height and temperature in the tropical region if data were available for the southern hemisphere. Another means of determining the trend in the temperature and height field in the tropics, at least at the lower levels, would be to use published tables of such values (i.e. Newell, et al., 1972 and Oort and Rasmussen, 1971). Since I did not have such tables of data available at the 5 and 2 mb levels, for consistency in my extrapolation, no climatology was used for any of the levels investigated in the energy budget calculations.

In order to determine the vertical flux across the four levels I examined, I found it necessary to make use of climatological data from a number of sources. The equation for determining vertical flux across a given pressure surface requires a knowledge of the potential temperature gradient at that level. For the 100 mb level, I made use of temperature data at the 150 and 82 mb levels. The 150 mb temperatures were obtained from

Professor R.E. Newell based on a stratospheric study of 1964 data for latitudes 20-85°N. The remaining latitudes were extrapolated from available tables (Newell, et al., 1972). For the 82 mb level I made use of data provided by the Oxford University Department of Atmospheric Physics (Oxford, 1972) which contained mean temperatures from 0 to 80°N. Again, 90°N was extrapolated based on Newell, et al. (1972). For the 10 mb level, I used data from the 16 mb level as given in the Oxford (1972) publication, and 5 mb data which was generated in the study. Similarly, the 5 mb level made use of potential temperatures which I calculated for the 10 and 2 mb surfaces. For the 2 mb level, I used mean temperatures at the 40 and 45 km levels as given in AFCRL Report #71-0410 (Groves, 1971) which lists the mean temperatures and pressures for latitudes 0° to 80°N. The remaining values were extrapolated from my 2 mb data which lies within the 40-45 km range.

Utilizing the statistical formulas and notation as outlined in Section II, the following quantities were computed for each pressure level:

a) At each latitude circle by week:

$[T]$, $[u]$, $[uv]$, $[\theta]$, horizontal energy flux, vertical energy flux

b) At each latitude-longitude point by month:

$\bar{u}$, $\bar{v}$, $\bar{T}$, $\bar{\theta}$, $\overline{vT}$, $\bar{T}^*$

c) At each latitude circle by month:

$[\bar{u}]$, $[\bar{v}]$, $[\bar{T}]$, $[\bar{\theta}]$, $[\overline{vT}]$ $[\bar{T}]''$, $[\bar{v}^*\bar{T}^*]$, $[\overline{v'T'}]$, $[\bar{v}^*\bar{T}^* + \overline{v'T'}]$, $[\bar{T}^{*2}]$, $[\bar{u}^{*2}]$, $[\bar{v}^{*2}]$, $[\bar{u}^{*2} + \bar{v}^{*2}]$, $[\bar{\theta}^*\bar{v}^*]$, $[\bar{u}^*\bar{v}^*]$, $[\overline{u'v'}]$, $[\bar{u}^*\bar{v}^* + \overline{u'v'}]$, $[\overline{uv}]$, $[\sqrt{\overline{u'^2}}]$, $[\sqrt{\overline{v'^2}}]$, $[\sqrt{\overline{T'^2}}]$, $\sqrt{[\bar{u}^{*2}]}$, $\sqrt{[\bar{v}^{*2}]}$, $\sqrt{[\bar{T}^{*2}]}$, $[\overline{u'^2} + \overline{v'^2}]$, Sensible heat transfer by standing eddies, momentum transfer by standing eddies, vertical energy flux, horizontal energy flux.

d) The following totals and area averages:
$\tilde{\bar{T}}$, $\tilde{\bar{\theta}}$, vertical energy flux, and $\widetilde{[T]}$ by week.

Finally, the total energy contents (A_E, A_Z, K_E, K_Z) and conversion rates (C_A, C_E, C_K) were computed for each month.

Values of these quantities are presented in tabular form and/or in figures at the end of this study. In addition, a discussion of these quantities and their relationship to the energetics of the stratosphere is given in Section V.

IV. PRESENTATION AND DISCUSSION OF EQUATIONS

The equations utilized in describing the energetics of the stratosphere have been derived and/or discussed by a number of authors in the past (Lorenz, 1955 and 1967; Saltzman, 1957; Oort, 1963; Peixoto, 1965; Richards, 1967; and Newell, et al., 1970 among others). Herein it will be assumed that the reader is familar with these derivations and only modifications made for this study will be discussed. Although there were some terms in the energy budget which could not be calculated, they will be included in this presentation in order to indicate the calculations necessary for a complete study of the energetics involved.

A. Zonal Available Potential Energy Equation

$$A_Z = \frac{C_p}{2} \int \gamma \, [\bar{T}]''^2 \, dM$$

gives the maximum amount of mean zonal available potential energy as a function of the latitudinal variation of the time and globally averaged temperature over an isobaric surface. This expression is the Lorenz approximation to the exact formulation and is more generally used as the latter requires the data in potential temperature coordinates. The rate of change of A_Z in a layer is a function of the vertical and horizontal motion and radiational heating and/or cooling taking place in that layer, and the energy budget equation for A_Z is:

$$\frac{\partial A_Z}{\partial t} = G_Z - C_Z - C_A \quad .$$

B. The "Generation of A_Z" Equation

$$G_Z = \int \gamma \left[\bar{Q}\right]'' \left[\bar{T}\right]'' dM$$

gives the rate of generation of zonal available potential energy by non-adiabatic processes (which in the stratosphere are radiational heating and cooling). Generation occurs when there is heating at the warmer latitudes and cooling at colder latitudes. I was unable to compute this term in the energy budget due to the uncertainty in the contribution to total $\bar{Q}$ by the ozone heating and/or cooling in the 9.6 μm band and to uncertainty in the ozone distribution between 30 and 50 kilometers. An alternate means of getting at $\bar{Q}$ will be discussed at the end of this section.

C. The "A_Z to K_Z Conversion" Equation

$$C_Z = -\int \left[\bar{\omega}\right]'' \left[\bar{\alpha}\right]'' dM \cong \int f \left[\bar{u}_g\right] \left[\bar{v}\right] dM$$

represents the rate of conversion from zonal available potential energy into zonal kinetic energy integrated over the entire mass of the region in question. Physically, the conversion of A_Z to K_Z is a result of the mean sinking motion in the colder latitudes and rising motion in the warmer latitudes. Since weekly fields of vertical motion were not computed, I could not use $\left[\bar{\omega}\right]'' \left[\bar{\alpha}\right]''$ to compute C_Z. Also, any terms which involve mean meridional motions cannot be evaluated with my computed values of $\left[\bar{v}\right]$, since the geostrophic approximation gives $\left[\bar{v}\right] = 0$, using the equation

$$\oint \frac{g}{fa \cos \phi} \frac{\partial H}{\partial \lambda} \, d\lambda$$

What was actually needed for determination of the integrand $[\bar{u}_g] [\bar{v}]$ was the ageostrophic $[\bar{v}]$, which I could not compute without a knowledge of $\bar{Q}$ or $\bar{\omega}$.

D. The "A_Z to A_E Conversion" Equation

$$C_A = - C_p \int \gamma \left[\bar{v}^* \bar{T}^* + \overline{v'T'}\right] \frac{1}{a} \frac{\partial [\bar{T}]}{\partial \phi} \, dM - C_p \int \gamma \left(\frac{[\bar{T}]}{[\bar{\theta}]} \right) \left[\bar{\omega}^* \bar{T}^* + \overline{\omega' T'}\right] \frac{\partial}{\partial p} [\bar{\theta}]'' \, dM$$

which represents the conversion rate from zonal available potential energy to eddy available potential energy integrated over the entire mass of the region in question. In the atmosphere this conversion would result from an eddy transport of sensible heat from warmer toward colder latitudes. The second term of C_A could not be computed owing to the lack of information about vertical motion for the 10 to 2 mb layer.

E. Eddy Available Potential Energy Equation

$$A_E = \frac{C_p}{2} \int \gamma \left[\bar{T}^{*2}\right] dM$$

gives the maximum amount of eddy available potential energy as a function of the variance of the temperature from the zonal average. Again, this is the Lorenz Approximation to the exact formulation. The rate of change of A_E in the layer is a function of the vertical and horizontal motion as well as the radiational heating and/or cooling taking place, and the energy budget equation for A_E is:

$$\frac{\partial A_E}{\partial t} = G_E - C_E + C_A \ .$$

F. The "Generation of A_E" Equation

$$G_E = \int \gamma \left[\bar{Q}^{*}\bar{T}^{*}\right] dM$$

represents the total generation of eddy available potential energy by non-adiabatic processes (radiational heating and cooling). In this case, one would find generation of A_E, for example, where heating occurs in the warmer regions and cooling in the colder regions at the same latitudes. As in the case of G_Z, I was unable to compute this term due to a lack of knowledge about the effect of the ozone in the stratosphere on $\bar{Q}$.

G. The "A_E to K_E Conversion" Equation

$$C_E = - \int \left[\bar{\omega}^{*}\bar{\alpha}^{*} + \overline{\omega'\alpha'}\right] dM$$

represents the rate of conversion of available eddy potential energy to eddy kinetic energy integrated over the entire mass of the region of the atmosphere in question. The actual process of converting A_E to K_E in the atmosphere can be resolved into the sinking of colder air and rising of warmer air. Since I had no means of computing ω values for the region in question, this term could not be calculated in this study.

H. The Zonal Kinetic Energy Equation

$$K_Z = \frac{1}{2} \int \left([\bar{u}]^2 + [\bar{v}]^2 \right) dM$$

represents the mean zonal kinetic energy and is a function of the time mean and zonal mean atmospheric circulation in the horizontal when integrated over a volume represented by the 10 to 2 mb north polar cap region. The rate of change of K_Z in the region is a function of the horizontal transport of angular momentum and the mean meridional overturning, and the resulting energy budget equation for K_Z is:

$$\frac{\partial K_Z}{\partial t} = C_Z - C_K \quad .$$

I. The "K_Z to K_E Conversion" Equation

$$C_K = - \int \left[\bar{u}^* \bar{v}^* + \overline{u'v'} \right] \cos \phi \, \frac{1}{a} \frac{\partial}{\partial \phi} \left(\frac{[\bar{u}]}{\cos \phi} \right) dM - \int \left[\bar{u}^* \bar{\omega}^* + \overline{u'\omega'} \right] \frac{\partial [\bar{u}]}{\partial p} \, dM$$

represents the rate of conversion of zonal kinetic energy to eddy kinetic energy as a result of Reynold's stresses within the volume over which the conversion is integrated. In the atmosphere, the eddy transport of angular momentum is, on the average, toward latitudes having higher angular velocities, giving rise to a conversion of K_E into K_Z. Again, the portion of the C_K equation involving vertical transport of angular momentum had to be dropped since ω is unknown.

J. The Eddy Kinetic Energy Equation

$$K_E = \frac{1}{2}\int\left(\left[\bar{u}^{*2} + \bar{v}^{*2}\right] + \left[\overline{u'^2} + \overline{v'^2}\right]\right)dM$$

which gives the kinetic energy due to the time and zonally averaged horizontal eddy motions within the volume over which the energy contents are integrated, and merely represents the excess of total kinetic energy over the zonal kinetic energy. Changes in K_E are brought about by the vertical transport of sensible heat and angular momentum, horizontal transport of angular momentum, and by transfer of energy from below, so that the energy budget equation for K_E is:

$$\frac{\partial K_E}{\partial t} = C_E + C_K + \left[\overline{pw}\right]$$

(Kung, 1966 and 1969).

K. The Vertical Energy Flux Equation

$$\left[\overline{pw}\right] = -\frac{f}{g}\left[\bar{u}\right]\frac{\left[\bar{\theta}^{*}\bar{v}^{*}\right]}{\frac{\partial\left[\bar{\theta}\right]}{\partial p}}$$

gives the total amount of energy transferred from below by vertical eddy motions. In this way baroclinic eddy activity in the troposphere supplies energy to the stratosphere. A vertical flux upward would result from a transport of potential temperature northward by standing eddies. This is the Eliassen and Palm (1961) approximation strictly applicable to stationary adiabatic standing waves.

The above-mentioned equations then represent the complete energy budget of the region from 10 to 2 mb. As was noted in the discussion, a problem arises in the determination of the energetics because ω, $[\bar{v}]_{ag}$ and $\bar{Q}$ are unknown for purposes of this study. If one were to start from the surface and work up to the 2 mb layer, mass divergence techniques (i.e. Kung, 1972) might be used to get at the ω term, although it is quite possible that the vertical velocities would blow up long before reaching 2 mb. Knowing ω, though, one could use a continuity equation of the form

$$\frac{1}{a \cos \phi} \frac{\partial}{\partial \phi} [\bar{v}] \cos \phi + \frac{\partial [\bar{\omega}]}{\partial p} = 0 \qquad (6)$$

to determine $[\bar{v}]$ without resorting to the geostrophic approximation and, hence, obtain reasonable values. If Q were known, then ω could be found from:

$$\omega = \frac{\frac{\partial T}{\partial t} + \frac{u}{a \cos \phi} \frac{\partial T}{\partial \lambda} + \frac{v}{a} \frac{\partial T}{\partial \phi} - Q/C_p}{\frac{R}{C_p} \frac{T}{p} - \frac{\partial T}{\partial p}} \qquad (7)$$

Once ω, $[\bar{v}]$, and $\bar{Q}$ are known, then one is able to compute G_Z, G_E, C_Z, and C_E.

An alternate method which I examined for determination of the unknowns involved the use of the continuity equation (6) and the conservation of angular momentum equation:

$$\frac{\partial \overline{[u]}}{\partial t} + \frac{[\bar{v}]}{a \cos\phi} \frac{\partial\left([\bar{u}] \cos\phi\right)}{\partial\phi} + [\bar{\omega}] \frac{\partial [\bar{u}]}{\partial p} + \frac{1}{a \cos^2\phi}$$

$$\frac{\partial}{\partial\phi}\left[\left(\left[\bar{u}^*\bar{v}^*\right] + \left[\overline{u'v'}\right]\right)\cos^2\phi\right] + \frac{\partial}{\partial p}\left(\left[\bar{u}^*\bar{\omega}^*\right] + \left[\overline{u'\omega'}\right]\right)$$

$$-f[\bar{v}] = 0 \qquad (8)$$

This method was used in the determinations made by Richards (1967) for the lower stratosphere in which the $\left(\left[\bar{u}^*\bar{\omega}^*\right] + \left[\overline{u'\omega'}\right]\right)$ term was considered to be so small as to be negligible so that equations (6) and (8) have only two unknowns $\left([\bar{v}] \text{ and } [\bar{\omega}]\right)$ and can be solved simultaneously to determine $[\bar{v}]$ and $[\bar{\omega}]$ and also $\bar{Q}$, using (7). For the upper stratosphere, though, as a result of a discussion with Professor R.E. Newell, it was decided that the vertical transport of angular momentum by eddies is of the same order of magnitude as the other terms in (8) and therefore may not be dropped from the equation. As a result, we have 3 unknowns and 2 equations, precluding the possibility of solving the equations simultaneously. So it appears that a determination of the vertical velocity field is the key to computation of the missing terms in the energy budget for the upper stratosphere.

V. RESULTS AND DISCUSSION

The results of this study will be divided into five general categories as follows: (A) the monthly mean features of the middle and upper stratosphere in 1972; (B) the computed horizontal transport of angular momentum and sensible heat, and the horizontal and vertical energy flux; (C) the time-sequential change of computed quantities; (D) the time and space deviations of mean variables; and (E) the total energy budget of the 10-2 mb layer. The categories will be discussed in the order listed, although they are inter-related in some cases. In addition to being in tabular form, some of the parameters have been put in figure form to display the salient features. Heights shown on those figures are based on U.S. Standard Atmosphere, 1966 values for 15° North latitude and are provided just as a reference for the pressure levels given. For figures which display the variability of a parameter on a time-sequential basis (i.e. Figures 2-8 and 11-12), each point drawn for on the curves represents the zonal average of that quantity at a particular level and week, with tick marks on the horizontal scale representing the last Wednesday of each month. In addition, for the vertical energy flux curves in Figures 3-8, for purposes of clarity, separate curves for each level are not shown where the fluxes are essentially equal to zero and instead a single zero line is drawn. This is the case in the summer months and in some cases towards the end of the year at the lower and highest latitudes.

A. Mean Monthly Features

Tables 1, 2, and 3, give values of $[\bar{u}]$, $[\bar{T}]$, and $[\bar{\theta}]$, respectively, at each 10° latitude starting at 15°N for $[\bar{u}]$ and 5°N for $[\bar{T}]$ and $[\bar{\theta}]$ for each month and level. In addition, monthly cross-sections of $[\bar{u}]$ have been included for the 100 to 2 mb (approximately 16.5 to 43 km) region of the atmosphere (see Figure 1).

In January, the zonal wind is clearly westerly throughout the region with small easterly values indicated at low latitudes above 5 mb. The polar-night jet reached a maximum mean velocity of 59 m sec^{-1} at 5 mb and 65°N and extends downward, over a broad area, to the 100 mb level extending into the region just north of the upper portion of the middle latitude tropospheric jet, which appears at approximately 35°N at the 100 mb level with a maximum mean velocity of 24 m sec^{-1}. In February, the central velocity of the polar-night jet has decreased to 39 m sec^{-1}, although it is still positioned at approximately 65°N. If one follows the locus of the maximum downward it begins to move south at about 50 mb and extends into the tropospheric jet, which has increased in intensity slightly (26 m sec^{-1}) while remaining in relatively the same position.

There is a significant change in March, probably as a result of higher temperatures at the poles, with the maximum of the upper level jet being reduced to 30 m sec^{-1} and its position shifted considerably southward. The locus of maximum winds still appears to extend, after following a parabolic path, into what looks like a northward extension of the tropospheric jet, the center of which has remained relatively stationary although somewhat decreased in magnitude (22 m sec^{-1}). The low-latitude easterlies have temporarily disappeared also as westerlies have expanded to encompass the entire region.

In April there are signs of evolution into a summer regime and the same general pattern is displayed through August. By April, the polar vortex has virtually disappeared and easterlies have replaced westerlies, reaching a maximum velocity of -8 m sec^{-1} at 10 mb and 65°N. The westerly tropospheric jet still dominates the circulation at 100 mb, although its maximum value has decreased to 17 m sec^{-1}. By May, easterlies extend over all latitudes above 30 mb, and there are indications of formation of a low latitude easterly jet at and above the 2 mb level probably as a result of solar heating. This easterly summer jet increases to -35 m sec^{-1} in June and -44 m sec^{-1} in July at 2 mb. The position of the maximum shifts from south of 20°N in May to 25°N in June and July. Likewise, the tropospheric jet has shifted its position northward at 100 mb and has become more broad and less intense by July, with maximum values of 8 m sec^{-1} at 45°N. August appears to be a transition month from the distinct summer regime back to the normal winter circulation. The easterly jet at 25°N has disappeared, although easterly winds still dominate the region above 50 mb. The tropospheric jet is beginning to increase in value, the maximum velocity being 11 m sec^{-1} at 100 mb and 45°N. From September through December, one sees a rapid increase in the polar-night jet with the maximum velocity increasing from 11 m sec^{-1} in September to 59 m sec^{-1} in December remaining stationary at 2 mb and 55°N. An exception to the stationary position occurred in November when the polar-night jet at 2 mb extended from 25°N to 55°N with values of 40 to 44 m sec^{-1} throughout the region. By December, the middle latitude tropospheric jet has shifted southward to 35°N at 100 mb and increased in velocity to 28 m sec^{-1}. Overall, then, there appears to be two distinct regimes in the mean circulation field with velocity extremes which appear to be a function of the amount of solar heating.

Figure 11 represents a smoothed meridional distribution of weekly values of $[\bar{u}]$ at the 5 and 2 mb levels for 1972. Here again, the dominant westerly polar-night jet is evident at high latitudes in the winter season and the easterly jet at low latitudes in the summer months. The maximum velocity in the polar-night jet occurred in January at 65°N with speeds of 73 m sec^{-1} at 2 mb and 67 m sec^{-1} at the 5 mb level. The summer easterly jet attained maximum speeds in July at 25°N of 44 m sec^{-1} at the 2 mb level and 28 m sec^{-1} at 5 mb. Note that the westerlies change over to easterlies earlier at high latitudes than at low latitudes in the Spring and the higher latitudes again precede the lower latitudes in converting back to westerlies in the fall transition.

The same type of 2-season pattern appears in an examination of the mean monthly values of $[\bar{T}]$ (Table 2). The January values of $[\bar{T}]$ appear to represent a typical winter regime, at least at the lower levels (Newell, 1966 and Richards, 1967), with the semi-permanent dome of cold air at the 100 mb level in the tropics with temperatures of 197.7°K at 5°N. A second cold air dome is evident in the polar regions at the 10 mb level with temperatures about 5 degrees warmer. Between these cold regions there is an extension of warm air from the sub-tropical middle and upper stratosphere, which produces the temperature gradient reversal which is common to the lower stratosphere in winter. An opposite gradient appears at the 2 mb level where there are high temperatures in the tropics as well as in the polar region, and low temperatures in the middle latitudes at 55°N. Also of significance is the fact that at the 10 and 5 mb levels the temperature gradient is in the same direction as the gradient of $[\bar{T}]$ in the troposphere.

This feature becomes important in a discussion of the zonal available potential energy as will be seen later.

February values of $[\bar{T}]$ display the same pattern as January at the 100, 10 and 2 mb levels. As at 2 mb, the 5 mb level now displays higher temperatures at the pole and the tropics than at middle latitudes which produces a temperature gradient reversal above 10 mb which is the mirror image of that found below 10 mb. In conjunction with the decrease in velocity of the polar-night jet as the polar vortex weakens, there are signs of warming at the higher latitudes in February and March. This is especially evident by April where the temperatures at 85°N have increased by 30° at 10 mb and 20° at 5 mb. The rate at which the warming proceeds in the spring appears to be quite variable, with some levels showing sudden warmings in some years and very gradual increases in others (see Reed et al., 1963 and Richards, 1967). It is interesting to note that there is a temperature gradient reversal at the 100, 5 and 2 mb levels in February and none at 10 mb. In April, the temperature structure completely changes such that the temperature gradient reversal is at the 10 mb level only, with the lowest temperatures at middle latitudes. This $[\bar{T}]$ gradient reversal in turn disappears as we move into a typical summer regime (Newell, 1966 and Richards, 1967) in May where the greatest temperature contrast with latitudes occurs at 100 mb. The $[\bar{T}]$ values reflect the path of the sun quite well as the maximum temperatures occur at the highest latitudes in July just after solar heating has reached a maximum in the northern hemisphere.

The values of $[\bar{T}]$ in August and September clearly show the effects of reduced heating as the temperatures drop appreciably at the high latitudes with only modest changes occurring at middle and low latitudes. In fact, temperatures have dropped enough at the 10 mb level in the high latitudes to set up a temperature gradient reversal at that level, which is equal and opposite in nature to that found in the April $[\bar{T}]$ distribution. It appears that the occurrence of a temperature gradient reversal at 10 mb signals a transition between the winter and summer regimes. This is something that should be investigated as more data becomes available. By October, the winter regime is quite well established again with the cold air split into two regions: the semi-permanent cold dome at 100 mb in the tropics and the cold polar dome at 10 mb. A striking feature of the October through December distributions of $[\bar{T}]$ is the extremely low temperatures at high latitudes at the 5 and 2 mb levels. The upper half of Figures 5 though 8 show the weekly pattern of the zonally averaged temperature, $[T]$, at the higher latitudes and indicate a temperature difference between January and December at 2 mb of 24°C at 85°N, 21°C at 75°N, and 16°C at 65°N. It is possible that once more data has been collected in the 10 to 2 mb region, the temperature difference between January and December might decrease somewhat, but the fact that there is a difference is not unreasonable in view of the effects of solar heating and dynamics. The difference in solar angle between December and January results in greater solar heating, hence higher temperatures, in January. In addition, as will be shown later in a discussion of vertical energy flux, the dynamics are such that greater energy is being transported upward in January which contributes toward maintaining a higher temperature. The weekly patterns of zonally averaged temperatures at the higher latitudes (Figures 6-8) indicate a stratospheric warming occurred the third week in January thereby reinforcing the idea of higher temperatures resulting from dynamics. It should be remembered that there is no data readily available for December, 1971, for comparison. The distributions of mean potential temperature, $[\bar{\theta}]$, display the same general patterns as those discussed for the monthly distributions of $[\bar{T}]$, which is not surprising since the potential temperature at each constant pressure surface is equal to the temperature times a constant.

Figure 10 contains zonal cross-sections of the January values of $\bar{u}$, $\bar{v}$, and $\bar{T}$ from which the zonal averages $[\bar{u}]$, $[\bar{v}]$, and $[\bar{T}]$ at 55°N were derived. Large variations with longitude are quite evident indicating the necessity for adequate spatial sampling in any scheme of statistical analysis which is based upon zonal means. For example, several rocket stations clustered in the North American sector would give a biased view. Besides zonal means, any parameters which are to be computed based on combinations of $\bar{u}$, $\bar{v}$, or $\bar{T}$, such as momentum transport by standing waves, would be seriously affected if poor sampling techniques were used. Profiles of radiational heating are also longitudinally dependent since its computation is based on values of T.

B. Horizontal and Vertical Transport Quantities

Note: Henceforth, the terms $[\overline{uv}]$, $[\bar{u}^*\bar{v}^*]$, and $[\overline{u'v'}]$ will be referred to as angular momentum transports even though they represent a transport only after they have been multiplied by the torque arm. Similarly, the terms $[\overline{vT}]$, $[\bar{v}^*\bar{T}^*]$, and $[\overline{v'T'}]$ will be referred to as sensible heat transports even though they represent a transport only after they have been multiplied by the specific heat capacity.

(1) Eddy transport of angular momentum:

Values of $[\overline{uv}]$, the total mean transport of angular momentum across a latitude circle, and $[\bar{u}^*\bar{v}^*]$, the standing eddy transport of angular momentum, are given in Tables 4 and 5, respectively. Possibly as a result of the limited time scale imposed by taking monthly averages of once-weekly values of u and v, the standing eddy transport in most cases is greater than the transient eddy transport throughout the year and the transient eddy terms are quite noisy from one pressure level to the next. The reader should be alerted to the fact that since only one week of values per month went into the computation of all terms at the 5 and 2mb levels in May, June, and July, the transient eddy term will necessarily be zero during those summer months since it is based on a deviation from a time mean. Of more interest for purposes of discussion is the distribution of standing eddy transport of mean relative zonal angular momentum per mb of vertical distance across a complete latitude circle. This transport is computed as follows:

$$\int_{(1mb)}^{P} \int_{0}^{2\pi} \bar{u}^*\bar{v}^* \, a^2 \cos^2\phi \, d\lambda \, \frac{dp}{g} \, .$$

Values of this quantity are given in Table 6 and the values in the following discussion will all be in units of gm cm^2 mb^{-1} sec^{-2} when multiplied by 10^{20}.

In January, transport of angular momentum is almost entirely northward, with the maximum occurring in the upper stratosphere (almost five times as much at 2mb as at 100mb) just south of the main axis of the polar-night jet. North of the jet core, there is a small amount of southward transport of angular momentum in the upper stratosphere. By February, the angular momentum transport is reduced considerably at the 5 and 2mb levels and yet has remained unchanged at the 100mb level and increased significantly at the 10mb level. This change is reflected in the February $[\bar{u}]$ distribution (Figure 1) which shows a sharp reduction in westerly wind speeds in the upper stratosphere with little change in the lower and middle stratosphere. By March, the transport values are smaller at all levels while still remaining northward except at low latitudes and at 100mb at high latitudes. The parabolic path taken by the polar-night jet axis on the March zonal wind distribution (Figure 1) is reflected in the maximum transport values as the locus moves from 35°N at 100mb to 55°N at 5mb then back to 35°N at 2mb.

A drastic change in the values of angular momentum transport occurs in April as there are small northward transports at high latitudes and relatively large southward transports at middle and low latitudes, the resultant giving rise to easterlies in the April zonal wind cross-section (Figure 1). Another meteorological parameter which may be related to the change in the standing eddies in the stratosphere is the mean surface albedo. Baroclinic activity in the troposphere is clearly affected by changes in the mean albedo and surface heating. As will be discussed later, an extensive amount of energy is transported upward, as a result of eddy activity, from the troposphere to the stratosphere in winter, with considerably less vertical transport taking place in late spring and in the summer. With a decrease in the amount of energy being supplied by the troposphere to the stratosphere in April, the amplitude of the standing waves in the stratosphere changes, which is reflected in the decreased amounts of angular momentum transported by standing eddies in the stratosphere in the late spring and in summer. Hence, changes in the mean surface albedo are linked to changes in the troposphere and, in turn, the stratosphere.

The months of May through August exhibit mainly noise at the high latitudes with extensive southward transport of angular momentum present at middle and low latitudes at the higher levels. Northward transport is still evident at the 100mb level, supplying angular momentum to the sub-tropical tropospheric jet. The transports in September and October begin to show a resemblance to their March and April counterparts, especially at the lower levels. October in particular shows a pattern of convergence into the accelerating polar vortex with maximum northward transport of angular momentum more or less taking place just south of the maximum zonal wind. Just as there was an abrupt transition from March to April in the standing eddy transport of angular momentum, there is in October an opposite and equally abrupt transition to a strong winter regime. One might look for equally abrupt changes in mean albedo for the earth's surface, as snowfall at high latitudes (i.e., Siberia) changes the radiational heating at the surface and in the atmosphere. November displays large northward angular momentum transports, especially in the upper stratosphere, with two regions of maximum transport at 15°N and 65°N at the 2mb level, giving rise to the broad jet core of westerly wind previously discussed for November (Figure 1). There is still some residual southward transport at low latitudes at the 10 and 5mb levels which persists into December, although somewhat reduced in magnitude. As was the case for January, December displays strong northward transport of angular momentum at the middle and upper latitudes at all levels with maximum values that are comparable except at the 2mb level, where December values are less than those computed for January. This in turn gives rise to a polar-night jet core which appears to be above the 2mb level in December but moves downward and poleward in January, as evidenced by increased standing eddy transports of angular momentum at the 2mb level in January. In general, then, momentum convergence takes place in the region of maximum westerly flow in the middle and upper stratosphere in winter. In the summer, transports were quite noisy (probably owing to the small sample size) and small, indicating the small role played by eddy activity in the general circulation of the stratosphere during the summer months.

(2) Eddy transport of sensible heat:

Values of $[\overline{vT}]$, the total mean transport of sensible heat across a latitude circle, and $[\bar{v}^*\bar{T}^*]$, the standing eddy transport of sensible heat, are given in Tables 7 and 8, respectively. As in the case of the angular momentum transports, certain limitations are imposed on the transient eddy transport by the sampling technique used in this study. The discussion will again be confined to the distribution of standing eddy transport, in the horizontal, of sensible heat per mb of vertical distance across a latitude circle, which is computed as follows:

$$C_p \int_{(1mb)}^{P} \int_{0}^{2\pi} \overline{v}^* \overline{T}^* \, a \cos\phi \, d\lambda \, \frac{dp}{g} .$$

Values of the sensible heat transport by standing eddies are given in Table 9 and the values referred to in the following discussion will be in units of ergs mb^{-1} sec^{-1} when multiplied by 10^{17}.

Northward transport of sensible heat by standing eddies is prominent at all latitudes and levels in January, with maximum transports occurring at approximately 55°N. The flux values significantly increase with height, with the maximum 2mb flux being 10 times as great as the maximum at 100mb. If one compares the values in Table 7 ($[\overline{v}^*\overline{T}^*]$ + $[\overline{v'T'}]$) with the sum of Tables 8 ($[\overline{v'T'}]$) and 9 ($[\overline{v}^*\overline{T}^*]$) from Richards (1967), the total eddy transport in 1965 and 1972 was similar in terms of changes with height and latitude, although the 1965 values were, on the average, larger than the 1972 values. This difference may be a result of, among other things, the fact that the transient eddy transport determined from the 1972 data may have been small due to the limited amount of data available. It also seems probable that there could be a lot of variability in the eddy transport of sensible heat from one year to the next. With maximum fluxes occurring at 55°N, it follows that convergence of sensible heat is taking place north of 55°N and divergence to the south. Even greater northward transports are evident in February with flux values still increasing with height, and the maximum flux of sensible heat still at 55°N. Northward transports of sensible heat still dominate all latitudes and levels in March, but a drastic reduction in the flux values has taken place. At the 2mb level, for example, the maximum flux value is one-sixth what it was in February. By April there are indications of both northward and southward transports of sensible heat and the numbers have been reduced to the noise level of the data.

The transport values remain quite small through September, although a noteworthy change in the sign of the transport occurs between August and September. Whereas the transports are all northward at the 100 and 10mb levels in August and September, they are generally southward at the 5 and 2mb levels. By October, northward transport is increasing and becoming more widespread at all levels, except for some residual southward flux at the low latitudes in the upper stratosphere. The region of maximum transport of sensible heat appears again at 55°N with convergence north of that demarcation and divergence south of it. The numbers tend to increase at all levels through December, although as was the case with the angular momentum transport, do not increase to the levels attained in January of the same year, especially at the 5 and 2mb levels. The region around 40°N has become an area of sensible heat divergence in November and December, as the transports are all southward to the south of the demarcation and northward to the north of it. In general, though, the distributions for the winter months show predominantly northward transport of sensible heat by standing eddies with predominantly negative standing eddy transports in the upper stratosphere and positive (northward) transports in the middle and lower stratosphere in summer.

(3) The Vertical energy flux:

The vertical energy fluxes are shown in Table 10. In most cases, the flux values calculated for the 100 and 10mb levels were less than those calculated by Newell and Richards (1969) for the years 1964 and 1965. Otherwise, the features of the two sets of values are quite similar. Largest flux values occur at about 65°N throughout the winter months (January through March, November and December) and the predominant direction of the energy flux is upward, especially at the 5 and 2mb levels. The exception occurs at 100mb where downward flux is the case from 35°N to the tropics. The maximum flux values occurred in February and in all cases the flux values decrease with height. By May, the polar vortex has completely vanished, which is evident from the flux values, as there is no significant flux remaining at high latitudes. The 100mb level does maintain a small amount of flux throughout the summer months at around 40°N which may be related to the tropospheric jet which is present in the summer cross-sections of $[\bar{u}]$ (Figure 1). Above the 100mb level, the flux is mainly downward and quite small.

These small downward flux values last until September at the 100 and 10mb levels and until October at the 5 and 2mb levels, when a transition to a winter situation begins to occur. In September, a maximum value of upward flux is clearly indicated at the 100mb level at 55°N with positive values dominating the lower and middle stratosphere. By October, only the 2mb level is not displaying upward vertical energy flux of significant magnitude. Virtually all flux of energy is upward in November and December with maximum values somewhat less than those indicated in January of 1972. In summary, then, upward flux of energy is the dominant feature throughout the winter months with values peaking in February. The summer months, on the other hand, are characterized by small flux values of varying sign which are at the noise level of the computations. The reader is reminded that the formula used in computing the vertical energy flux (as well as the formula for computing the horizontal flux, which is discussed below) is based on an approximation to an exact formulation. In the approximation, Eliassen and Palm (1961) assume a straight westerly flow where the motion is considered to be stationary and adiabatic, to which they in turn apply a geostrophic approximation. Hence, the vertical energy flux so computed can only give an indication of relative magnitude and phase of the flux.

(4) The Horizontal energy flux:

The horizontal energy fluxes are shown in Table 11. In January, the flux is decidedly equatorward at all levels and at all latitudes except near the pole at the 5 and 2mb levels. The maximum flux occurs at 35°N at the 100mb level but moves poleward with height, showing up at 65°N at 2mb. From February on, though, the situation becomes more complex with the four levels each displaying a different pattern of horizontal flux. Except at the 100mb level, where the tropospheric jet is active, the horizontal flux values reduce to the noise level during the summer months. By October, the flux is generally southward and increasing, with maximum values at the lower levels. In November and December, there are southward fluxes throughout the region with maximum values almost comparable in size to those computed in January. Newell and Richards (1969) found a northward flux at high latitudes for November and December 1964 and a southward flux for 1965, as is found here for 1972. Thus, there is a fair amount of variability from year to year. In general, in 1972, the horizontal flux is southward at all levels in winter months at low and middle latitudes and relatively small (except at the 100mb level) in the summer.

(5) Total energy flux divergence:

To gain a better understanding of the effects of large horizontal and vertical energy fluxes in the 100 to 2mb region, the energy flux divergence was computed in the vertical and horizontal planes. The horizontal energy flux divergence was computed from values given in Table 11 using the following equation, given in finite difference notation:

$$\text{H div} = (a \cos\phi)^{-1} \frac{\Delta(F \cos\phi)}{\Delta\phi}$$

where F denotes the flux at latitude ϕ and $\Delta\phi$ is the increment of latitude used (10°). The vertical energy flux divergence was computed from values in Table 10 using the following equation, also in finite difference notation:

$$\text{V div} = \frac{\Delta F}{\Delta Z} = -\frac{\bar{p}\, g}{R\, \bar{T}} \frac{\Delta F}{\Delta p}$$

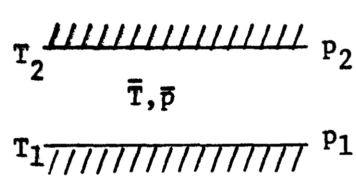

where the F again denotes the flux at each latitude, $\bar{p}$ is the average pressure in the layer ($\bar{p} = \frac{p_1 + p_2}{2}$), $\bar{T}$ is the average temperature in the layer ($\bar{T} = \frac{T_1 + T_2}{2}$), and Δp is the pressure difference in the layer ($\Delta p = p_2 - p_1$). The horizontal flux divergence and vertical flux divergence were combined to give the total flux divergence for the 55 to 3.5mb layer. Since the total divergence was insignificant in the summer months, the pattern of the flux divergence in the winter months of December through March only has been included in this study for purposes of discussion (Figure 9). In Figure 9, divergence is represented by positive numbers. A region of energy flux convergence separates areas of divergence at high and low levels in January. By February, convergence dominates almost the entire cross-section, except at 55mb at the higher latitudes and at low latitudes at the higher levels. The divergent region at low levels, which was quite strong and broad in January, occupies a small area at 55mb around 70°N in February. March displays almost no divergence to speak of and the maximum convergence area is at and below the 55mb level at 60°N. By December, as was the case in January, convergence again separates high and low level divergence at middle and high latitudes. So, except for the divergent region at the high latitudes at 3.5mb in January (presumably associated with the polar-night jet), the winter months of 1972 seem to indicate a large amount of absorbed energy in the upper stratosphere and a divergence of energy in the middle and lower stratosphere north of about 55°N. By April, the energy flux divergence was essentially reduced to zero, remaining so throughout the summer and fall. In December, divergence is again indicated at high and low levels at the high latitudes, and at all levels in the tropics. Energy is still being absorbed in the middle latitudes at around 10mb indicating the possible buildup of a pattern similar to that observed in the previous January.

C. The Weekly Variation of Temperature and Vertical Energy Flux

The variation of the temperature distribution by latitude on a monthly basis which was discussed previously leads one to conclude that there is a significant variation in temperature throughout the year which follows a different pattern depending on the level in the stratosphere. Figure 12 depicts the annual variation in the temperature averaged over an isobaric surface. In addition, Table 12 gives the temperature averaged over a given isobaric surface by month. One can learn more about the behavior of the temperature, though, since it is latitudinally dependent, if one examines its weekly variation at each latitude for the 100, 10, 5, and 2mb pressure levels. Figures 2 through 8 represent the resulting patterns when the zonally averaged temperature is plotted at the 4 levels for each week of 1972, when known. In addition, the vertical flux computed on a once-weekly basis is included in Figures 2 through 8, for latitudes 35°N to 85°N, for purposes of discussion. It can be seen that at low latitudes where heating is more uniform and the dynamics are of minor importance, the zonally averaged temperature bears no distinct variation with time but instead undergoes sporadic variations throughout the year. With increasing latitude, though, the temperature variation becomes more distinct, especially at the higher levels, so that at 85°N and 2mb, there was an annual variation of 59°C in 1972. Imposed on this annual variation in [T], which mirrors the path of the sun, is a number of small variations which seem to correlate well with vertical fluxes of energy occurring in the stratosphere. Starting with 45°N and more so northward, sudden impulses of energy which are transported upward are invariably followed a week later by a distinct rise in temperature at the upper levels in the stratosphere (especially at 5 and 2mb). Then, just as the vertical flux returns to small values the following week, so also does the temperature return to its normal pattern of a gradual increase (in the first half of the year) with time. The large vertical fluxes spoken of here appear much more prevalent in the first few months of 1972 as opposed to November and December. Of course, this pattern may have been peculiar to 1972 and not the normal situation. If this is the typical pattern, though, one might look again to the changes in the surface albedo for a clue as to the cause. In November, the albedo is just beginning to rise as snow accumulates on high ground and at high latitudes. Vertical fluxes are correspondingly small and therefore the fluxes have no effect on the temperature, which continues to drop, unimpeded, from its summer maximum. By December and January, the mean albedo has reached a maximum and we hypothesize that as a result the vertical fluxes of energy are more frequent and greater in magnitude, having an effect on the stratospheric temperatures which in turn are on the upswing. This situation lasts until April when the snow is melting and the albedo is decreasing rapidly, and we hypothesize that the vertical flux decrease is associated with this change. Thereafter there is a smooth continual rise in temperature. This type of scheme would account for the temperatures being higher in the first part of the year than in the last as the data shows, and would give the lowest temperatures at the higher latitudes in November at each level, which was also found. It is necessary to examine the corresponding albedo data on a weekly basis to see if indeed there is a correlation.

These figures clearly indicate the need for a sampling scheme which utilizes data on a smaller time scale than once a week. The variation of the vertical flux is quite significant and cannot be adequately examined using values determined on a once-a-week basis. Stratospheric warmings, for example, can begin and end in a period of a week and go undetected if too coarse a time grid is used for analysis. The reader should take note of the strong vertical energy fluxes in February which resulted in temperature increases at the higher latitudes that were equal to or greater than the maximum temperature attained due to solar heating in July at the 5 and 2mb levels (see Figures 6 through 8).

D. Time and Space Deviations of Mean Quantities

Monthly distributions of $[\bar{T}]^{\prime\prime}$, the deviation of the area averaged temperature from the zonal average, are given in Table 13. The sign of $[\bar{T}]^{\prime\prime}$ at 100mb displays a different pattern to that found at the 10, 5, and 2mb levels. Throughout 1972 at 100mb, the high and middle latitudes displayed a value of $[\bar{T}]''$ which was positive whereas $[\bar{T}]''$ at low latitudes was negative. The 10, 5, and 2mb levels, on the other hand, display negative values of $[\bar{T}]''$ at high latitudes in winter and at low latitudes in the summer, and positive values of $[\bar{T}]''$ at low latitudes in the winter and high latitudes in the summer. Another noteworthy feature of the $[\bar{T}]''$ values in 1972 is the distinct summer maximum at the 100mb level at high latitudes, indicating large differences in the zonal average and global average of $\bar{T}$ in the summer at low levels and high latitudes.

Tables 14, 15, and 16 give monthly values of zonally averaged time standard deviations of u, v, and T, respectively. Again, the reader is reminded that since there was only one set of weekly data for the months of May, June, and July, deviations from a time mean will be zero for those months. Since $\overline{u'^2}$ is used in determining the Eddy Kinetic Energy in the layer, Table 14 can give a rough idea of what effect $\overline{u'^2}$ will have on the total K_E. It is quite clear that for the computation of the K_E in the 10 to 2mb layer, the value of $\overline{u'^2}$ contributes the most to the K_E content at 2mb, especially at middle latitudes. Even though my sampling technique was limited to, at best, once-weekly values at the 100, 10, 5, and 2mb levels, the values in Tables 14, 15, and 16 compare quite favorably with those computed by Richards (1967) for the 100 to 10mb layer.

Tables 17, 18, and 19 give the monthly values of the spatial standard deviations of $\bar{u}$, $\bar{v}$, and $\bar{T}$, respectively. All three variables attained maximum values in winter at high latitudes in 1972, with the $\sqrt{[\bar{u}^{*2}]}$ field displaying an especially peculiar pattern. In winter, the values of $\sqrt{[\bar{u}^{*2}]}$ display double maxima at all four levels with a distinct minimum at 65°N. In the computations of the K_E in the winter, this would give rise to a double maxima on a plot of K_E on a height vs latitude cross-section. The double maxima in the $\sqrt{[\bar{u}^{*2}]}$ values seem to occur to the north and south of the major axis of the polar-night jet so that the polar vortex is at the point of minimum deviation in $[\bar{u}]$ (i.e., at 65°N). As the polar vortex decelerates in the spring, the maxima and minimum disappear, only to reappear again in November when the polar-night jet has come into place and has begun accelerating. The spatial standard deviations of $\bar{T}$ given in Table 19 are relatively small at all latitudes and levels, with the values at 10, 5, and 2mb somewhat larger than the $\sqrt{[\bar{T}^{*2}]}$ values computed at 100mb. Except at 100mb, the maximum spatial deviations of $\bar{T}$ occurred in January in 1972, which gives maximum values of A_E in January as will be discussed later.

E. The Total Energy Budget

As I pointed out in the presentation of the energy budget equation for K_E (Section IV), the amount of energy transported vertically through the action of stationary adiabatic waves is an important part of the total energy budget. Table 20 gives monthly values of the total vertical energy flux and the resultant divergence between levels (a positive number indicates divergence). It is evident that all of the layers shown absorb significant amounts of energy in the winter whereas energy is transported out of the upper layers to varying degrees in the summer months. It was rather surprising at first that such large amounts of energy are transported upward across even the 2mb level, indicating that the region above 2mb is quite active in winter. It should be remembered that the diabatic effects in the stratosphere increase with height as do the errors in the vertical energy flux approximation, so that the vertical energy flux computed at the 2mb level, for example, could be off by a significant amount.

The total energy contents and conversion rates by month for the 10 to 2mb layer are given in Table 21. In addition, the conversion rate for A_Z to A_E using standing eddy transport of sensible heat only is given (the column labeled ALT C_A) and the conversion rate for K_Z to K_E using standing eddy transport of angular momentum only is given also (the column labeled ALT C_K). A positive sign on C_A indicates a conversion from A_Z to A_E and a positive sign on C_K indicates a conversion from K_Z to K_E. To better illustrate the energy budget values, a series of box diagrams are included for purposes of discussion (see Figure 13).

One of the first things to note is that the conversion rates and the energy involved in the convergence of the vertical flux display marked seasonal variations in both magnitude and sign, with a maximum in winter and a minimum that is normally opposite in sign in summer. Also noteworthy is the fact that the convergence of the vertical energy is quite comparable in size and often greater than the conversion rates C_A and C_K. Further, the contribution of the standing eddies to the conversion rate is, in most cases, greater than the contribution from transient eddies. In the discussion of sensible heat transports via eddy processes, it was pointed out that the transport was predominantly northward throughout the winter months with some southward transport indicated in the summer months at some latitudes. From the equation for C_A given in Section IV, it can be seen that the sign of the mean available potential energy conversion in the 10 to 2mb layer will depend on the sign of the mean temperature gradient at that latitude as well as on the direction of transport. When the temperature gradient reversed in the spring, a corresponding change in the sign of the available potential energy conversion rate occurred. Hence, the conversion of available potential energy is from A_Z to A_E in the winter and the conversion reverses in the summer months, resulting in the A_E being depleted.

A parallel situation exists in the kinetic energy conversion, although the situation is more complicated. The sign of the angular momentum transport in winter months is such that the eddy processes are feeding momentum to the polar vortex. From the equation for calculating the conversion C_K given in Section IV, it can be seen that the sign of the mean kinetic energy conversion in the 10 to 2mb layer will depend on the sign of the mean zonal wind gradient as well as on the direction of the transport. In the winter, the polar-night jet at high latitudes dominates the $[\bar{u}]$ cross-section, whereas in the summer we have the easterly jet at low latitudes, both of which result in the same sign for the zonal wind gradient. So the sign of the transport term becomes important in determining the direction of the conversion. In the winter there is a conversion of K_E to K_Z which reverses in April when the seasonal transition occurs, then reverses back again in July and remains a K_E to K_Z conversion for the rest of the year, except for October.

The entire energy cycle of the atmosphere appears to be very much dependent on season with a distinct energy cycle in winter and energy values at the noise level in the summer. The transport processes and the baroclinicity of the atmosphere drive the energy cycle from eddy kinetic energy through the cycle to eddy available potential energy in the winter and generally in the reverse direction in the summer. The kinetic energy values attain a maximum in the winter when the polar vortex is in an accelerated state, and drop to a minimum in the summer, although it is noteworthy that the zonal kinetic energy maintained relatively high values in the summer months when the easterly jet at high levels in the tropics was at a maximum (June and July).

As was discussed by Newell (1965) a few years ago, the middle and upper stratosphere resembles the tropospheric heat engine during the winter season. Radiational processes are a source of A_Z and horizontal eddy processes in turn convert this A_Z into A_E. Further conversion of this eddy available potential energy into eddy kinetic energy may occur but this calculation awaits determination of the corresponding vertical velocity field. In addition, Eddy processes convert energy transported from the troposphere into eddy kinetic energy in the stratosphere and in turn convert eddy kinetic energy into K_Z, supplying energy to the mean circulatory motions in the stratosphere. Although I was unable to compute C_Z, it seems probable that the conversion would be from K_Z to A_Z in winter in the upper stratosphere, resulting from rising motion at the colder latitudes and sinking motion in the warmer latitudes. Richards (1967) found subsidence at the lower latitudes, where temperatures are warmest, and rising motion at the higher latitudes in the region of colder temperatures, at the 10mb level in 1965. This appears to be the normal winter pattern for the vertical motion field, at least at the 10mb level, indicating a conversion of zonal kinetic energy to zonal available potential energy in winter. In summer, the C_Z conversion rate would reduce to the noise level of the data so that the sign of the conversion would be indiscernible.

During the summer months, the middle and upper stratosphere resemble a refrigerator with radiational processes now destroying A_Z as they transport heat against the temperature gradient. The idea of heat engines and refrigerated regions in the atmosphere has been discussed extensively in other publications although not for the upper stratospheric region (see Barnes, 1962 and Newell, 1966).

VI. CONCLUSION

Although this study entailed an extensive amount of calculations and computer time, it by no means resulted in a complete picture of the energetics of the stratosphere. Assumptions had to be made about the relative importance of some terms whereas certain of the necessary parts of the energy cycle, such as the generation of available potential energy, could not be computed at all. In addition, due to the limited amount of data, some terms, such as those involving transient eddies, were given less weight in the overall calculations than they may deserve. With these shortcomings in mind, though, the study did reveal some remarkable facts about the circulation and energetics of the upper stratosphere.

Eddy processes do indeed play an important role in maintaining the energy budget in all regions of the stratosphere. In addition, the troposphere, through the action of a vertical flux of energy, exerts a significant influence on the stratosphere, with its effects seemingly still felt above the 2mb level. The 10 to 2mb region appears to function as a heat engine in winter with an internal heat source and a probable destruction of A_E through radiational processes. The result is more cooling in the warmer regions and warming in the colder regions at the same latitude. In contrast, the 10 to 2mb layer acts as a refrigerated region in the summer, having to rely on external sources of heat to maintain itself.

The final point to be made is that almost all of the quantities computed appear to have strong seasonal dependence. This fact alone points up the need for more than once-monthly data at the 5 and 2mb levels in the summer months before one can adequately examine the monthly changes in the energy cycle and the stratospheric circulation as a whole.

100 mb

Lat.	Jan.	Feb.	Mar.	Apr.	May	June	July	Aug.	Sept.	Oct.	Nov.	Dec.
85	1.0	5.0	0.9	0.7	0.0	0.3	1.4	1.6	-0.6	4.3	0.4	4.8
75	8.3	16.8	9.4	4.2	0.2	0.0	3.5	4.8	1.2	8.2	3.8	11.7
65	15.1	17.6	15.0	6.1	1.5	0.2	2.3	4.5	4.5	10.5	10.5	14.4
55	21.1	15.2	16.4	8.4	5.2	3.1	3.0	6.2	10.1	12.0	15.9	18.2
45	22.4	18.6	14.9	13.0	9.8	8.5	8.2	10.5	13.2	14.8	19.8	22.4
35	24.0	26.1	20.6	17.4	13.9	10.0	5.1	4.2	11.4	15.8	24.8	27.7
25	21.8	25.0	22.1	15.7	13.6	1.1	-4.1	-4.0	3.6	11.2	18.5	20.8
15	13.0	12.9	12.5	11.6	11.2	-3.6	-4.7	-6.2	-0.4	7.2	9.2	13.7

10 mb

Lat.	Jan.	Feb.	Mar.	Apr.	May	June	July	Aug.	Sept.	Oct.	Nov.	Dec.
85	15.0	15.3	5.3	-1.2	-1.2	-2.1	-1.9	-0.3	1.8	4.9	5.1	7.7
75	39.5	36.7	15.6	-5.1	-4.4	-6.8	-4.7	-2.1	5.3	14.1	15.0	22.9
65	49.2	39.9	17.8	-8.1	-8.5	-11.7	-9.3	-4.7	5.9	17.4	20.2	32.1
55	39.9	27.4	11.3	-7.0	-8.5	-14.3	-13.8	-7.1	5.3	14.9	21.4	30.1
45	22.5	16.0	7.1	0.6	-4.7	-12.3	-15.1	-9.9	3.4	10.8	19.9	21.7
35	10.0	8.7	6.9	7.2	-1.3	-9.8	-16.2	-13.9	-1.5	6.2	14.8	16.1
25	4.9	8.1	6.0	7.7	-4.2	-12.9	-21.3	-19.5	-7.4	1.6	7.3	11.0
15	4.5	4.7	6.6	4.1	-5.3	-17.4	-22.3	-17.8	-5.3	-6.9	2.8	6.0

TABLE 1. Zonal Average of Mean Monthly Zonal Wind, $[\bar{u}]$. Units: m sec^{-1}.

5 mb

Lat.	Jan.	Feb.	Mar.	Apr.	May	June	July	Aug.	Sept.	Oct.	Nov.	Dec.
85	14.5	12.8	0.8	-0.9	-2.9	-4.1	-4.0	-0.9	1.3	6.2	6.2	8.8
75	43.1	34.8	10.5	-5.5	-6.5	-8.2	-14.5	-3.4	6.9	19.1	17.6	31.6
65	59.0	39.9	19.3	-7.2	-9.2	-9.6	-15.0	-4.8	7.5	23.1	26.5	41.9
55	50.9	29.7	17.5	-3.7	-10.4	-12.4	-16.5	-8.5	8.5	21.7	29.5	43.8
45	31.6	15.2	14.6	3.0	-10.8	-14.7	-18.4	-11.5	5.9	18.4	27.9	34.8
35	13.0	7.9	18.2	8.1	-7.9	-16.7	-23.2	-15.2	-1.8	11.0	25.8	25.5
25	2.2	8.7	8.5	3.9	-6.4	-23.2	-27.7	-16.6	-6.8	6.8	23.0	16.9
15	-3.6	-3.0	0.4	-3.8	-7.5	-8.7	-23.2	-14.1	-6.6	5.1	17.3	11.8

2 mb

Lat.	Jan.	Feb.	Mar.	Apr.	May	June	July	Aug.	Sept.	Oct.	Nov.	Dec.
85	17.7	12.8	0.8	-0.8	-1.3	-1.6	-2.0	-2.3	1.8	8.0	3.5	9.4
75	43.7	27.5	8.0	-1.7	-5.2	-2.5	-10.4	-4.8	8.5	24.8	20.1	33.7
65	57.8	31.8	15.7	-1.0	-9.1	-12.3	-15.3	-10.0	11.4	28.8	35.2	50.5
55	52.3	27.6	21.5	1.9	-10.3	-17.6	-20.5	-12.3	11.1	30.9	41.1	59.3
45	42.4	24.4	28.6	5.5	-9.7	-20.7	-26.6	-15.4	9.1	29.1	43.7	54.7
35	27.8	18.2	29.7	7.0	-11.6	-28.2	-31.7	-19.8	5.4	25.6	44.0	50.2
25	14.3	14.3	17.7	5.3	-16.6	-35.0	-44.2	-11.3	-0.9	24.6	40.7	30.2
15	-2.2	4.7	6.7	3.2	-29.5	-29.1	-24.1	-7.3	-7.1	21.8	29.9	18.0

TABLE 1 - Continued

100 mb

Lat.	Jan.	Feb.	Mar.	Apr.	May	June	July	Aug.	Sept.	Oct.	Nov.	Dec.
85	209.2	206.5	213.0	227.5	226.9	229.2	230.5	228.8	224.2	220.5	215.0	205.9
75	210.6	209.1	214.4	225.8	226.0	228.1	228.8	227.4	223.8	220.8	216.5	208.8
65	213.9	213.2	217.1	223.0	224.1	225.5	225.6	224.8	222.5	219.9	217.8	213.2
55	217.4	217.0	218.4	219.2	220.6	221.5	221.2	220.6	219.5	217.6	217.0	216.2
45	216.5	216.7	216.5	214.8	216.0	215.6	214.6	213.9	214.1	213.5	213.6	215.1
35	210.7	210.2	210.4	209.2	209.8	208.0	207.0	206.2	206.8	207.2	207.2	209.4
25	203.7	201.7	202.5	202.5	202.5	201.7	201.3	200.8	200.6	200.8	200.0	202.3
15	199.2	197.3	197.8	198.1	197.7	198.6	197.9	197.7	197.2	196.3	195.5	197.4
5	197.7	196.2	196.3	196.5	196.3	197.5	196.3	196.2	195.8	193.7	193.4	195.1

10 mb

Lat.	Jan.	Feb.	Mar.	Apr.	May	June	July	Aug.	Sept.	Oct.	Nov.	Dec.
85	203.6	213.8	227.2	232.5	237.1	242.1	244.2	238.7	227.3	214.2	208.3	203.3
75	208.2	216.7	227.5	231.7	236.9	241.4	243.4	238.3	228.4	216.2	210.2	206.5
65	214.2	220.5	227.0	230.3	236.2	239.8	241.3	237.4	230.0	219.6	213.5	211.5
55	220.1	223.6	226.2	229.2	235.1	237.3	238.6	236.0	231.0	223.5	217.6	216.8
45	225.5	226.8	226.8	229.6	234.3	234.8	236.4	234.5	231.6	226.7	222.2	221.5
35	229.3	229.5	228.7	231.5	234.2	233.3	234.5	233.0	231.9	228.9	226.3	225.6
25	231.1	230.7	230.4	233.6	234.7	232.9	233.3	231.8	231.7	230.0	228.9	228.6
15	231.9	231.4	231.4	234.7	235.2	232.9	232.3	231.0	231.3	230.7	230.2	230.0
5	232.1	232.0	231.9	235.2	235.5	233.1	231.3	230.5	230.8	231.2	231.0	230.8

TABLE 2. Zonal Average of Mean Monthly Temperature, $[\bar{T}]$. Units: ^{o}K.

5 mb

Lat.	Jan.	Feb.	Mar.	Apr.	May	June	July	Aug.	Sept.	Oct.	Nov.	Dec.
85	221.7	245.5	236.1	241.0	250.6	255.0	259.8	254.4	237.7	222.5	214.7	211.9
75	223.8	241.3	233.9	241.6	249.8	254.5	258.5	252.9	238.5	224.3	216.3	213.3
65	227.7	237.0	232.4	242.9	249.6	253.7	256.3	250.3	239.7	227.5	219.8	216.8
55	232.4	235.8	233.9	244.6	249.6	252.4	253.5	247.5	240.9	231.3	224.9	223.2
45	236.2	236.8	237.8	246.1	249.2	250.7	250.5	245.2	242.1	235.3	230.7	231.9
35	239.1	238.8	242.0	247.1	248.1	248.8	247.2	243.6	243.6	239.0	236.5	239.7
25	241.4	240.9	244.7	247.5	246.5	247.1	244.2	243.1	245.1	242.9	241.6	243.7
15	242.7	242.5	245.5	247.6	245.0	245.8	242.1	243.5	246.0	246.2	245.3	244.8
5	243.0	243.2	245.7	247.6	243.8	245.1	241.0	244.4	246.7	248.2	247.1	244.8

2 mb

Lat.	Jan.	Feb.	Mar.	Apr.	May	June	July	Aug.	Sept.	Oct.	Nov.	Dec.
85	251.1	256.0	246.3	254.6	271.9	277.2	279.7	270.6	250.4	231.0	226.9	227.3
75	249.7	254.3	246.4	256.5	271.3	276.7	279.2	269.8	251.9	234.5	228.0	228.5
65	247.0	251.2	247.6	260.0	270.4	274.3	278.0	267.7	254.0	240.0	231.0	231.7
55	245.6	249.0	251.0	263.2	269.2	271.1	276.1	265.0	255.8	245.6	236.8	238.2
45	248.8	251.5	256.8	265.4	268.2	268.8	273.4	262.9	257.4	251.2	245.0	247.1
35	254.7	257.1	262.7	266.5	267.3	266.6	270.0	261.6	259.2	256.6	252.9	255.7
25	259.6	261.0	266.6	266.6	266.5	264.4	266.3	261.0	260.7	260.7	258.5	260.8
15	261.9	262.3	268.3	266.5	265.2	262.8	263.1	261.1	261.8	263.3	261.9	262.2
5	262.2	262.5	269.1	266.5	264.0	261.5	261.9	261.4	262.4	264.8	263.8	262.4

TABLE 2 – Continued

100 mb

Lat.	Jan.	Feb.	Mar.	Apr.	May	June	July	Aug.	Sept.	Oct.	Nov.	Dec.
85	404.2	399.0	411.5	439.5	438.3	442.7	445.3	441.9	433.0	426.0	415.3	397.8
75	406.8	404.0	414.2	436.3	436.5	440.6	441.9	439.4	432.3	426.6	418.2	403.4
65	413.3	411.7	419.3	430.7	432.8	435.6	435.9	434.3	429.9	424.8	420.8	411.9
55	420.0	419.1	421.9	423.4	426.2	427.9	427.4	426.2	424.1	420.3	419.1	417.6
45	418.1	418.6	418.2	414.9	417.2	416.5	414.5	413.3	413.5	412.3	412.7	415.5
35	407.0	406.0	406.4	404.0	405.3	401.8	399.8	398.4	399.5	400.2	400.2	404.5
25	393.4	389.5	391.2	391.3	391.2	389.6	388.8	387.8	387.5	387.8	386.3	390.8
15	384.8	381.1	382.2	382.7	382.0	383.7	382.3	381.9	380.9	379.2	377.7	381.4
5	381.8	379.0	379.2	379.5	379.1	381.6	379.2	379.0	378.2	374.1	373.6	376.9

10 mb

Lat.	Jan.	Feb.	Mar.	Apr.	May	June	July	Aug.	Sept.	Oct.	Nov.	Dec.
85	760.0	797.8	847.8	867.6	884.7	903.6	911.4	890.7	848.4	799.4	777.2	758.9
75	776.9	808.6	848.8	864.8	884.2	901.0	908.2	889.5	852.4	807.0	784.5	770.6
65	799.4	822.7	847.2	859.4	881.6	895.0	900.4	886.1	858.4	819.7	796.6	789.3
55	821.4	834.5	844.1	855.2	877.3	885.7	890.5	880.7	862.1	834.1	812.2	809.1
45	841.7	846.5	846.4	856.7	874.3	876.1	882.1	875.2	864.4	846.2	829.4	826.8
35	855.8	856.4	853.4	863.9	874.0	870.6	875.2	869.4	865.4	854.2	844.4	842.1
25	862.4	860.9	859.9	871.7	875.9	869.2	870.6	864.9	864.9	858.4	854.1	853.0
15	865.3	863.4	863.7	876.0	877.7	869.2	866.9	861.9	863.3	860.9	859.1	858.5
5	866.2	865.9	865.6	877.7	879.0	869.8	863.3	860.2	861.2	862.9	861.9	861.5

TABLE 3. Zonal Average of Mean Monthly Potential Temperature, $[\bar{\theta}]$. Units: ^{o}K.

5 mb

Lat.	Jan.	Feb.	Mar.	Apr.	May	June	July	Aug.	Sept.	Oct.	Nov.	Dec.
85	1008.6	1117.3	1074.2	1096.4	1140.3	1160.4	1182.2	1157.6	1081.7	1012.4	976.8	964.2
75	1018.2	1098.2	1064.5	1099.3	1136.5	1158.0	1176.1	1150.5	1085.1	1020.7	984.0	970.7
65	1036.3	1078.6	1057.5	1105.3	1135.6	1154.3	1166.0	1138.9	1090.6	1035.2	1000.0	986.6
55	1057.4	1072.9	1064.3	1113.0	1135.6	1148.6	1153.7	1126.0	1096.0	1052.5	1023.1	1015.6
45	1074.8	1077.7	1082.0	1119.7	1133.8	1140.6	1139.8	1115.5	1101.8	1070.5	1049.8	1055.3
35	1087.9	1086.7	1101.1	1124.3	1128.8	1131.9	1125.0	1108.3	1108.6	1087.7	1076.2	1090.5
25	1098.2	1096.3	1113.2	1126.3	1121.8	1124.5	1111.2	1106.0	1115.0	1105.0	1099.2	1108.9
15	1104.3	1103.3	1117.2	1126.6	1115.0	1118.5	1101.5	1108.2	1119.4	1120.4	1116.0	1114.1
5	1105.6	1106.8	1118.1	1126.8	1109.4	1115.3	1096.4	1112.0	1122.6	1129.3	1124.4	1113.9

2 mb

Lat.	Jan.	Feb.	Mar.	Apr.	May	June	July	Aug.	Sept.	Oct.	Nov.	Dec.
85	1485.0	1513.9	1456.4	1505.8	1608.0	1639.5	1653.8	1600.2	1480.9	1365.9	1342.1	1344.4
75	1476.9	1503.8	1456.9	1516.8	1604.2	1636.5	1650.9	1595.3	1489.7	1386.5	1348.1	1351.2
65	1460.7	1485.3	1464.2	1537.4	1598.7	1621.9	1644.1	1582.9	1502.1	1419.3	1365.9	1370.4
55	1452.4	1472.3	1484.5	1556.2	1592.2	1603.4	1633.0	1567.0	1512.4	1452.1	1400.1	1408.6
45	1471.5	1487.0	1518.3	1569.4	1585.7	1589.5	1616.5	1554.6	1522.3	1485.5	1448.9	1461.3
35	1506.4	1520.3	1553.7	1575.6	1580.8	1576.3	1596.7	1547.1	1532.7	1517.3	1495.8	1512.2
25	1534.9	1543.4	1576.3	1576.3	1575.9	1563.7	1574.9	1543.6	1541.6	1541.7	1528.4	1542.0
15	1549.0	1551.3	1586.4	1576.1	1568.2	1553.9	1556.0	1543.8	1547.9	1557.3	1548.7	1550.7
5	1550.6	1552.2	1591.3	1575.6	1561.4	1546.6	1548.8	1545.6	1551.8	1565.6	1559.8	1551.6

TABLE 3 - Continued

100 mb

Lat.	Jan.	Feb.	Mar.	Apr.	May	June	July	Aug.	Sept.	Oct.	Nov.	Dec.
85	0.0	0.0	0.0	0.0	0.0	0.0	0.0	0.0	0.0	0.0	0.0	0.0
75	3.0	-11.6	-6.0	-5.3	-2.5	-0.8	-2.0	-0.5	-5.2	0.1	-15.7	9.6
65	4.9	-9.9	-5.9	-1.1	-3.0	-2.4	0.9	-0.7	-4.5	-0.7	-9.9	4.9
55	-0.4	6.5	-6.4	2.4	-0.8	0.0	2.6	4.2	-3.1	14.9	-8.9	20.5
45	11.1	15.8	5.6	0.4	0.5	0.2	5.8	0.8	4.1	18.4	6.2	21.5
35	23.8	22.5	10.8	12.9	5.2	-1.4	7.0	8.4	14.0	16.3	20.4	23.9
25	3.6	6.4	6.0	8.3	5.0	7.4	2.6	7.3	12.7	7.5	8.5	3.6
15	1.6	-0.2	3.7	-7.4	1.7	6.4	-4.9	-1.6	2.1	-3.8	1.5	3.2

10 mb

Lat.	Jan.	Feb.	Mar.	Apr.	May	June	July	Aug.	Sept.	Oct.	Nov.	Dec.
85	0.0	0.0	0.0	0.0	0.0	0.0	0.0	0.0	0.0	0.0	0.0	0.0
75	2.8	-21.7	70.2	8.9	1.5	0.4	0.0	1.2	1.9	-0.1	26.5	16.6
65	10.5	-25.4	45.9	9.4	-0.4	-0.1	0.0	0.7	3.6	5.0	56.9	35.7
55	65.9	46.3	69.5	23.2	0.1	1.5	0.2	1.0	2.9	12.5	68.3	45.6
45	53.2	49.9	33.2	13.8	-0.4	1.0	-0.7	0.4	-0.6	10.9	32.5	21.4
35	13.7	23.7	12.9	7.8	2.1	0.5	-1.1	-0.4	2.5	1.9	8.5	8.4
25	-6.0	-3.3	-0.7	1.2	2.3	-1.2	-3.1	-5.8	-1.6	-1.5	-0.7	0.1
15	4.3	-2.5	-1.8	7.5	1.8	-1.0	-3.8	-3.9	-2.8	-3.3	-1.0	1.7

TABLE 4. Monthly Values of $[\overline{uv}]$. Units: $m^2\ sec^{-2}$.

5 mb

Lat.	Jan.	Feb.	Mar.	Apr.	May	June	July	Aug.	Sept.	Oct.	Nov.	Dec.
85	0.0	0.0	0.0	0.0	0.0	0.0	0.0	0.0	0.0	0.0	0.0	0.0
75	-5.6	-62.9	59.2	9.7	5.7	1.7	3.0	1.8	3.1	4.5	50.6	27.9
65	29.6	-76.9	89.7	4.1	-2.4	1.1	1.7	-3.3	-2.0	-10.6	60.8	62.5
55	11.5	75.8	75.6	4.7	-2.7	0.4	1.8	-3.4	3.3	0.7	59.6	80.2
45	9.4	83.2	35.7	-4.4	-2.9	0.3	0.8	-0.7	-4.0	-5.4	17.6	48.5
35	40.2	40.0	31.6	-0.2	1.0	0.2	4.7	0.5	5.1	0.7	12.9	33.0
25	-6.7	2.5	7.8	-9.6	-0.7	0.1	5.3	-3.0	-4.4	-2.8	-9.5	8.7
15	32.6	0.4	21.9	7.3	-0.4	-0.7	33.0	-1.1	4.7	6.0	-25.6	46.8

2 mb

Lat.	Jan.	Feb.	Mar.	Apr.	May	June	July	Aug.	Sept.	Oct.	Nov.	Dec.
85	0.0	0.0	0.0	0.0	0.0	0.0	0.0	0.0	0.0	0.0	0.0	0.0
75	4.3	-87.0	52.1	8.9	2.8	0.0	1.0	2.6	6.6	6.9	79.1	59.5
65	82.6	-2.7	57.9	2.6	-7.0	0.2	0.3	-19.3	-1.2	0.6	115.2	101.3
55	141.5	133.2	56.4	3.7	-0.9	0.6	0.2	-13.3	8.1	-2.3	97.1	128.5
45	136.2	127.7	30.2	0.8	-3.9	0.8	1.2	0.4	1.9	-8.4	24.8	101.7
35	127.4	65.0	30.6	2.9	0.0	-0.4	-1.5	0.4	11.0	4.7	10.6	37.1
25	67.9	0.3	4.7	-0.8	-7.1	-7.7	-2.0	-6.1	-2.9	0.9	-17.5	23.0
15	8.4	2.3	74.7	23.5	-2.1	-14.8	1.1	-4.0	8.0	2.2	25.2	32.3

TABLE 4 - Continued

100 mb

Lat.	Jan.	Feb.	Mar.	Apr.	May	June	July	Aug.	Sept.	Oct.	Nov.	Dec.
85	0.0	0.0	0.0	0.0	0.0	0.0	0.0	0.0	0.0	0.0	0.0	0.0
75	12.6	-20.9	-2.0	-9.1	-1.0	-0.2	2.4	-0.8	-1.7	0.7	-8.3	10.1
65	8.5	-23.3	-4.8	-5.4	-2.5	-0.5	1.6	1.1	-1.3	2.2	-5.3	0.7
55	6.1	0.8	-8.3	-0.1	-1.1	0.2	2.4	1.2	-0.9	7.8	-11.5	8.5
45	13.1	10.7	0.1	-1.3	-2.4	-0.9	2.1	-2.1	0.8	10.0	5.9	12.1
35	14.0	14.1	3.1	3.0	0.0	0.4	5.2	6.8	7.7	1.8	13.4	8.4
25	1.7	0.9	2.1	1.2	3.4	7.4	1.0	6.0	7.9	5.4	5.7	4.8
15	1.2	-2.3	1.4	-6.2	0.3	3.8	-3.3	0.0	2.7	-7.3	0.5	4.7

10 mb

Lat.	Jan.	Feb.	Mar.	Apr.	May	June	July	Aug.	Sept.	Oct.	Nov.	Dec.
85	0.0	0.0	0.0	0.0	0.0	0.0	0.0	0.0	0.0	0.0	0.0	0.0
75	14.7	5.5	22.4	7.5	0.7	0.1	0.0	0.3	1.4	-2.6	26.1	18.0
65	20.4	31.1	31.6	6.4	-0.5	-0.1	0.6	0.7	2.6	4.6	46.1	34.1
55	48.0	70.5	55.2	9.6	-0.3	1.2	0.1	0.9	2.0	8.7	39.5	39.0
45	26.2	47.2	26.6	6.9	-0.1	0.8	-0.1	0.1	-0.1	8.6	15.2	16.0
35	3.6	18.6	9.1	3.6	1.5	1.7	-0.6	-1.8	1.2	-0.1	3.2	6.5
25	-6.6	-3.5	-1.2	0.4	1.7	-0.1	-3.4	-4.9	-0.9	-1.4	-0.7	-0.3
15	5.6	-3.6	-0.9	0.9	1.0	-0.9	-2.5	-6.7	-1.8	-1.5	-1.1	0.5

TABLE 5. Zonally Averaged Spatial Covariances of $\bar{u}$ and $\bar{v}$, $\left[\bar{u}^{*}\bar{v}^{*}\right]$. Units: m^2 sec^{-2}.

5 mb

Lat.	Jan.	Feb.	Mar.	Apr.	May	June	July	Aug.	Sept.	Oct.	Nov.	Dec.
85	0.0	0.0	0.0	0.0	0.0	0.0	0.0	0.0	0.0	0.0	0.0	0.0
75	-6.2	-74.6	14.4	4.2	5.7	1.7	3.0	2.4	-0.5	-2.9	68.2	34.4
65	69.9	-30.3	69.7	1.7	-2.4	1.1	1.7	-1.1	-0.4	-1.4	76.8	65.5
55	56.5	26.6	53.8	0.1	-2.7	0.4	1.8	-1.1	0.2	6.6	48.2	49.7
45	19.3	22.5	28.2	-1.4	-2.9	0.3	0.8	-0.5	-1.9	-1.4	5.4	33.4
35	24.8	16.7	21.1	1.3	1.0	0.2	4.7	0.3	-0.2	2.3	1.9	15.0
25	6.9	5.0	9.1	-5.4	-0.7	0.1	5.3	-0.5	-1.3	-1.3	0.2	3.1
15	16.3	0.6	16.1	6.4	-0.4	-0.7	33.0	-4.7	0.1	1.5	-1.5	23.4

2 mb

Lat.	Jan.	Feb.	Mar.	Apr.	May	June	July	Aug.	Sept.	Oct.	Nov.	Dec.
85	0.0	0.0	0.0	0.0	0.0	0.0	0.0	0.0	0.0	0.0	0.0	0.0
75	-1.3	-33.3	3.8	5.5	2.8	0.0	1.0	-1.4	-0.1	11.5	101.9	42.3
65	133.0	8.1	21.4	1.5	-7.0	0.2	0.3	-7.6	-0.9	9.2	136.5	49.0
55	134.5	69.6	29.9	2.0	-0.9	0.6	0.2	-1.6	2.1	5.7	84.0	72.9
45	96.7	58.9	18.9	0.0	-3.9	0.8	1.2	3.4	0.6	-1.0	22.8	61.1
35	60.0	42.4	22.3	1.4	0.0	-0.4	-1.5	2.2	0.0	0.9	8.0	29.7
25	28.6	2.5	-1.9	-0.6	-7.1	-7.7	-2.0	-0.8	-1.8	2.6	5.5	7.9
15	1.3	-0.4	40.6	3.6	-2.1	-14.8	1.1	-1.8	4.3	0.5	24.3	23.5

TABLE 5 - Continued

100 mb

Lat.	Jan.	Feb.	Mar.	Apr.	May	June	July	Aug.	Sept.	Oct.	Nov.	Dec.
85	0.0	0.0	0.0	0.0	0.0	0.0	0.0	0.0	0.0	0.0	0.0	0.0
75	22.0	-36.5	-3.5	-15.9	-1.8	-0.4	4.2	-1.5	-2.9	1.2	-14.5	17.5
65	39.7	-108.0	-22.2	-25.3	-11.8	-2.5	7.4	5.3	-6.2	10.2	-24.8	3.3
55	52.0	6.7	-70.8	-0.4	-9.7	1.7	20.9	9.9	-7.5	67.1	-98.0	73.0
45	170.3	139.4	0.8	-16.6	-31.2	-11.1	27.5	-26.9	10.5	130.1	76.3	157.6
35	244.3	246.7	54.3	52.1	0.3	7.7	90.2	119.5	134.6	30.9	233.7	147.1
25	37.0	20.0	45.8	25.6	73.1	157.6	21.6	127.5	168.0	115.7	121.6	102.8
15	28.8	-54.9	33.4	-150.9	6.1	92.8	-79.4	0.0	64.5	-178.1	10.9	115.2

10 mb

Lat.	Jan.	Feb.	Mar.	Apr.	May	June	July	Aug.	Sept.	Oct.	Nov.	Dec.
85	0.0	0.0	0.0	0.0	0.0	0.0	0.0	0.0	0.0	0.0	0.0	0.0
75	25.5	9.5	39.0	13.1	1.2	0.2	0.1	0.5	2.4	-4.5	45.4	31.4
65	94.9	144.3	146.9	29.5	-2.3	-0.5	2.8	3.3	12.2	21.3	214.2	158.4
55	410.4	603.1	472.4	81.9	-2.6	10.4	1.0	7.6	17.3	74.6	338.3	334.0
45	340.4	613.7	345.6	89.8	-1.8	10.2	-1.3	1.0	-1.5	111.9	197.7	208.6
35	63.1	324.0	158.5	62.9	26.1	29.4	-10.0	-30.6	20.4	-1.1	55.0	113.7
25	-141.2	-75.0	-25.6	7.5	35.4	-2.3	-73.1	-103.9	-18.4	-30.6	-15.6	-7.1
15	136.5	-88.5	-21.8	20.8	23.5	-21.3	-60.8	-161.7	-43.2	-35.2	-27.4	11.2

TABLE 6. Relative Angular Momentum Transport by Standing Eddies, $\iint \bar{u}^* \bar{v}^* a^2 \cos^2\phi \, d\lambda \, \frac{dp}{g}$.

Units: 10^{20} gm cm^2 mb^{-1} sec^{-2}. (NOTE: 0.0 represents < $\pm 0.05 \times 10^{20}$)

5 mb

Lat.	Jan.	Feb.	Mar.	Apr.	May	June	July	Aug.	Sept.	Oct.	Nov.	Dec.
85	0.0	0.0	0.0	0.0	0.0	0.0	0.0	0.0	0.0	0.0	0.0	0.0
75	-10.7	-129.9	25.2	7.4	10.0	3.0	5.3	4.1	-0.8	-5.1	118.8	59.9
65	324.5	-140.5	323.8	7.9	-11.0	5.1	7.9	-4.9	-1.7	-6.6	356.5	304.3
55	483.5	227.6	460.2	1.3	-23.0	3.2	15.2	-9.7	1.4	56.5	412.7	424.9
45	251.4	292.0	366.8	-17.9	-37.2	3.8	9.9	-6.3	-24.1	-17.7	70.5	433.7
35	432.0	291.2	368.7	23.1	17.4	4.0	81.8	5.7	-3.4	39.4	33.6	262.5
25	147.5	106.5	194.6	-114.6	-13.9	2.8	114.1	-11.1	-27.8	-27.8	3.6	67.1
15	396.2	14.9	389.7	156.2	-8.5	-17.1	801.9	-115.2	2.1	35.7	-37.4	567.3

2 mb

Lat.	Jan.	Feb.	Mar.	Apr.	May	June	July	Aug.	Sept.	Oct.	Nov.	Dec.
85	0.0	0.0	0.0	0.0	0.0	0.0	0.0	0.0	0.0	0.0	0.0	0.0
75	-2.2	-58.0	6.7	9.7	4.9	0.0	1.8	-2.5	-0.2	20.1	177.5	73.7
65	617.9	37.6	99.6	6.8	-32.5	0.8	1.4	-35.3	-4.1	42.8	633.9	227.4
55	1150.4	595.8	255.4	17.2	-7.8	5.5	1.8	-14.0	17.9	48.8	718.4	623.7
45	1257.7	766.1	246.1	-0.3	-50.8	10.6	15.2	44.2	8.1	-13.6	296.5	794.6
35	1047.7	740.2	389.9	24.8	0.0	-6.7	-26.8	37.9	-0.4	15.8	139.8	518.6
25	611.9	53.6	-39.9	-13.4	-151.7	-164.2	-41.7	-18.1	-37.7	55.1	117.1	168.9
15	30.4	-9.6	985.5	86.9	-51.2	-358.3	25.6	-42.7	104.0	12.3	590.7	570.5

TABLE 6 - Continued

100 mb

Lat.	Jan.	Feb.	Mar.	Apr.	May	June	July	Aug.	Sept.	Oct.	Nov.	Dec.
85	-1.6	-0.3	-2.6	-0.7	0.1	-0.2	0.3	0.1	0.6	0.1	-0.9	0.6
75	1.4	7.3	-4.0	1.1	0.7	-0.2	0.6	1.1	1.8	1.7	-0.8	4.8
65	11.5	30.1	8.8	5.7	2.4	1.0	1.2	1.7	2.4	7.0	8.4	7.8
55	13.6	32.1	11.7	7.8	2.4	1.2	1.8	1.7	3.2	8.9	12.7	8.0
45	5.2	11.9	4.4	5.2	1.4	0.0	1.0	0.0	2.3	4.3	6.0	5.2
35	-0.9	-0.1	1.7	1.4	-0.2	0.3	-0.3	-1.1	0.9	1.1	0.2	-0.4
25	-0.6	-0.6	0.6	0.0	-0.5	2.4	1.9	-0.2	0.5	0.1	-1.9	-4.2
15	0.1	-0.3	1.3	-0.4	0.2	2.5	2.7	0.3	0.8	0.8	1.0	-3.7
5	0.1	-0.1	0.5	-0.1	0.0	0.9	0.9	0.2	0.3	0.0	0.8	-1.0

10 mb

Lat.	Jan.	Feb.	Mar.	Apr.	May	June	July	Aug.	Sept.	Oct.	Nov.	Dec.
85	2.3	12.7	6.4	-0.7	1.0	0.2	0.0	0.1	0.2	0.3	3.5	1.6
75	25.5	67.7	27.3	-1.4	3.2	1.3	0.4	1.0	1.9	4.1	22.9	12.8
65	50.8	87.5	28.8	4.9	2.1	1.4	0.6	1.6	2.9	11.0	32.8	25.5
55	44.7	70.0	22.6	10.7	1.4	1.7	1.1	1.6	1.6	11.0	25.6	28.5
45	22.3	28.1	10.7	6.8	0.6	1.5	0.7	1.5	0.3	4.0	10.6	17.7
35	5.6	4.5	2.2	0.4	-0.2	1.0	0.0	1.2	-0.1	0.5	2.2	6.2
25	0.4	0.4	0.3	0.5	-0.2	0.4	0.5	0.7	0.1	0.2	0.2	1.2
15	0.1	0.0	-0.3	0.6	0.0	0.5	0.5	0.0	0.1	1.0	-0.4	0.0
5	-0.1	-0.1	-0.1	0.5	0.0	0.3	0.1	0.0	-0.1	0.4	-0.4	0.0

TABLE 7. Monthly Values of $\left[\overline{vT}\right]$. Units: $^{o}K\ m\ sec^{-1}$.

5 mb

Lat.	Jan.	Feb.	Mar.	Apr.	May	June	July	Aug.	Sept.	Oct.	Nov.	Dec.
85	1.9	17.6	7.0	-1.8	0.8	0.0	0.0	-0.4	0.5	0.5	3.7	2.4
75	29.0	93.0	36.2	-8.7	2.9	0.2	0.1	-2.3	1.9	1.8	23.9	20.7
65	76.7	139.6	43.2	-8.9	1.1	0.2	0.2	-0.8	1.1	3.1	32.6	34.8
55	92.5	134.0	29.9	-4.2	0.0	0.2	0.7	0.3	0.3	4.1	23.9	21.6
45	68.4	70.9	16.3	-0.2	-0.1	0.1	0.8	0.3	0.3	3.1	11.8	6.7
35	29.5	20.9	6.1	0.6	-0.2	0.0	0.4	0.4	-0.3	2.1	5.4	-0.6
25	5.4	2.0	1.9	0.7	-0.2	0.0	0.3	0.1	-0.2	0.3	3.2	-0.2
15	0.4	-1.4	0.1	0.7	-0.3	-0.3	0.1	-0.1	-0.5	-1.1	3.1	-0.4
5	0.2	-0.4	-0.1	0.3	-0.2	-0.5	0.0	0.0	-0.6	-0.6	1.3	0.7

2 mb

Lat.	Jan.	Feb.	Mar.	Apr.	May	June	July	Aug.	Sept.	Oct.	Nov.	Dec.
85	0.1	27.6	6.4	-2.4	0.3	0.1	-0.2	-1.3	0.5	0.8	16.1	2.6
75	27.0	142.6	35.1	-7.4	1.4	0.1	-1.1	-7.8	3.0	4.9	77.3	28.4
65	131.8	194.5	45.0	0.2	1.9	0.0	-1.8	-8.6	3.4	5.6	82.7	45.6
55	180.0	174.7	35.3	5.9	0.7	0.3	-1.7	-2.6	2.9	3.4	60.0	31.1
45	109.6	101.5	22.6	5.6	-0.1	0.3	-0.3	-1.0	2.2	-0.2	25.7	15.3
35	44.8	31.2	9.2	2.3	1.2	-0.9	1.1	-0.6	0.7	-1.5	7.5	4.1
25	15.6	2.5	4.4	0.4	1.4	-2.1	0.8	0.9	0.1	-0.7	2.1	0.4
15	4.2	-1.4	2.4	1.5	0.7	-1.5	-0.5	2.9	-0.2	-0.3	-4.0	-0.6
5	-1.0	-0.6	0.6	1.6	-0.8	-0.6	-1.1	2.4	-0.4	-0.1	-2.5	0.0

TABLE 7 - Continued

100 mb

Lat.	Jan.	Feb.	Mar.	Apr.	May	June	July	Aug.	Sept.	Oct.	Nov.	Dec.
85	-0.5	-0.9	-0.6	-0.5	-0.1	-0.2	0.2	0.1	0.1	0.0	-0.6	0.5
75	0.5	-0.8	0.5	2.2	0.3	0.0	0.6	0.4	0.5	0.4	0.3	4.8
65	4.8	15.1	8.8	6.2	1.2	0.6	0.4	0.3	1.5	3.0	8.2	7.2
55	9.3	22.8	9.9	5.1	0.7	0.2	0.7	0.6	1.9	4.6	11.8	6.7
45	3.9	9.7	3.6	2.2	-0.3	-0.3	1.1	0.2	1.4	1.9	5.1	3.9
35	-1.5	-0.1	1.3	0.3	-0.8	0.5	0.3	-0.1	0.0	0.5	-1.1	-0.3
25	-1.1	-1.5	0.7	-0.3	-0.1	2.4	1.8	0.4	0.2	-0.3	-1.6	-2.9
15	-0.2	-0.7	1.0	-0.5	0.6	2.7	2.3	0.6	0.6	0.1	0.9	-2.1
5	0.0	-0.2	0.4	-0.3	0.0	0.8	0.6	0.2	0.3	-0.3	0.8	-0.7

10 mb

Lat.	Jan.	Feb.	Mar.	Apr.	May	June	July	Aug.	Sept.	Oct.	Nov.	Dec.
85	5.1	12.8	5.3	-0.8	0.3	0.1	0.0	0.1	0.1	0.1	4.7	1.6
75	35.5	63.6	21.9	-2.4	1.6	0.9	0.3	1.0	1.0	2.0	27.5	12.7
65	43.9	75.7	23.1	-0.6	1.6	1.2	0.2	1.3	1.7	6.2	33.8	23.9
55	28.0	55.7	18.0	2.4	0.9	1.5	0.5	1.0	1.0	6.3	22.3	24.4
45	13.2	19.2	8.0	2.2	0.1	1.2	0.3	0.7	0.2	2.2	6.8	14.6
35	3.3	3.0	1.1	-0.6	-0.4	0.6	-0.1	0.8	0.2	0.3	1.2	5.4
25	0.5	0.4	0.1	-0.3	-0.5	0.1	0.4	0.5	0.3	0.2	0.2	1.1
15	0.0	0.1	-0.1	0.0	-0.3	0.4	0.5	0.3	0.2	0.7	-0.1	0.1
5	0.0	0.0	0.0	0.0	-0.1	0.2	0.1	0.2	0.0	0.4	-0.1	0.0

TABLE 8. Zonally Averaged Spatial Covariances of $\bar{v}$ and $\bar{T}$, $\left[\bar{v}^*\bar{T}^*\right]$. Units: ^{o}K m sec^{-1}.

5 mb

Lat.	Jan.	Feb.	Mar.	Apr.	May	June	July	Aug.	Sept.	Oct.	Nov.	Dec.
85	4.8	16.9	3.5	-0.9	0.8	0.0	0.0	-0.2	0.0	0.0	5.6	1.9
75	38.2	98.0	22.6	-4.6	2.9	0.2	0.1	-1.9	-0.2	0.7	31.4	15.2
65	63.3	125.6	31.9	-5.5	1.1	0.2	0.2	-1.1	-0.4	2.2	34.9	27.1
55	50.8	88.0	23.6	-2.9	0.0	0.2	0.7	0.0	-0.5	2.3	21.3	18.6
45	27.1	37.2	12.9	-0.3	-0.1	0.1	0.8	0.5	-0.1	1.8	7.3	7.4
35	10.1	8.5	5.2	0.2	-0.2	0.0	0.4	0.6	-0.6	1.5	0.7	2.5
25	2.0	0.3	2.2	0.1	-0.2	0.0	0.3	0.1	-0.3	0.1	-0.2	1.1
15	-0.2	-0.7	0.3	0.2	-0.3	-0.3	0.1	-0.3	-0.2	-1.0	0.0	-1.1
5	0.3	-0.2	-0.2	0.1	-0.2	-0.5	0.0	-0.3	-0.3	-0.5	0.2	-1.3

2 mb

Lat.	Jan.	Feb.	Mar.	Apr.	May	June	July	Aug.	Sept.	Oct.	Nov.	Dec.
85	2.1	28.3	4.1	-0.7	0.3	0.1	-0.2	0.2	-0.1	0.3	17.6	1.0
75	39.0	145.0	23.6	-2.6	1.3	0.1	-1.1	-1.0	-0.5	1.3	81.5	15.4
65	117.5	170.8	29.3	-1.0	1.9	0.0	-1.8	-2.7	-0.6	1.4	75.5	35.4
55	123.7	131.6	20.5	0.9	0.7	0.3	-1.7	-1.2	-0.5	0.5	39.5	32.2
45	53.3	69.6	11.9	1.7	-0.1	0.3	-0.3	-0.9	-0.2	-1.0	8.1	15.1
35	12.8	22.7	4.2	1.2	1.2	-0.9	1.1	-0.6	-0.4	-1.1	0.1	3.7
25	2.6	4.9	1.6	0.0	1.4	-2.1	0.8	0.3	-0.7	-0.7	0.2	0.9
15	1.6	0.9	0.4	0.0	0.7	-1.5	-0.5	1.6	-0.9	-0.4	-2.2	-0.6
5	-0.4	-0.2	-0.1	0.4	-0.8	-0.6	-1.1	1.5	-0.5	0.0	-1.1	0.0

TABLE 8 - Continued

Lat.	Jan.	Feb.	Mar.	Apr.	May	June	July	Aug.	Sept.	Oct.	Nov.	Dec.
100 mb												
85	-0.2	-0.3	-0.2	-0.2	0.0	-0.1	0.1	0.0	0.0	0.0	-0.2	0.2
75	0.5	-0.8	0.6	2.3	0.3	0.0	0.6	0.4	0.5	0.5	0.4	5.0
65	8.3	26.2	15.3	10.7	2.1	1.0	0.7	0.5	2.6	5.1	14.2	12.4
55	21.8	53.7	23.2	11.9	1.7	0.6	1.6	1.3	4.4	10.8	27.8	15.7
45	11.3	28.1	10.6	6.5	-0.8	-0.8	3.3	0.7	4.2	5.6	14.6	11.3
35	-5.1	-0.5	4.5	1.1	-2.5	1.6	0.9	-0.4	0.0	1.6	-3.8	-1.2
25	-4.1	-5.5	2.6	-1.0	-0.4	8.9	6.6	1.5	0.6	-1.3	-5.9	-10.6
15	-0.8	-2.8	4.1	-1.9	2.3	10.5	9.2	2.2	2.5	0.6	3.7	-8.4
5	0.1	-1.0	1.6	-1.0	0.1	3.3	2.6	0.8	1.3	-1.2	3.1	-2.8
10 mb												
85	1.8	4.6	1.9	-0.3	0.1	0.0	0.0	0.0	0.0	0.0	1.7	0.6
75	37.7	67.5	23.2	-2.6	1.7	1.0	0.4	1.0	1.0	2.2	29.2	13.5
65	76.1	131.2	40.0	-1.1	2.8	2.1	0.4	2.2	3.0	10.7	58.6	41.5
55	66.0	131.1	42.3	5.7	2.2	3.4	1.1	2.4	2.4	14.8	52.4	57.3
45	38.2	55.9	23.2	6.5	0.4	3.4	1.0	1.9	0.6	6.2	19.8	42.4
35	11.2	10.0	3.8	-2.1	-1.2	1.9	-0.4	2.7	0.6	1.0	4.0	18.2
25	2.0	1.4	0.3	-0.9	-2.0	0.5	1.5	1.9	1.1	0.9	0.8	4.1
15	0.2	0.6	-0.5	-0.1	-1.3	1.6	2.1	1.2	0.8	3.0	-0.2	0.4
5	-0.1	0.1	-0.2	-0.1	-0.2	0.7	0.6	0.7	-0.1	1.5	-0.4	0.0

TABLE 9. Sensible Heat Transport by Standing Eddies, $C_p \iint \bar{v}^* \bar{T}^* a \cos\phi \, d\lambda \, \frac{dp}{g}$.

Units: 10^{17} ergs mb^{-1} sec^{-1}. (NOTE: 0.0 represents $<\pm 0.05 \times 10^{17}$).

5 mb

Lat.	Jan.	Feb.	Mar.	Apr.	May	June	July	Aug.	Sept.	Oct.	Nov.	Dec.
85	1.7	6.0	1.3	-0.3	0.3	0.0	0.0	-0.1	0.0	0.0	2.0	0.7
75	40.6	104.0	24.0	-4.9	3.1	0.2	0.2	-2.0	-0.2	0.8	33.4	16.2
65	109.8	217.8	55.3	-9.5	1.9	0.4	0.4	-2.0	-0.7	3.8	60.4	47.0
55	119.5	207.0	55.5	-6.7	0.1	0.5	1.7	0.1	-1.1	5.3	50.2	43.8
45	78.7	108.0	37.3	-0.8	-0.3	0.3	2.4	1.5	-0.4	5.2	21.3	21.6
35	34.0	28.5	17.4	0.6	-0.7	0.1	1.5	2.0	-2.1	5.1	2.3	8.3
25	7.5	1.2	8.3	0.3	-0.6	0.0	1.3	0.3	-1.3	0.6	-0.7	4.2
15	-0.8	-2.8	1.3	0.8	-1.2	-1.2	0.6	-1.0	-0.7	-3.8	0.2	-4.4
5	1.1	-1.0	-1.0	0.3	-0.8	-1.9	0.0	-1.3	-1.0	-2.1	0.7	-5.2

2 mb

Lat.	Jan.	Feb.	Mar.	Apr.	May	June	July	Aug.	Sept.	Oct.	Nov.	Dec.
85	0.8	10.1	1.5	-0.2	0.1	0.0	-0.1	0.1	0.0	0.1	6.3	0.3
75	41.4	153.9	25.1	-2.7	1.4	0.1	-1.2	-1.1	-0.5	1.4	86.5	16.4
65	203.6	296.0	50.7	-1.8	3.2	0.0	-3.1	-4.7	-1.1	2.4	130.8	61.4
55	290.9	309.7	48.3	2.1	1.6	0.8	-4.0	-2.8	-1.2	1.2	93.0	75.7
45	154.5	201.6	34.6	5.0	-0.4	0.8	-0.8	-2.6	-0.5	-3.0	23.4	43.7
35	43.0	76.4	14.0	4.0	4.0	-2.9	3.6	-1.9	-1.2	-3.7	0.2	12.6
25	9.8	18.2	6.1	0.0	5.2	-7.6	3.1	1.2	-2.5	-2.6	0.9	3.4
15	6.4	3.5	1.5	0.2	2.6	-5.8	-1.9	6.4	-3.7	-1.6	-8.7	-2.2
5	-1.4	-1.0	-0.3	1.6	-3.3	-2.6	-4.4	6.3	-2.0	-0.1	-4.4	0.1

TABLE 9 - Continued

100 mb

Lat.	Jan.	Feb.	Mar.	Apr.	May	June	July	Aug.	Sept.	Oct.	Nov.	Dec.
85	-1.9	-11.0	-1.4	-1.2	0.0	-0.2	0.8	0.2	-0.1	-0.3	-0.8	9.4
75	15.1	-33.3	13.1	25.6	0.2	0.0	4.9	4.1	1.4	11.5	4.6	208.3
65	214.9	642.2	326.3	94.5	4.3	0.3	1.9	3.1	16.4	86.8	268.6	327.6
55	459.6	774.0	365.0	91.4	7.8	1.4	4.1	7.0	40.4	127.7	469.8	295.2
45	167.1	352.9	105.5	51.4	-4.5	-3.8	16.1	4.3	34.9	54.0	196.1	165.8
35	-56.4	-5.7	42.1	7.9	-14.9	6.9	2.0	-0.6	0.2	11.1	-42.4	-14.3
25	-28.1	-41.7	16.4	-4.3	-1.6	2.9	-8.0	-1.7	0.7	-4.0	-32.0	-65.2
15	-1.9	-6.3	8.4	-3.7	4.2	-6.3	-7.4	-2.3	-0.2	0.6	5.5	-19.4

10 mb

Lat.	Jan.	Feb.	Mar.	Apr.	May	June	July	Aug.	Sept.	Oct.	Nov.	Dec.
85	15.5	34.1	5.4	0.2	-0.1	-0.1	0.0	0.0	0.0	0.1	5.1	2.7
75	273.5	416.7	65.6	2.4	-1.2	-1.1	-0.3	-0.3	0.9	5.6	85.1	61.7
65	384.4	530.7	76.2	0.9	-2.2	-2.3	-0.3	-0.9	1.7	19.4	127.6	149.4
55	176.8	244.8	33.4	-2.6	-1.2	-3.0	-0.9	-1.1	0.8	15.1	78.4	125.2
45	39.9	42.2	7.8	0.2	-0.1	-1.8	-0.6	-0.8	0.1	3.2	18.8	44.3
35	3.6	2.8	0.8	-0.5	0.0	-0.5	0.2	-1.2	0.0	0.2	2.0	9.3
25	0.2	0.2	0.0	-0.1	0.2	-0.1	-0.7	-0.8	-0.2	0.0	0.1	0.9
15	0.0	0.0	0.0	0.0	0.1	-0.3	-0.6	-0.3	0.0	-0.2	0.0	0.0

TABLE 10. Vertical Energy Flux, $\left[\overline{pw}\right]$. Units: ergs cm^{-2} sec^{-1}.

5 mb

Lat.	Jan.	Feb.	Mar.	Apr.	May	June	July	Aug.	Sept.	Oct.	Nov.	Dec.
85	3.2	10.2	0.2	0.0	-0.1	0.0	0.0	0.0	0.0	0.0	2.1	1.0
75	76.9	160.5	12.8	1.3	-0.9	-0.1	-0.1	0.3	-0.1	0.8	32.0	27.1
65	173.4	231.7	30.6	1.8	-0.4	-0.1	-0.1	0.2	-0.1	2.6	49.7	59.9
55	113.6	113.7	17.9	0.4	0.0	-0.1	-0.5	0.0	-0.2	2.2	29.7	37.7
45	32.6	21.2	6.7	0.0	0.0	0.0	-0.5	-0.2	0.0	1.2	7.9	9.8
35	3.9	2.0	2.6	0.0	0.0	0.0	-0.3	-0.3	0.0	0.5	0.5	1.8
25	0.1	0.1	0.4	0.0	0.0	0.0	-0.2	0.0	0.0	0.0	-0.1	0.4
15	0.0	0.0	0.0	0.0	0.0	0.0	0.0	0.0	0.0	-0.1	0.0	-0.2

2 mb

Lat.	Jan.	Feb.	Mar.	Apr.	May	June	July	Aug.	Sept.	Oct.	Nov.	Dec.
85	0.9	10.0	0.1	0.0	0.0	0.0	0.0	0.0	0.0	0.1	1.6	0.2
75	39.7	110.2	5.4	0.1	-0.2	0.0	0.5	0.2	-0.1	0.9	42.4	12.3
65	158.2	141.9	12.8	0.0	-0.5	0.0	1.0	1.0	-0.2	1.1	68.6	42.6
55	151.4	86.3	10.8	0.0	-0.2	-0.2	1.2	0.5	-0.2	0.4	39.5	45.2
45	46.9	34.7	7.3	0.2	0.0	-0.2	0.2	0.4	0.0	-0.7	7.6	17.5
35	6.1	7.2	2.3	0.2	-0.3	0.5	-0.8	0.2	0.0	-0.6	0.1	3.3
25	0.4	0.9	0.4	0.0	-0.4	1.1	-0.6	-0.1	0.0	-0.3	0.1	0.4
15	0.0	0.0	0.0	0.0	-0.2	0.4	0.1	-0.1	0.1	-0.1	-0.6	-0.1

TABLE 10 - Continued

100 mb

Lat.	Jan.	Feb.	Mar.	Apr.	May	June	July	Aug.	Sept.	Oct.	Nov.	Dec.
85	0.0	0.0	0.0	0.0	0.0	0.0	0.0	0.0	0.0	0.0	0.0	0.0
75	-172.5	586.8	31.1	59.2	0.4	0.0	-12.6	6.2	3.1	-8.6	50.6	-195.9
65	-210.3	667.4	115.1	51.8	5.9	0.2	-5.6	-8.0	9.4	-36.7	89.3	-16.9
55	-205.4	-19.0	216.0	0.7	9.4	-0.9	-11.5	-11.2	14.1	-150.2	291.7	-249.9
45	-473.1	-320.9	-1.5	27.0	38.0	11.7	-28.0	35.4	-17.3	-241.7	-189.0	-438.7
35	-556.4	-610.8	-106.3	-86.5	-0.4	-7.4	-44.1	-48.8	-148.1	-47.2	-557.7	-389.2
25	-64.8	-40.5	-81.6	-32.2	-80.3	-13.9	7.2	41.0	-49.4	-105.7	-183.8	-172.8
15	-27.1	51.6	-30.2	126.3	-5.0	24.2	-27.3	0.0	1.7	94.3	-7.4	-115.0
5	-47.7	16.8	82.3	70.8	8.5	-73.9	27.5	22.8	-7.5	-82.4	-91.8	-145.7

10 mb

Lat.	Jan.	Feb.	Mar.	Apr.	May	June	July	Aug.	Sept.	Oct.	Nov.	Dec.
85	0.0	0.0	0.0	0.0	0.0	0.0	0.0	0.0	0.0	0.0	0.0	0.0
75	-97.0	-32.2	-53.3	5.7	0.5	0.1	0.0	0.1	-1.1	5.9	-64.8	-69.6
65	-163.3	-195.9	-86.3	7.8	-0.6	-0.2	0.8	0.5	-2.4	-12.7	-152.2	-180.4
55	-303.1	-300.6	-95.9	10.1	-0.4	2.5	0.2	0.9	-1.6	-20.2	-135.4	-188.9
45	-90.8	-116.3	-29.0	-0.6	-0.1	1.4	-0.2	0.1	0.1	-14.3	-47.4	-54.7
35	-5.5	-24.4	-9.5	-3.9	0.3	2.5	-1.4	-3.7	0.3	0.1	-7.2	-16.2
25	4.9	4.3	1.1	-0.4	1.0	-0.2	-10.9	-14.2	-1.0	0.4	0.8	0.6
15	-3.8	2.6	0.9	-0.5	0.8	-2.3	-8.4	-17.9	-1.4	-1.5	0.5	-0.4
5	1.5	-3.8	-0.6	1.5	-0.5	-3.2	-2.8	23.6	-5.7	-26.9	1.7	0.6

TABLE 11. Horizontal Energy Flux, $\left[\overline{pv}\right]$. Units: 10^2 ergs cm^{-2} sec^{-1}.

(NOTE: 0.0 represents < $\pm 0.05 \times 10^2$)

5 mb

Lat.	Jan.	Feb.	Mar.	Apr.	May	June	July	Aug.	Sept.	Oct.	Nov.	Dec.
85	0.0	0.0	0.0	0.0	0.0	0.0	0.0	0.0	0.0	0.0	0.0	0.0
75	20.6	187.5	-11.3	1.7	2.6	1.0	3.0	0.6	0.2	4.3	-96.5	-88.8
65	-315.4	88.6	-100.7	0.9	-1.5	0.7	1.7	-0.4	0.2	2.5	-161.0	-220.6
55	-215.7	-58.4	-70.2	0.0	-1.9	0.3	2.0	-0.7	-0.1	-10.8	-110.2	-169.9
45	-45.1	-25.2	-30.2	0.3	-2.2	0.3	1.0	-0.4	0.8	1.9	-11.4	-87.1
35	-23.5	-9.6	-27.6	-0.8	0.6	0.3	7.7	0.4	0.0	-1.8	-3.7	-27.9
25	-1.1	-3.1	-5.5	1.5	-0.3	0.2	10.6	-0.7	-0.6	0.6	-0.3	-3.8
15	4.2	0.1	-0.5	1.7	-0.2	-0.4	55.3	-4.8	0.0	-0.5	1.9	-19.6
5	-9.1	0.8	0.8	0.5	0.7	-1.4	36.5	0.0	-4.4	0.2	12.5	-0.3

2 mb

Lat.	Jan.	Feb.	Mar.	Apr.	May	June	July	Aug.	Sept.	Oct.	Nov.	Dec.
85	0.0	0.0	0.0	0.0	0.0	0.0	0.0	0.0	0.0	0.0	0.0	0.0
75	1.6	25.1	-0.9	0.2	0.4	0.0	0.3	-0.2	0.0	-8.5	-62.6	-43.5
65	-216.9	-7.1	-9.5	0.0	-1.6	0.1	0.1	-2.0	0.3	-7.7	-145.0	-74.4
55	-199.5	-53.7	-17.8	-0.1	-0.2	0.3	0.1	-0.5	-0.6	-5.0	-101.5	-126.4
45	-115.0	-39.8	-14.7	0.0	-1.0	0.4	0.8	1.4	-0.2	0.8	-28.3	-94.2
35	-45.6	-20.9	-17.6	-0.3	0.0	-0.3	-1.3	1.1	0.0	-0.6	-9.7	-40.6
25	-11.0	-1.0	0.9	0.1	-3.1	-7.1	-2.3	-0.3	0.0	-1.7	-6.0	-6.4
15	0.1	0.0	-7.1	-0.3	-1.6	-11.4	0.7	-0.3	0.8	-0.3	-19.4	-11.3
5	-16.5	1.4	-9.5	0.3	-36.4	-31.8	0.0	-0.7	-0.4	0.3	-10.5	-1.9

TABLE 11 - Continued

Month	100 mb	10 mb	5 mb	2 mb
Jan.	207.3	226.9	238.2	255.8
Feb.	206.1	228.3	240.4	257.8
Mar.	207.1	229.6	241.5	261.7
Apr.	208.1	232.8	246.6	265.3
May	208.4	235.4	247.4	267.4
June	208.7	235.0	249.0	267.0
July	208.0	235.4	247.5	269.4
Aug.	207.5	233.5	245.6	263.2
Sept.	206.9	231.4	244.0	259.3
Oct.	205.8	227.8	239.7	255.7
Nov.	205.0	225.1	236.6	251.8
Dec.	205.6	224.4	236.5	252.9

TABLE 12. Mean Temperature Averaged Over an Isobaric Surface, $\tilde{\bar{T}}$. Units: ^{o}K.

100 mb

Lat.	Jan.	Feb.	Mar.	Apr.	May	June	July	Aug.	Sept.	Oct.	Nov.	Dec.
85	2.0	0.4	5.9	19.5	18.5	20.5	22.5	21.2	17.2	14.7	9.9	0.3
75	3.3	3.1	7.3	17.8	17.6	19.4	20.7	19.9	16.9	15.0	11.5	3.2
65	6.7	7.1	9.9	14.9	15.6	16.8	17.6	17.3	15.6	14.1	12.8	7.6
55	10.2	10.9	11.3	11.1	12.2	12.9	13.2	13.1	12.6	11.8	11.9	10.6
45	9.2	10.6	9.4	6.7	7.6	6.9	6.5	6.4	7.1	7.6	8.6	9.5
35	3.5	4.1	3.3	1.1	1.4	-0.7	-1.1	-1.3	-0.1	1.4	2.1	3.8
25	-3.6	-4.4	-4.6	-5.5	-5.9	-7.0	-6.8	-6.8	-6.3	-5.1	-5.1	-3.3
15	-8.0	-8.8	-9.3	-9.9	-10.7	-10.1	-10.1	-9.8	-9.7	-9.5	-9.5	-8.2
5	-9.6	-9.9	-10.9	-11.6	-12.2	-11.1	-11.7	-11.3	-11.1	-12.2	-11.6	-10.5

10 mb

Lat.	Jan.	Feb.	Mar.	Apr.	May	June	July	Aug.	Sept.	Oct.	Nov.	Dec.
85	-23.2	-14.5	-2.4	-0.3	1.7	7.1	8.8	5.2	-4.1	-13.6	-16.9	-21.1
75	-18.8	-11.6	-2.1	-1.0	1.5	6.4	8.0	4.9	-3.0	-11.5	-14.9	-17.9
65	-12.7	-7.9	-2.6	-2.5	0.9	4.8	5.9	4.0	-1.4	-8.1	-11.7	-12.9
55	-6.9	-4.7	-3.4	-3.6	-0.3	2.3	3.2	2.5	-0.4	-4.3	-7.5	-7.6
45	-1.4	-1.5	-2.8	-3.2	-1.1	-0.2	1.0	1.1	0.2	-1.0	-2.9	-2.9
35	2.4	1.1	-0.9	-1.3	-1.2	-1.7	-0.8	-0.5	0.5	1.1	1.1	1.2
25	4.1	2.4	0.8	0.8	-0.7	-2.1	-2.1	-1.7	0.4	2.2	3.7	4.2
15	4.9	3.0	1.8	2.0	-0.2	-2.1	-3.1	-2.5	-0.1	2.9	5.1	5.6
5	5.2	3.7	2.4	2.4	0.1	-1.9	-4.0	-3.0	-0.6	3.4	5.8	6.4

TABLE 13. Deviation of the Area Average From the Zonal Average of the Mean Temperature, $[\bar{T}]''$.

Units: ^{o}K.

5 mb

Lat.	Jan.	Feb.	Mar.	Apr.	May	June	July	Aug.	Sept.	Oct.	Nov.	Dec.
85	-16.6	5.2	-5.4	-5.7	3.2	6.0	12.3	8.8	-6.3	-17.2	-21.9	-24.6
75	-14.5	1.0	-7.5	-5.0	2.4	5.5	11.0	7.2	-5.6	-15.4	-20.3	-23.1
65	-10.5	-3.3	-9.1	-3.7	2.2	4.7	8.8	4.7	-4.3	-12.2	-16.8	-19.7
55	-5.8	-4.6	-7.6	-2.0	2.2	3.4	6.0	1.9	-3.2	-8.4	-11.7	-13.3
45	-2.0	-3.5	-3.7	-0.5	1.8	1.7	3.0	-0.5	-1.9	-4.5	-5.9	-4.5
35	0.9	-1.6	0.5	0.4	0.7	-0.3	-0.3	-2.0	-0.4	-0.7	0.0	3.2
25	3.1	0.6	3.2	0.9	-0.9	-1.9	-3.3	-2.5	1.0	3.1	5.0	7.2
15	4.5	2.1	4.1	1.0	-2.4	-3.2	-5.5	-2.1	2.0	6.5	8.7	8.4
5	4.8	2.9	4.2	1.0	-3.6	-3.9	-6.5	-1.2	2.7	8.4	10.5	8.3

2 mb

Lat.	Jan.	Feb.	Mar.	Apr.	May	June	July	Aug.	Sept.	Oct.	Nov.	Dec.
85	-4.7	-1.8	-15.4	-10.6	4.6	10.3	10.3	7.4	-8.9	-24.8	-24.8	-25.5
75	-6.1	-3.5	-15.3	-8.8	3.9	9.8	9.8	6.6	-7.4	-21.3	-23.8	-24.4
65	-8.8	-6.6	-14.1	-5.3	3.0	7.3	8.7	4.5	-5.3	-15.7	-20.8	-21.1
55	-10.2	-8.8	-10.7	-2.1	1.9	4.2	6.8	1.8	-3.6	-10.2	-15.0	-14.6
45	-7.0	-6.3	-4.9	0.1	0.8	1.8	4.0	-0.3	-1.9	-4.5	-6.8	-5.7
35	-1.1	-0.7	1.0	1.2	-0.1	-0.4	0.6	-1.6	-0.2	0.8	1.2	2.9
25	3.7	3.2	4.9	1.3	-0.9	-2.5	-3.1	-2.1	1.3	5.0	6.7	7.9
15	6.1	4.6	6.6	1.3	-2.2	-4.2	-6.3	-2.1	2.4	7.6	10.1	9.4
5	6.4	4.7	7.4	1.2	-3.3	-5.4	-7.5	-1.8	3.1	9.0	12.0	9.5

TABLE 13 - Continued

100 mb

Lat.	Jan.	Feb.	Mar.	Apr.	May	June	July	Aug.	Sept.	Oct.	Nov.	Dec.
85	7.8	3.7	7.0	2.7	2.7	2.3	3.3	2.1	4.5	3.4	4.9	6.7
75	4.8	7.3	7.5	2.7	2.6	2.4	2.8	3.4	3.7	4.2	4.4	5.4
65	5.7	6.8	7.2	3.4	3.0	2.6	3.4	3.9	4.8	3.9	4.1	7.5
55	6.9	6.6	7.9	3.0	3.3	3.2	2.6	4.2	3.7	5.5	5.0	7.3
45	5.0	6.1	7.7	5.5	4.3	2.8	4.9	5.3	4.9	6.2	5.5	7.8
35	5.3	5.3	4.8	5.3	4.9	4.3	4.7	4.7	5.1	5.8	6.6	6.8
25	4.5	6.0	5.4	5.4	4.0	4.3	3.7	3.8	4.6	5.7	6.7	6.6
15	6.0	5.4	5.1	7.5	5.2	7.3	6.0	4.7	5.8	5.0	5.4	7.8

10 mb

Lat.	Jan.	Feb.	Mar.	Apr.	May	June	July	Aug.	Sept.	Oct.	Nov.	Dec.
85	7.7	14.7	15.4	3.0	2.2	1.2	0.8	1.4	2.3	4.8	7.3	4.6
75	10.9	17.3	19.5	4.2	1.6	1.7	2.4	1.9	2.9	3.9	5.5	5.3
65	9.9	15.7	15.7	3.5	2.1	1.3	2.4	2.7	4.2	4.0	4.1	6.1
55	9.3	14.3	9.8	5.3	2.6	1.8	2.0	3.8	4.2	4.0	7.2	6.9
45	12.2	16.1	9.5	6.5	2.4	2.4	2.2	3.6	4.2	4.4	9.2	6.4
35	11.3	11.2	7.2	6.8	4.4	3.2	2.2	3.4	5.5	4.3	7.6	5.6
25	7.1	7.8	4.0	6.7	5.0	4.0	3.2	4.2	6.4	4.4	4.2	4.1
15	3.9	4.6	3.8	5.6	5.5	6.7	5.7	7.1	11.3	5.7	4.7	1.8

TABLE 14. Zonally Averaged Time Standard Deviations of u, $\left[\sqrt{\overline{u'^2}}\right]$. Units: m sec^{-1}.

5 mb

Lat.	Jan.	Feb.	Mar.	Apr.	May	June	July	Aug.	Sept.	Oct.	Nov.	Dec.
85	11.8	17.4	15.4	2.6	0.0	0.0	0.0	1.2	4.1	5.9	10.2	7.2
75	13.8	26.3	23.1	3.8	0.0	0.0	0.0	3.3	3.4	4.6	6.8	8.8
65	13.8	22.1	19.2	3.7	0.0	0.0	0.0	3.6	3.9	3.8	7.9	7.6
55	15.6	17.0	14.3	3.6	0.0	0.0	0.0	3.9	4.2	3.9	8.9	10.9
45	15.4	20.9	11.3	5.4	0.0	0.0	0.0	3.3	6.8	6.5	10.4	10.9
35	14.8	17.5	10.7	6.3	0.0	0.0	0.0	4.7	6.7	7.0	8.5	11.5
25	15.7	11.5	11.0	3.9	0.0	0.0	0.0	3.4	8.0	7.3	12.2	10.8
15	9.3	4.5	8.4	5.0	0.0	0.0	0.0	4.6	4.6	7.4	12.2	10.6

2 mb

Lat.	Jan.	Feb.	Mar.	Apr.	May	June	July	Aug.	Sept.	Oct.	Nov.	Dec.
85	13.6	17.7	11.2	6.1	0.0	0.0	0.0	2.8	5.0	7.4	12.5	11.0
75	17.3	25.4	18.0	4.5	0.0	0.0	0.0	3.8	6.2	6.0	6.8	10.7
65	16.1	25.0	13.9	3.2	0.0	0.0	0.0	6.0	5.4	6.4	8.9	7.7
55	16.8	21.1	12.3	4.0	0.0	0.0	0.0	7.5	6.2	6.6	9.2	13.1
45	19.1	17.9	10.6	6.1	0.0	0.0	0.0	7.8	9.3	7.1	10.8	15.8
35	20.4	18.0	11.7	8.6	0.0	0.0	0.0	8.1	12.2	6.8	9.9	14.9
25	24.2	15.1	10.3	7.1	0.0	0.0	0.0	4.2	12.0	8.2	16.0	11.6
15	19.3	11.8	12.9	6.8	0.0	0.0	0.0	0.7	8.9	12.8	20.4	10.7

TABLE 14 - Continued

100 mb

Lat.	Jan.	Feb.	Mar.	Apr.	May	June	July	Aug.	Sept.	Oct.	Nov.	Dec.
85	4.4	3.4	4.4	2.4	1.9	1.6	2.3	1.8	2.9	2.5	3.2	4.4
75	7.7	7.3	9.2	4.1	3.2	2.5	3.6	3.5	4.3	4.7	5.5	7.0
65	6.9	7.5	9.7	4.3	3.6	2.4	3.7	4.7	4.3	6.1	5.9	7.0
55	5.9	5.7	7.5	5.0	4.3	3.2	4.5	5.6	4.9	6.3	6.2	8.2
45	5.2	4.4	5.3	4.9	4.3	3.7	4.8	5.6	4.2	6.6	6.7	8.1
35	4.9	5.1	5.9	5.5	3.9	3.2	4.1	4.4	4.0	6.2	6.3	6.8
25	4.8	4.6	5.4	5.5	4.0	3.9	3.6	3.9	3.7	5.6	5.3	6.2
15	4.2	3.7	4.2	4.7	4.2	4.7	3.9	3.9	2.9	5.8	4.4	4.9

10 mb

Lat.	Jan.	Feb.	Mar.	Apr.	May	June	July	Aug.	Sept.	Oct.	Nov.	Dec.
85	6.4	9.8	7.6	2.0	1.6	0.7	0.9	1.5	1.7	2.8	4.6	2.9
75	14.9	21.2	14.2	3.9	2.1	1.4	1.7	2.3	2.7	5.0	8.2	6.0
65	17.5	23.0	12.2	4.7	1.5	1.7	1.9	2.0	2.5	5.1	7.8	7.1
55	14.8	18.3	8.4	4.5	1.6	1.7	1.8	1.8	2.4	4.6	6.6	7.0
45	9.5	10.9	4.7	3.8	1.8	2.1	2.1	2.0	2.2	3.4	5.0	5.4
35	5.2	5.5	2.9	3.6	1.9	2.1	3.0	2.3	2.5	2.5	3.0	3.2
25	2.9	2.9	2.3	4.0	2.1	2.9	3.9	3.2	2.6	2.3	2.2	1.6
15	2.7	2.5	2.9	4.6	2.3	3.4	4.0	4.9	3.3	3.1	2.7	1.6

TABLE 15. Zonally Averaged Time Standard Deviations of v, $\left[\sqrt{\overline{v'^2}}\right]$. Units: m sec^{-1}.

5 mb

Lat.	Jan.	Feb.	Mar.	Apr.	May	June	July	Aug.	Sept.	Oct.	Nov.	Dec.
85	7.4	12.2	8.0	2.0	0.0	0.0	0.0	0.8	2.3	3.5	6.4	4.3
75	14.0	25.4	14.9	3.3	0.0	0.0	0.0	2.3	3.7	6.2	10.6	8.8
65	15.6	27.2	12.6	3.4	0.0	0.0	0.0	3.0	3.1	5.9	10.0	10.2
55	15.2	22.5	8.0	3.4	0.0	0.0	0.0	2.9	2.9	5.2	9.3	9.0
45	12.6	14.4	5.1	2.9	0.0	0.0	0.0	2.3	2.7	4.0	7.9	7.2
35	9.5	7.4	4.1	2.8	0.0	0.0	0.0	1.5	2.9	2.7	6.4	5.3
25	7.2	2.9	4.2	3.7	0.0	0.0	0.0	1.4	2.9	2.5	5.3	5.0
15	7.4	2.3	5.0	5.1	0.0	0.0	0.0	1.8	3.6	3.3	6.2	8.8

2 mb

85	9.4	11.8	6.5	3.5	0.0	0.0	0.0	2.6	2.9	4.2	7.2	5.9
75	17.6	22.9	11.8	6.0	0.0	0.0	0.0	4.5	5.0	7.5	11.9	11.5
65	17.8	24.2	10.2	4.7	0.0	0.0	0.0	3.6	4.2	6.6	10.3	11.7
55	17.1	20.2	7.6	3.4	0.0	0.0	0.0	3.3	3.7	5.3	9.9	9.7
45	14.7	13.7	6.3	2.3	0.0	0.0	0.0	3.0	3.8	4.3	8.6	7.0
35	10.6	8.4	4.9	1.8	0.0	0.0	0.0	2.1	4.1	3.7	7.7	6.3
25	8.1	5.9	5.4	2.5	0.0	0.0	0.0	1.3	3.8	3.1	6.8	5.6
15	9.5	5.0	7.6	3.7	0.0	0.0	0.0	1.4	4.3	2.2	7.8	5.7

TABLE 15 - Continued

100 mb

Lat.	Jan.	Feb.	Mar.	Apr.	May	June	July	Aug.	Sept.	Oct.	Nov.	Dec.
85	11.0	2.6	6.9	0.8	1.4	0.6	1.4	0.5	1.0	1.8	2.6	2.0
75	9.0	4.1	5.3	2.2	1.7	0.8	0.9	0.8	1.2	1.9	2.6	2.3
65	5.2	4.7	4.0	2.6	1.4	1.0	0.9	1.5	1.3	1.9	2.6	2.8
55	3.2	4.2	3.0	2.2	1.4	1.1	1.7	2.0	1.5	1.8	2.3	2.4
45	2.3	2.5	2.1	1.8	1.5	1.5	1.7	1.8	1.6	1.7	1.8	2.0
35	2.4	1.7	1.9	1.7	1.4	1.6	1.4	1.5	1.6	1.6	1.8	1.8
25	2.4	1.5	1.3	1.2	1.1	1.6	1.2	1.2	1.2	1.1	1.4	1.6
15	2.0	0.8	1.0	0.7	0.8	1.5	1.0	1.2	0.9	1.2	1.2	1.3
5	1.9	0.3	0.6	0.3	0.4	1.3	0.7	1.1	0.8	1.4	1.1	0.9

10 mb

Lat.	Jan.	Feb.	Mar.	Apr.	May	June	July	Aug.	Sept.	Oct.	Nov.	Dec.
85	2.9	10.7	4.0	1.7	2.8	2.7	1.6	3.0	6.4	3.6	1.6	3.1
75	3.9	9.3	2.6	2.3	2.7	2.1	1.4	2.6	5.0	3.7	2.8	2.8
65	6.2	8.2	2.8	2.7	2.6	2.0	1.2	1.9	3.4	3.4	3.7	2.9
55	7.4	6.6	2.7	3.0	2.4	2.2	1.0	1.3	2.3	2.8	3.5	3.0
45	5.9	4.4	2.4	2.8	1.9	2.3	1.0	1.1	1.6	2.2	2.6	2.6
35	3.7	2.6	2.0	2.0	1.4	2.2	1.0	1.0	1.1	1.6	1.7	1.7
25	2.8	2.0	2.0	1.4	1.0	1.9	1.0	1.0	0.8	1.0	0.9	0.8
15	2.5	1.9	2.1	1.4	0.5	1.7	1.0	0.9	0.5	0.6	0.6	0.2
5	2.2	1.9	2.0	1.4	0.3	1.9	0.6	0.5	0.5	0.5	0.4	0.2

TABLE 16. Zonally Averaged Time Standard Deviations of T, $\left[\sqrt{\overline{T'^2}}\right]$. Units: °K.

5 mb

Lat.	Jan.	Feb.	Mar.	Apr.	May	June	July	Aug.	Sept.	Oct.	Nov.	Dec.
85	3.4	23.2	7.8	2.3	0.0	0.0	0.0	7.2	4.4	3.5	4.2	5.0
75	6.0	16.7	6.1	3.8	0.0	0.0	0.0	5.6	4.0	3.8	4.0	4.5
65	7.7	9.9	4.7	4.7	0.0	0.0	0.0	3.4	3.2	3.3	3.6	4.5
55	7.4	6.9	3.7	4.3	0.0	0.0	0.0	1.6	2.5	2.7	3.8	4.6
45	6.4	5.3	2.3	3.2	0.0	0.0	0.0	0.7	2.0	2.2	3.9	4.1
35	4.4	3.5	2.5	2.2	0.0	0.0	0.0	0.5	1.5	1.7	3.4	3.5
25	2.8	1.7	2.6	1.7	0.0	0.0	0.0	0.8	1.5	1.4	2.7	2.6
15	3.2	1.7	2.5	1.7	0.0	0.0	0.0	1.6	1.3	1.5	2.9	2.0
5	4.0	2.2	3.1	2.0	0.0	0.0	0.0	2.8	1.1	1.8	3.3	2.0

2 mb

85	5.7	10.3	3.2	6.3	0.0	0.0	0.0	6.4	8.2	4.7	3.9	3.8
75	4.9	10.6	4.8	6.2	0.0	0.0	0.0	5.8	7.0	4.4	3.9	5.5
65	6.4	9.3	6.5	5.7	0.0	0.0	0.0	4.2	5.3	3.8	4.3	7.0
55	8.7	7.6	6.3	4.5	0.0	0.0	0.0	2.6	3.9	3.2	4.9	7.5
45	8.1	6.1	4.7	3.3	0.0	0.0	0.0	1.5	2.9	2.4	4.9	7.5
35	5.8	4.4	3.7	2.4	0.0	0.0	0.0	1.4	2.3	1.8	4.0	6.1
25	4.1	3.0	3.2	2.1	0.0	0.0	0.0	2.5	2.2	1.2	2.8	3.9
15	3.1	2.1	2.7	2.4	0.0	0.0	0.0	3.6	2.2	0.7	2.2	2.6
5	3.1	1.9	2.8	2.7	0.0	0.0	0.0	4.2	2.1	0.4	1.8	2.4

TABLE 16 - Continued

100 mb

Lat.	Jan.	Feb.	Mar.	Apr.	May	June	July	Aug.	Sept.	Oct.	Nov.	Dec.
85	7.8	6.2	5.9	5.6	1.4	3.2	1.9	1.6	2.2	2.1	2.0	5.3
75	7.3	8.5	5.8	2.7	1.5	1.6	2.3	2.4	2.4	2.6	5.7	6.1
65	5.9	5.5	2.6	2.8	1.8	2.1	1.8	1.3	1.7	3.2	3.1	3.2
55	7.5	7.1	7.0	3.4	3.0	3.1	2.8	2.8	3.7	4.1	4.7	7.4
45	9.4	11.0	6.6	5.3	3.4	4.3	5.7	5.7	4.5	7.7	6.1	8.9
35	8.6	8.8	6.2	5.6	3.9	5.7	5.5	4.6	6.3	8.0	11.2	9.5
25	6.2	5.7	4.6	3.7	3.9	4.5	8.2	6.4	5.7	7.6	5.4	5.6
15	6.0	4.9	5.1	5.4	7.5	11.7	9.2	6.6	6.7	6.2	4.6	6.7

10 mb

Lat.	Jan.	Feb.	Mar.	Apr.	May	June	July	Aug.	Sept.	Oct.	Nov.	Dec.
85	14.4	19.7	15.1	2.6	1.2	0.7	0.6	1.3	1.4	4.0	18.2	6.9
75	19.5	15.9	9.9	4.2	1.0	1.0	1.1	0.9	1.8	3.6	10.7	7.4
65	4.7	6.8	6.4	2.6	0.7	1.3	1.2	1.1	1.7	3.7	4.3	5.8
55	16.2	13.6	9.8	4.5	1.1	1.3	0.8	1.1	2.1	5.0	13.7	6.3
45	18.3	17.8	10.7	4.8	1.9	1.8	1.8	1.9	2.0	5.4	13.9	8.8
35	13.6	14.0	7.3	4.0	1.5	3.3	3.4	3.1	2.0	4.3	8.5	10.1
25	7.7	8.1	4.7	4.0	2.5	2.5	3.4	4.9	3.8	5.0	3.8	7.1
15	4.1	3.4	3.0	3.3	2.9	4.4	6.7	4.2	3.2	3.6	2.1	2.2

TABLE 17. Spatial Standard Deviations of $\bar{u}$, $\sqrt{\left[\bar{u}^{*2}\right]}$. Units: m sec^{-1}.

5 mb

Lat.	Jan.	Feb.	Mar.	Apr.	May	June	July	Aug.	Sept.	Oct.	Nov.	Dec.
85	15.7	22.9	9.1	2.0	4.6	2.3	2.8	3.0	2.0	3.5	24.0	6.9
75	20.5	17.2	9.3	3.4	2.4	1.9	2.7	1.9	2.2	4.1	12.3	11.9
65	12.9	8.8	8.0	1.5	4.2	1.9	2.0	2.2	1.0	2.8	8.5	7.8
55	16.4	17.0	11.1	3.1	3.8	0.8	1.5	1.4	2.2	3.0	15.4	8.4
45	24.2	16.7	9.0	2.3	2.9	2.3	3.2	1.6	3.4	4.4	17.2	13.6
35	19.4	14.0	10.2	2.0	4.0	1.4	3.4	3.1	2.0	4.8	11.5	15.1
25	12.2	10.2	6.1	2.4	1.8	1.6	5.0	3.6	3.0	4.3	3.2	9.7
15	7.0	2.0	5.6	4.7	2.0	5.4	11.1	3.8	2.0	3.0	5.8	7.4

2 mb

Lat.	Jan.	Feb.	Mar.	Apr.	May	June	July	Aug.	Sept.	Oct.	Nov.	Dec.
85	28.5	29.9	5.7	5.8	5.5	0.5	1.2	4.9	1.4	3.9	25.8	4.5
75	26.1	16.7	5.8	2.3	3.8	0.5	2.6	2.5	2.2	4.5	13.1	11.6
65	8.9	8.6	4.8	1.5	2.6	0.8	1.7	2.0	1.2	3.1	11.8	9.9
55	23.9	17.6	7.8	2.9	2.4	1.8	1.9	2.3	1.6	3.5	17.6	7.9
45	30.8	19.5	4.8	1.8	2.4	2.4	3.9	3.8	2.7	4.8	18.9	17.9
35	24.7	20.9	10.1	4.0	2.3	4.3	3.6	3.6	2.6	5.5	14.3	18.6
25	15.0	13.8	5.6	4.0	3.9	5.7	6.4	3.3	1.8	3.6	5.9	7.1
15	9.5	5.6	9.6	5.1	6.2	11.6	9.3	2.2	3.4	6.5	10.6	12.3

TABLE 17 - Continued

100 mb

Lat.	Jan.	Feb.	Mar.	Apr.	May	June	July	Aug.	Sept.	Oct.	Nov.	Dec.
85	5.6	6.0	4.8	3.2	1.4	2.2	1.6	1.4	1.8	2.3	2.2	5.2
75	11.6	13.2	10.2	5.3	2.9	4.0	2.6	2.9	3.3	4.4	4.4	10.9
65	12.0	14.7	9.8	3.9	2.8	3.2	3.1	3.4	3.2	5.2	5.5	10.6
55	9.2	12.0	6.6	3.7	3.0	3.1	3.7	3.5	3.0	5.2	5.5	8.1
45	5.6	6.7	4.2	3.9	3.3	3.0	4.4	3.7	3.4	5.0	5.4	5.5
35	3.8	3.8	3.6	3.4	3.4	3.3	4.4	3.3	3.5	5.3	4.9	4.6
25	3.3	3.6	3.7	4.1	3.8	4.7	4.2	3.1	3.9	4.4	4.3	4.9
15	3.5	3.2	3.3	4.7	4.2	4.9	3.6	3.2	3.7	6.2	4.7	4.7

10 mb

Lat.	Jan.	Feb.	Mar.	Apr.	May	June	July	Aug.	Sept.	Oct.	Nov.	Dec.
85	9.8	12.0	9.4	1.8	1.2	0.6	0.7	1.1	1.4	2.8	9.5	4.1
75	23.0	25.0	18.6	3.4	2.1	1.3	1.2	1.9	2.6	5.8	17.6	8.9
65	24.5	24.6	16.7	3.9	1.9	1.8	1.3	1.7	2.7	6.2	14.1	9.6
55	16.8	18.9	11.8	3.3	1.6	1.8	1.5	1.4	2.0	5.0	9.2	8.4
45	8.6	11.4	6.9	3.2	1.7	2.0	2.3	1.7	1.6	3.0	4.8	6.0
35	4.8	5.5	3.8	3.3	2.6	2.4	3.4	2.8	2.2	2.0	2.5	3.7
25	3.4	3.0	2.5	3.0	2.9	3.3	4.3	4.2	2.3	2.0	1.6	2.0
15	4.0	2.8	2.5	3.7	2.9	3.2	5.0	5.9	2.6	3.3	1.8	1.6

TABLE 18. Spatial Standard Deviations of $\bar{v}$, $\sqrt{[\bar{v}^{*2}]}$. Units: m sec^{-1}.

5 mb

Lat.	Jan.	Feb.	Mar.	Apr.	May	June	July	Aug.	Sept.	Oct.	Nov.	Dec.
85	9.3	12.6	6.6	1.5	3.3	2.9	2.2	2.0	1.5	2.8	12.6	4.8
75	21.0	24.7	13.8	2.5	4.8	3.1	3.3	3.1	2.9	5.9	22.3	11.2
65	23.5	23.6	12.4	2.4	2.8	1.3	3.3	2.8	2.8	6.4	16.2	12.9
55	19.0	18.3	8.3	1.6	2.0	1.3	3.1	2.5	2.3	5.6	10.0	10.5
45	11.2	11.7	5.3	1.8	2.5	0.9	2.9	2.3	2.1	4.2	5.1	6.9
35	6.4	6.0	3.3	2.7	2.1	0.7	3.1	2.0	2.7	2.5	2.0	3.8
25	5.3	2.2	3.0	3.6	1.3	0.9	4.5	2.1	2.8	1.7	2.0	4.7
15	5.3	2.3	3.9	4.2	2.1	2.1	6.8	3.7	3.3	2.6	4.3	8.3

2 mb

Lat.	Jan.	Feb.	Mar.	Apr.	May	June	July	Aug.	Sept.	Oct.	Nov.	Dec.
85	15.2	15.9	3.2	3.6	3.4	0.8	1.4	3.7	1.6	3.2	13.4	4.1
75	30.2	29.0	6.5	5.8	6.0	1.0	2.9	6.2	2.7	5.7	23.8	9.6
65	28.2	24.5	6.3	4.3	4.8	0.9	3.1	5.3	3.0	6.3	17.1	12.1
55	21.4	19.7	5.1	2.9	3.7	1.2	3.1	4.4	2.8	5.6	10.8	10.7
45	14.0	14.8	4.8	2.0	3.5	2.0	2.9	3.3	2.3	4.2	5.9	7.7
35	8.1	10.0	5.0	1.3	3.5	3.2	3.7	2.7	2.3	2.8	3.2	5.9
25	5.1	5.7	6.0	1.7	4.0	6.0	4.3	2.3	2.5	2.3	3.3	5.6
15	5.9	4.8	8.2	2.3	6.2	10.1	3.1	2.9	3.3	1.7	5.3	5.9

TABLE 18 - Continued

100 mb

Lat.	Jan.	Feb.	Mar.	Apr.	May	June	July	Aug.	Sept.	Oct.	Nov.	Dec.
85	0.5	1.3	1.7	0.6	0.2	0.3	0.3	0.2	0.2	0.2	1.1	0.2
75	1.7	3.5	4.0	1.6	0.5	1.0	0.4	0.7	0.4	0.5	2.9	1.1
65	3.1	4.9	4.3	2.4	0.9	1.3	1.1	1.1	1.0	1.6	3.7	2.3
55	3.0	4.1	3.1	2.7	1.2	1.2	1.3	1.2	1.6	2.4	3.6	2.7
45	1.8	2.7	2.1	2.0	1.0	1.3	1.6	1.5	1.8	1.8	2.6	2.4
35	1.8	1.5	1.2	1.3	1.4	2.1	2.6	2.1	1.7	1.7	0.8	1.5
25	1.9	1.4	1.4	1.5	1.8	2.5	3.1	2.3	2.0	2.3	2.0	2.3
15	1.6	1.3	1.3	1.1	1.1	1.6	2.2	1.5	1.6	2.1	2.1	2.5
5	0.8	0.7	0.6	0.4	0.5	1.1	1.2	0.8	1.2	1.3	1.3	2.0

10 mb

Lat.	Jan.	Feb.	Mar.	Apr.	May	June	July	Aug.	Sept.	Oct.	Nov.	Dec.
85	2.9	2.0	0.9	0.9	0.5	0.4	0.4	0.4	0.4	0.3	1.8	0.7
75	8.6	5.4	1.6	1.5	1.3	1.5	1.5	1.1	1.1	1.0	4.6	2.3
65	11.1	7.1	2.1	1.2	1.5	2.1	2.1	1.2	1.2	1.6	5.7	4.2
55	8.7	6.3	2.3	2.0	1.2	1.9	1.8	1.3	1.0	1.9	5.1	5.5
45	4.8	3.7	1.9	1.9	1.1	1.9	1.5	1.2	0.8	1.6	3.2	5.0
35	2.0	1.5	1.2	1.1	1.2	1.6	1.4	1.1	0.6	0.9	1.6	3.0
25	0.8	0.8	0.6	0.8	1.0	1.1	1.2	1.0	0.5	0.5	0.7	1.2
15	0.4	0.4	0.5	0.7	0.8	1.0	0.8	0.7	0.5	0.4	0.2	0.4
5	0.2	0.3	0.2	0.5	0.5	0.9	0.5	0.4	0.4	0.3	0.1	0.3

TABLE 19. Spatial Standard Deviations of $\bar{T}$, $\sqrt{[\bar{T}^{*2}]}$. Units: ^{o}K.

5 mb

Lat.	Jan.	Feb.	Mar.	Apr.	May	June	July	Aug.	Sept.	Oct.	Nov.	Dec.
85	3.2	2.2	1.4	0.9	0.5	0.1	0.1	0.8	0.2	0.2	1.0	0.5
75	8.7	6.4	3.6	2.2	1.0	0.3	0.4	1.6	0.5	0.7	2.5	1.7
65	10.7	8.2	4.5	2.9	0.7	0.4	0.7	1.5	1.0	1.3	3.2	3.2
55	8.5	7.1	4.2	3.2	0.3	0.6	1.0	1.3	1.6	1.9	3.0	3.6
45	4.8	4.7	3.2	2.7	0.2	0.5	1.5	1.2	1.9	2.3	2.0	3.1
35	2.7	2.4	2.1	1.8	0.3	0.3	1.7	0.9	1.8	2.0	1.4	2.4
25	2.1	1.5	1.6	1.1	0.5	0.5	1.7	0.7	1.6	1.4	1.4	1.9
15	1.3	1.0	1.3	0.7	0.8	0.8	1.4	0.9	1.6	1.0	1.1	1.4
5	0.8	0.7	1.1	0.6	1.1	0.6	0.9	1.1	1.7	1.0	0.9	1.0

2 mb

Lat.	Jan.	Feb.	Mar.	Apr.	May	June	July	Aug.	Sept.	Oct.	Nov.	Dec.
85	3.2	2.6	1.5	1.1	0.4	1.0	0.4	0.9	0.3	0.4	1.4	1.0
75	8.0	7.1	4.2	2.6	0.7	2.8	1.2	2.0	0.7	1.0	3.6	3.0
65	9.8	9.5	5.8	2.6	0.6	4.0	2.0	2.3	0.9	1.2	4.9	4.3
55	9.8	8.9	5.7	1.8	1.3	3.9	2.3	1.9	0.8	1.3	4.6	3.9
45	7.8	6.1	4.1	1.6	2.0	3.0	2.6	1.2	0.7	1.5	2.2	2.2
35	5.2	3.5	2.1	1.6	1.9	2.1	3.0	0.7	0.7	1.5	1.2	2.1
25	2.9	2.0	1.0	0.8	1.2	1.6	3.4	0.8	0.6	1.1	1.6	2.3
15	1.5	1.1	0.4	0.8	0.6	1.1	4.0	1.2	0.7	0.6	1.6	1.3
5	0.9	0.6	0.3	1.2	0.9	0.8	4.8	1.7	0.8	0.2	1.3	0.7

TABLE 19 - Continued

Month	100 mb	10 mb	5 mb	2 mb	100-10	10-5	5-2	10-2
Jan.	179.4	163.2	82.3	90.2	-16.2	-80.9	7.9	-73.0
Feb.	403.6	225.4	98.7	75.8	-178.2	-126.7	-22.9	-149.6
Mar.	215.1	33.2	15.0	9.1	-181.9	-18.2	-5.9	-24.1
Apr.	59.6	-0.4	0.6	0.2	-60.0	1.0	-0.4	0.6
May	-2.8	-0.8	-0.1	-0.5	2.0	0.7	-0.4	0.3
June	-0.2	-2.3	-0.1	0.7	-2.1	2.2	0.8	3.0
July	1.1	-1.0	-0.5	0.2	-2.1	0.5	0.7	1.2
Aug.	2.2	-1.6	-0.1	0.5	-3.8	1.5	0.6	2.1
Sept.	24.8	0.6	-0.04	0.1	-24.2	-0.6	0.1	-0.5
Oct.	69.7	9.1	1.7	0.1	-60.6	-7.4	-1.6	-9.0
Nov.	207.2	60.6	23.3	30.1	-146.6	-37.3	6.8	-30.5
Dec.	173.0	85.0	27.9	27.8	-88.0	-57.1	-0.1	-57.2

TABLE 20. Total Vertical Energy Flux (Units: 10^{18} ergs sec^{-1}) and Resultant Divergence Between Levels (positive sign indicates divergence).

Month	A_Z	A_E	K_E	K_Z	C_A	ALT C_A	C_K	ALT C_K
Jan.	1.3	0.9	7.7	7.9	58.7	33.6	-82.9	-80.1
Feb.	0.5	0.5	6.8	3.4	6.7	0.1	-41.4	-28.2
Mar.	0.8	0.2	3.2	1.9	10.4	7.2	-24.7	-19.7
Apr.	0.1	0.1	1.1	0.4	-0.3	-0.3	1.6	0.04
May	0.1	0.02	0.5	1.7	-0.1	-0.1	2.5	2.5
June	0.3	0.1	0.8	3.0	-0.1	-0.06	0.7	0.7
July	0.7	0.1	0.7	4.9	-0.4	-0.4	-0.6	-0.6
Aug.	0.2	0.03	0.5	1.9	0.2	0.03	-0.5	0.14
Sept.	0.2	0.04	1.0	0.4	0.3	-0.1	-0.7	0.3
Oct.	1.5	0.1	1.0	2.6	3.6	1.8	0.6	-0.9
Nov.	2.8	0.2	3.2	5.7	32.0	23.3	-13.9	-12.6
Dec.	3.2	0.2	3.6	7.6	26.9	24.8	-65.0	-42.1

TABLE 21. Total Energy Contents - A_Z, A_E, K_Z, and K_E (Units: 10^{25} ergs) and Conversion Rates - C_A, ALT C_A, C_K, and ALT C_K (Units: 10^{18} ergs sec^{-1}).

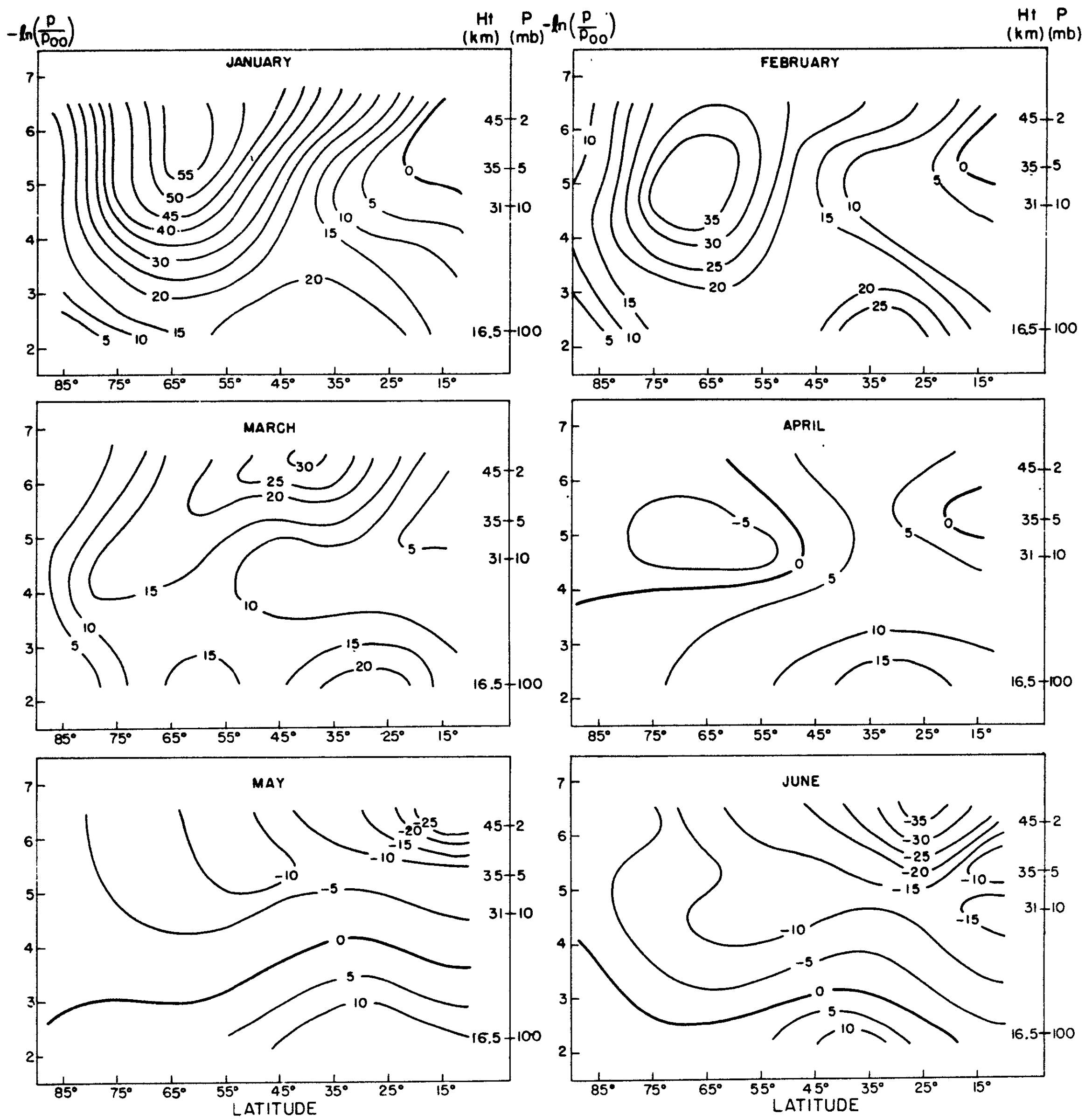

FIGURE 1. Mean Monthly Cross-Sections of Zonal Wind Component, $[\bar{u}]$. Units: m sec^{-1}.

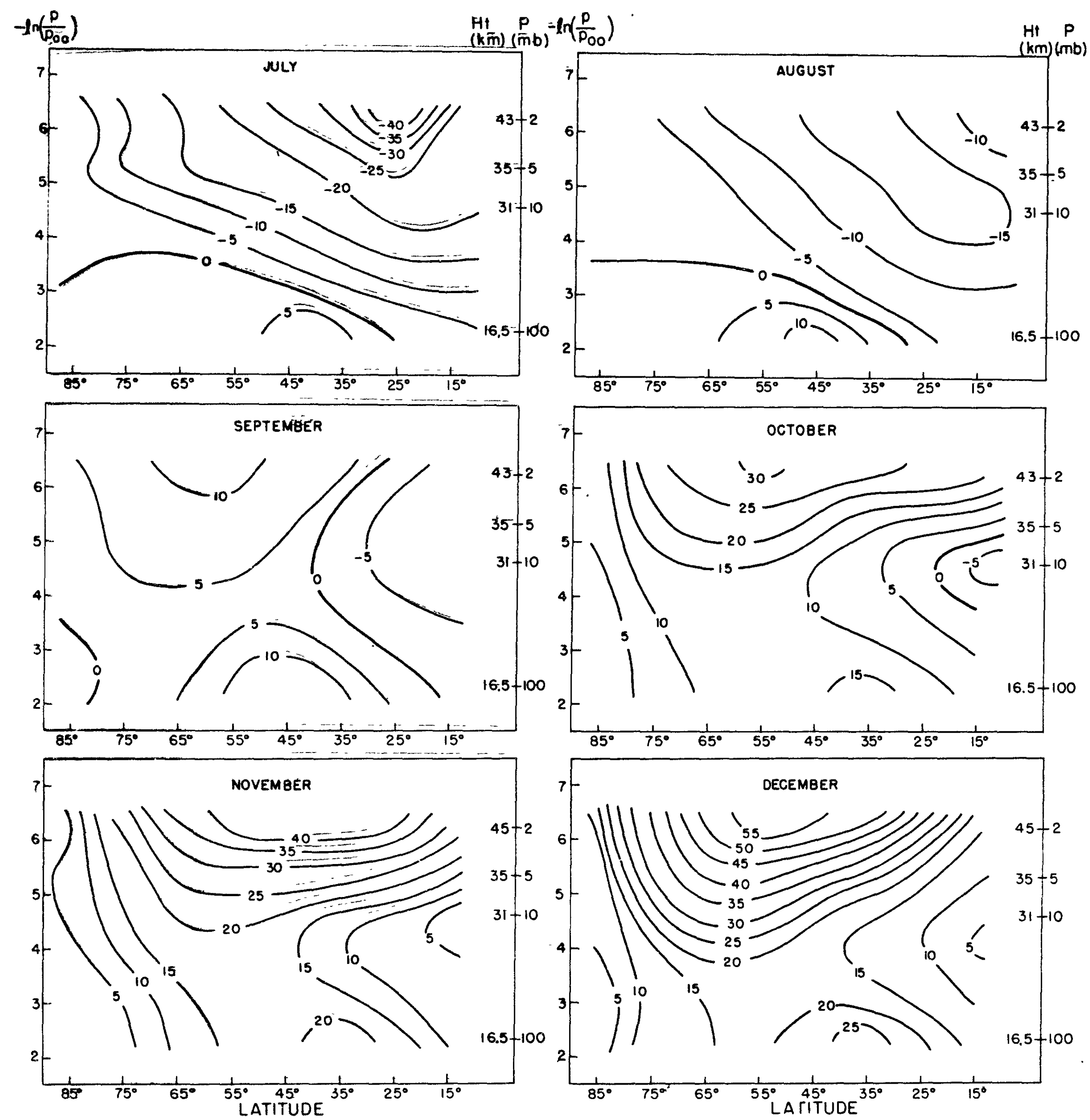

FIGURE 1 - Continued

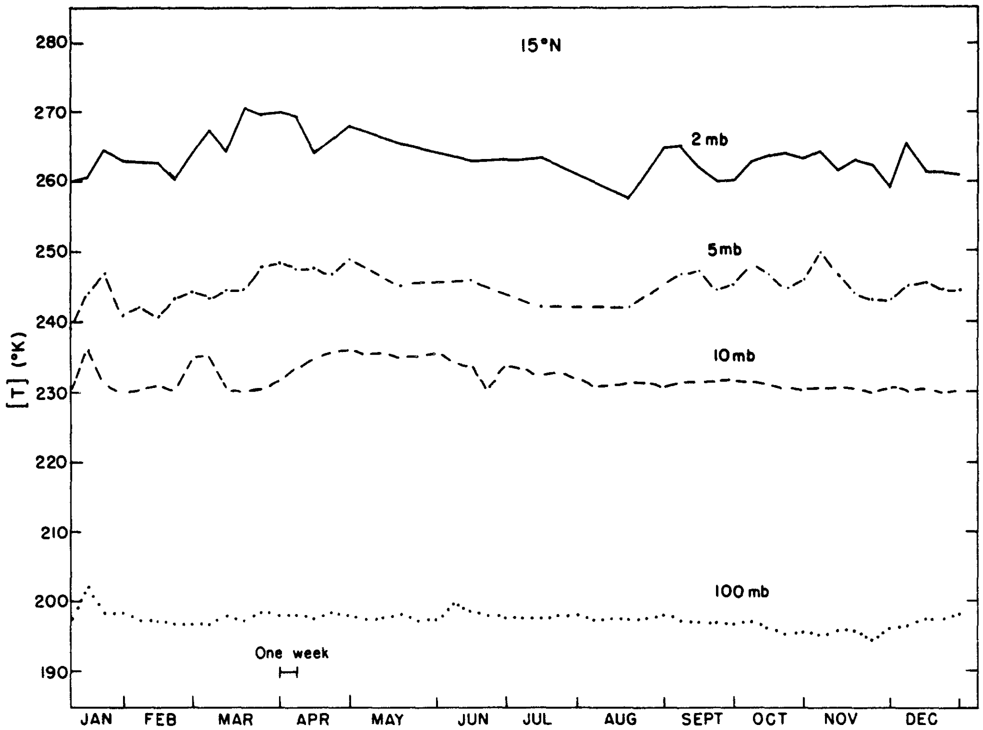

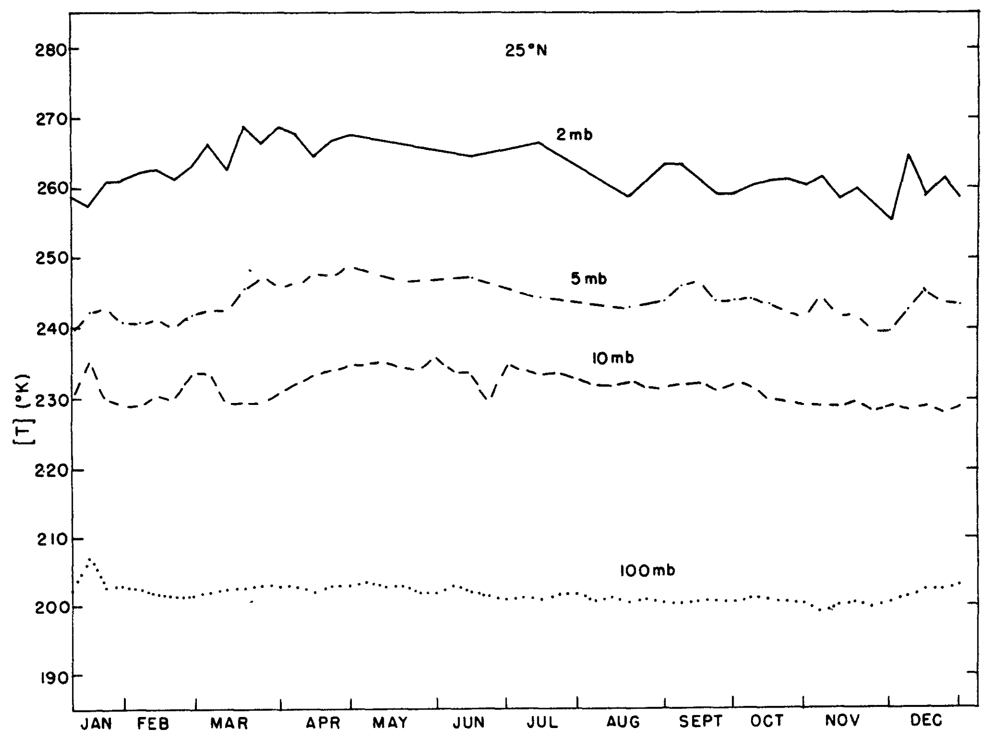

FIGURE 2. Weekly Pattern of Zonally Averaged Temperature, [T], at 15° and 25°N. Units: °K.

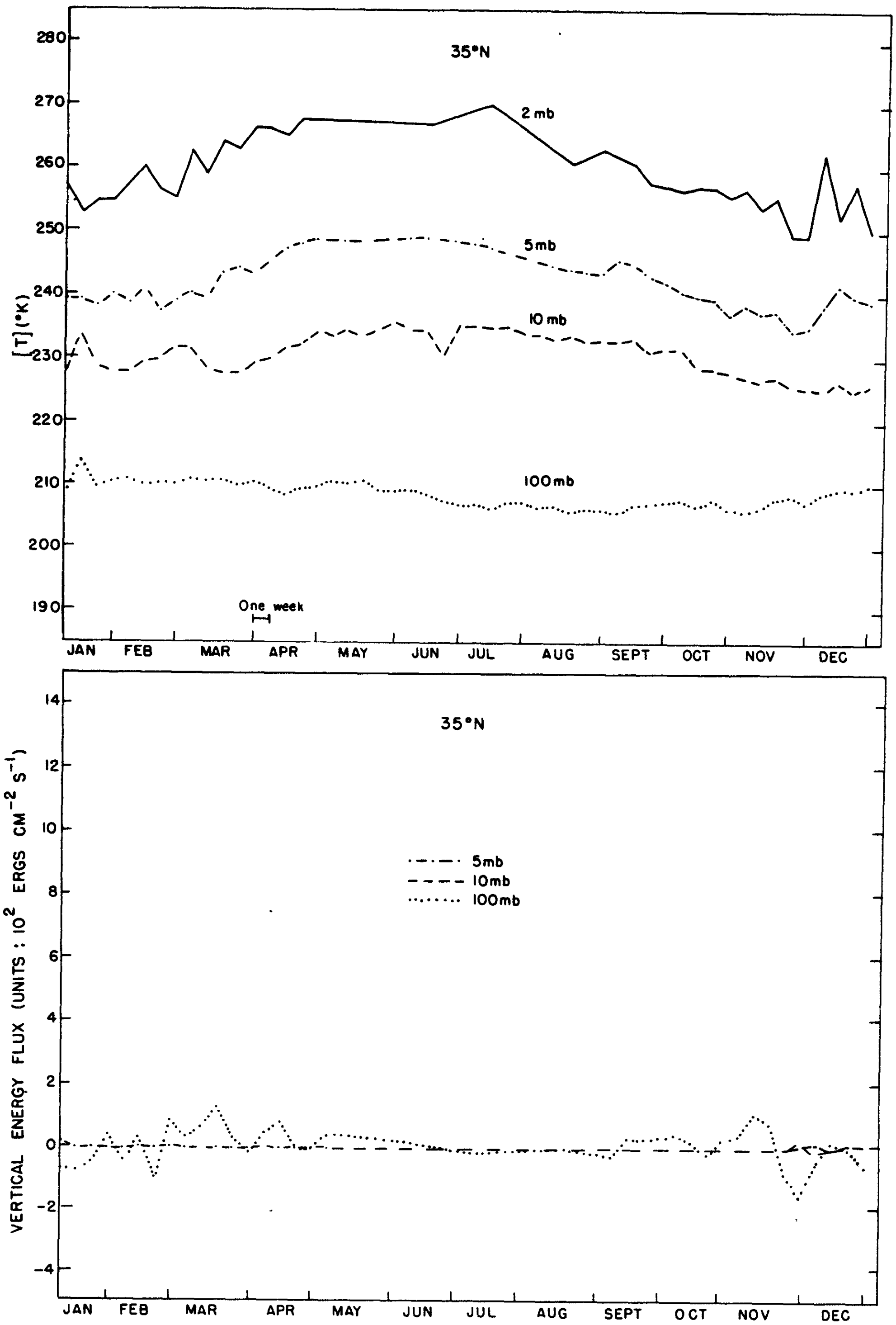

FIGURE 3. Weekly Pattern of Zonally Averaged Temperature, [T], in Units of ^oK, and Vertical Energy Flux, [pw], in Units of ergs cm^{-2} sec^{-1}, at 35^oN.

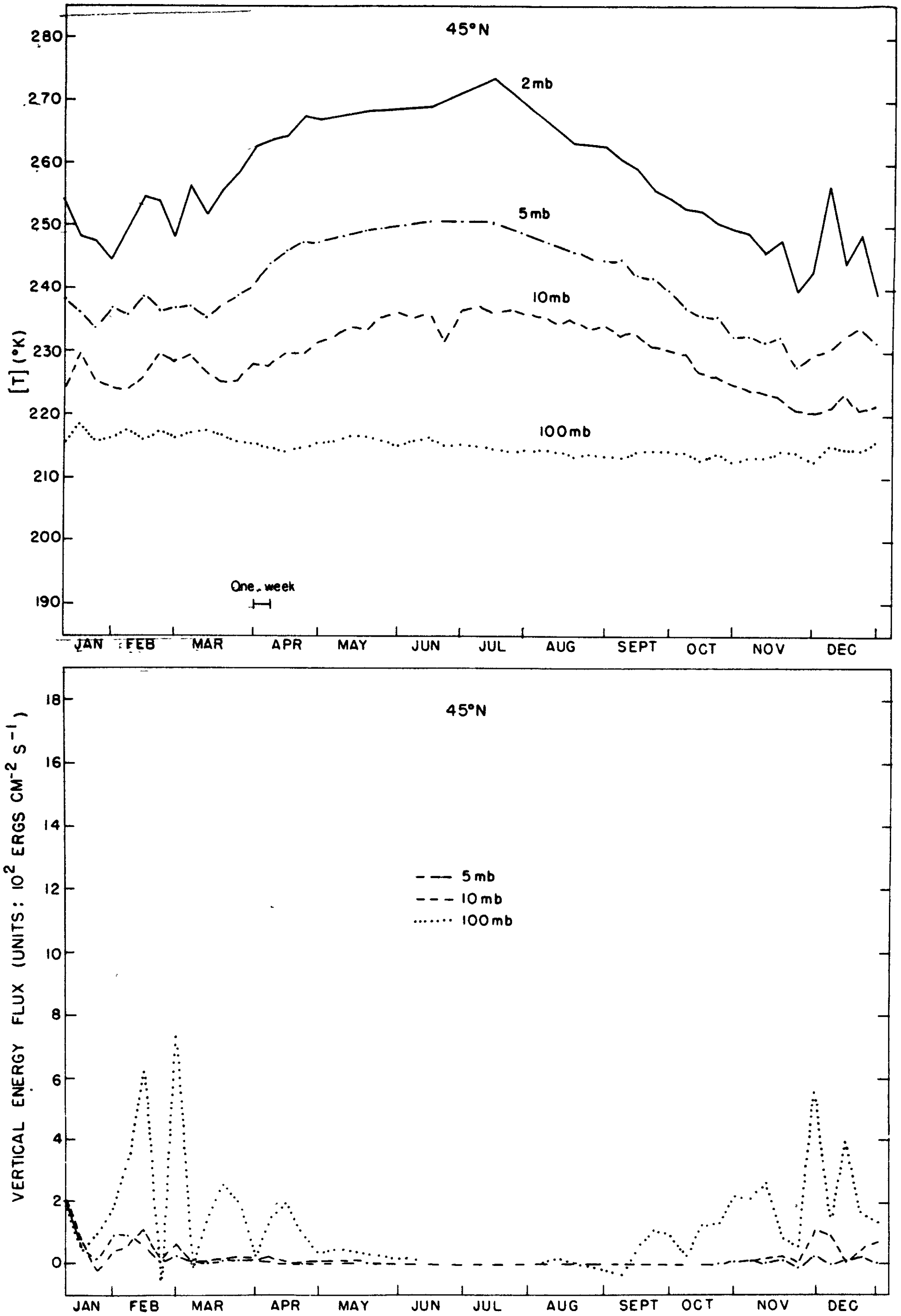

FIGURE 4. Weekly Pattern of Zonally Averaged Temperature, [T], in Units of °K, and Vertical Energy Flux, [pw], in Units of ergs cm^{-2} sec^{-1}, at 45°N.

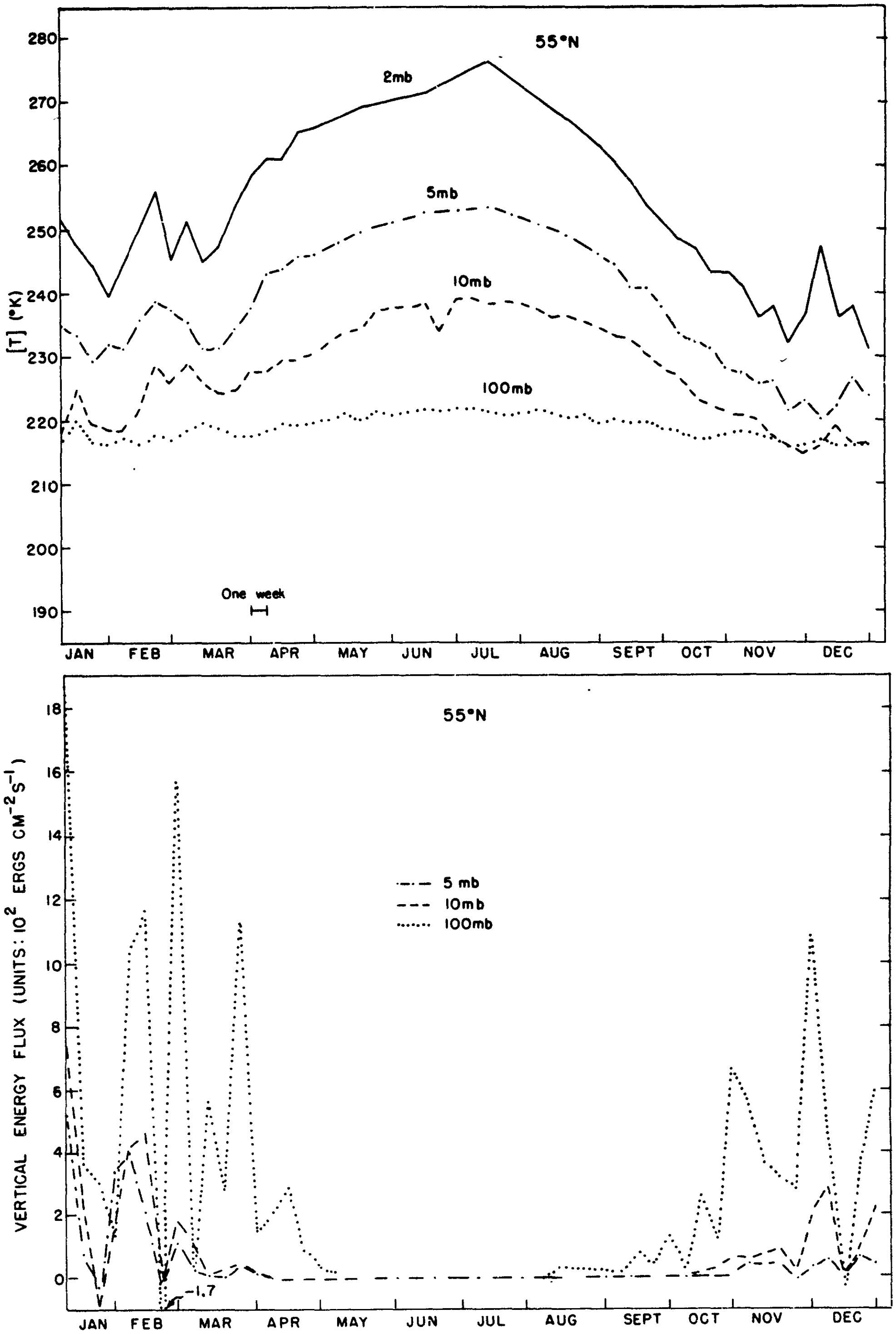

FIGURE 5. Weekly Pattern of Zonally Averaged Temperature, [T], in Units of ^{o}K, and Vertical Energy Flux, [pw], in Units of ergs cm^{-2} sec^{-1}, at 55^{o}N.

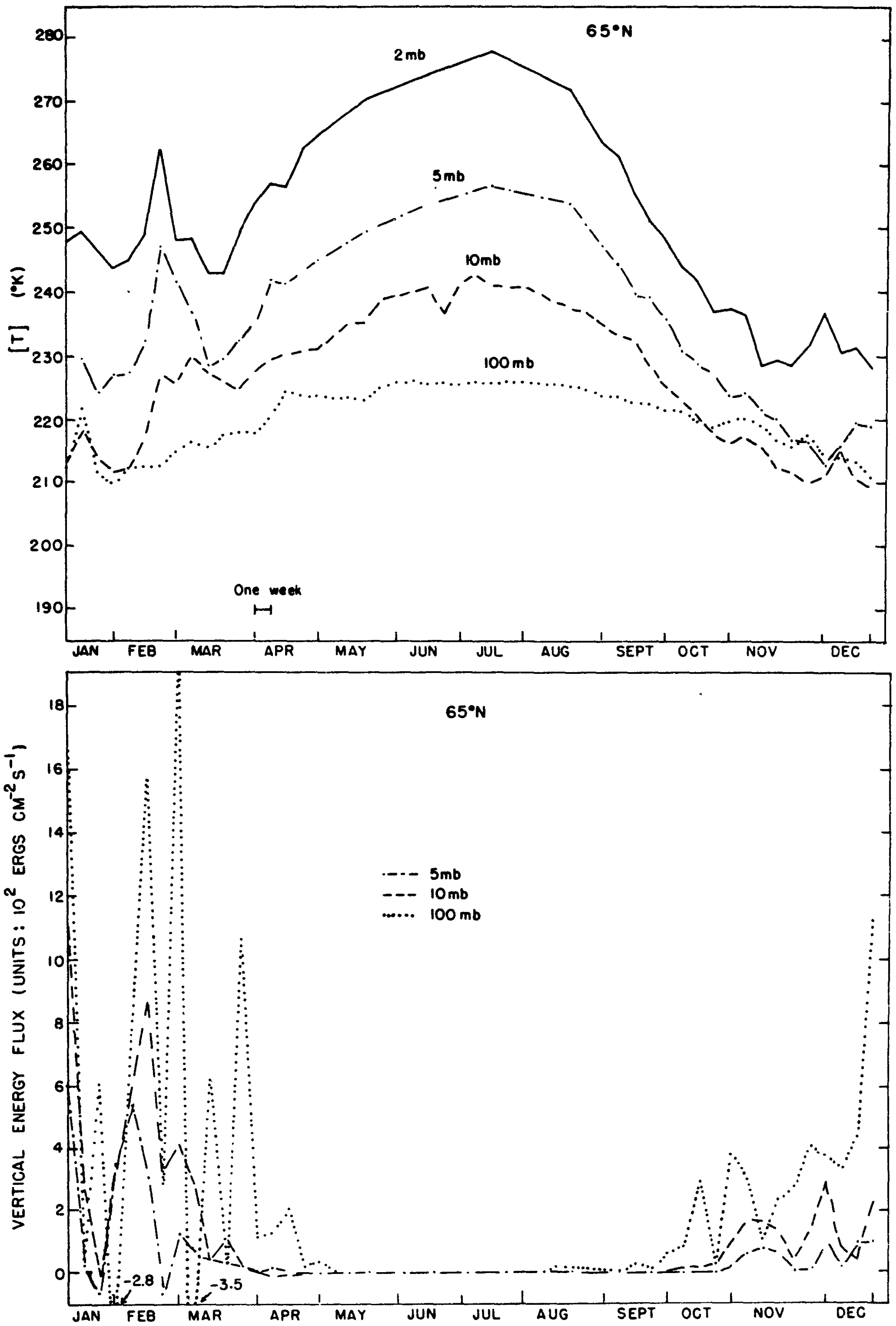

FIGURE 6. Weekly Pattern of Zonally Averaged Temperature, [T], in Units of °K, and Vertical Energy Flux, [pw], in Units of ergs cm^{-2} sec^{-1}, at 65°N.

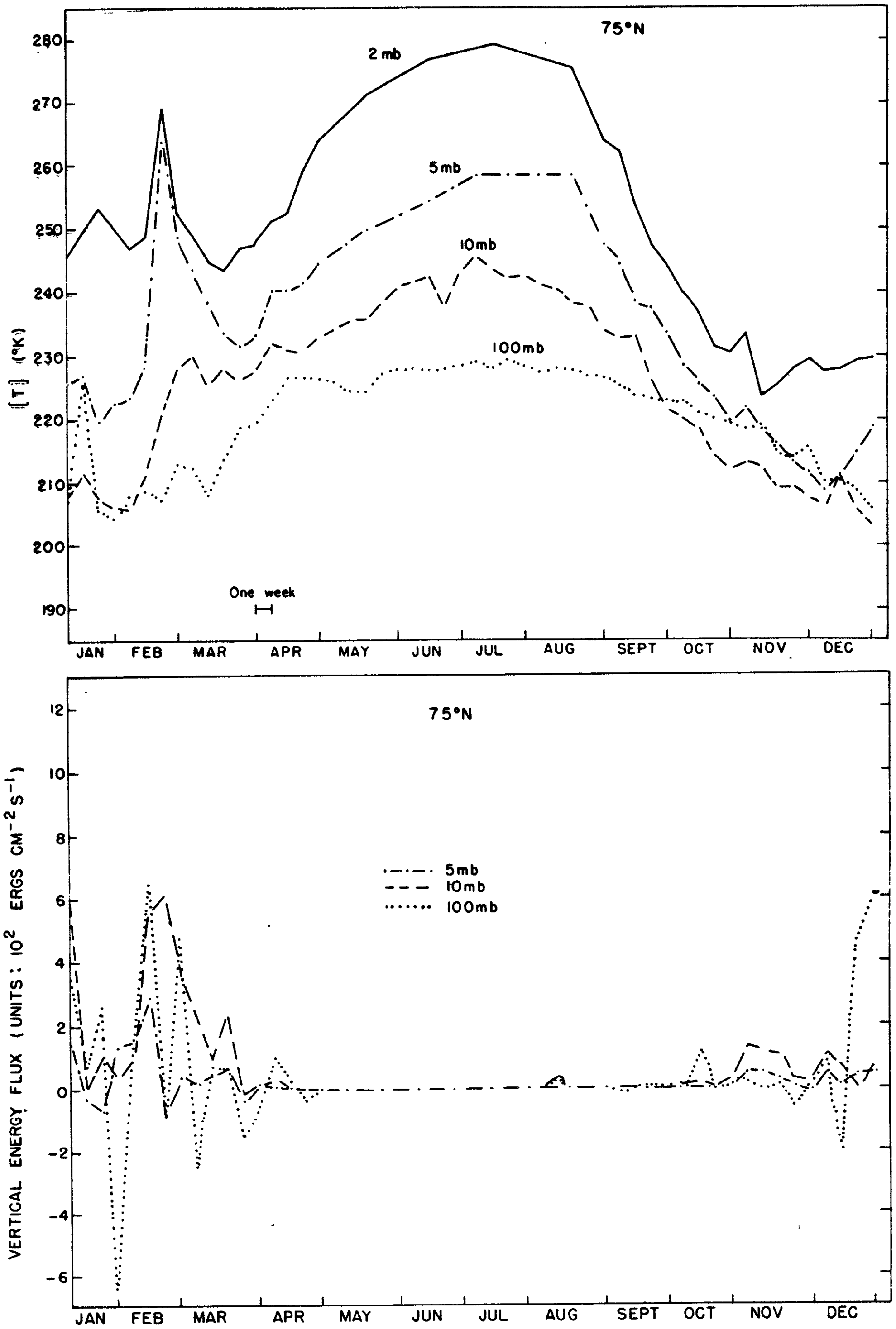

FIGURE 7. Weekly Pattern of Zonally Averaged Temperature, [T], in Units of °K, and Vertical Energy Flux, [pw], in Units of ergs cm^{-2} sec^{-1}, at 75°N.

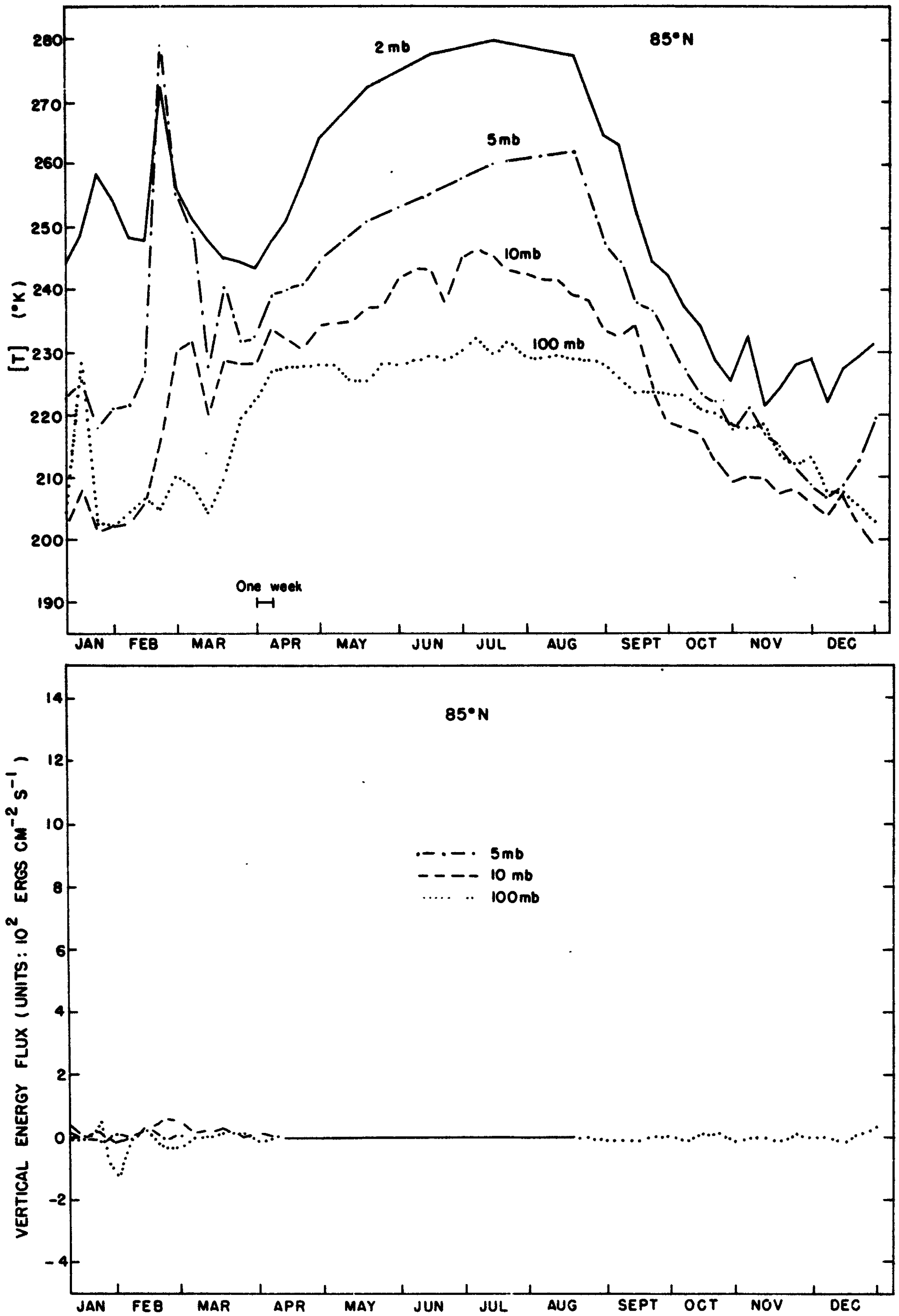

FIGURE 8. Weekly Pattern of Zonally Averaged Temperature, [T], in Units of ^{o}K, and Vertical Energy Flux, [pw], in Units of ergs cm^{-2} sec^{-1}, at 85^{o}N.

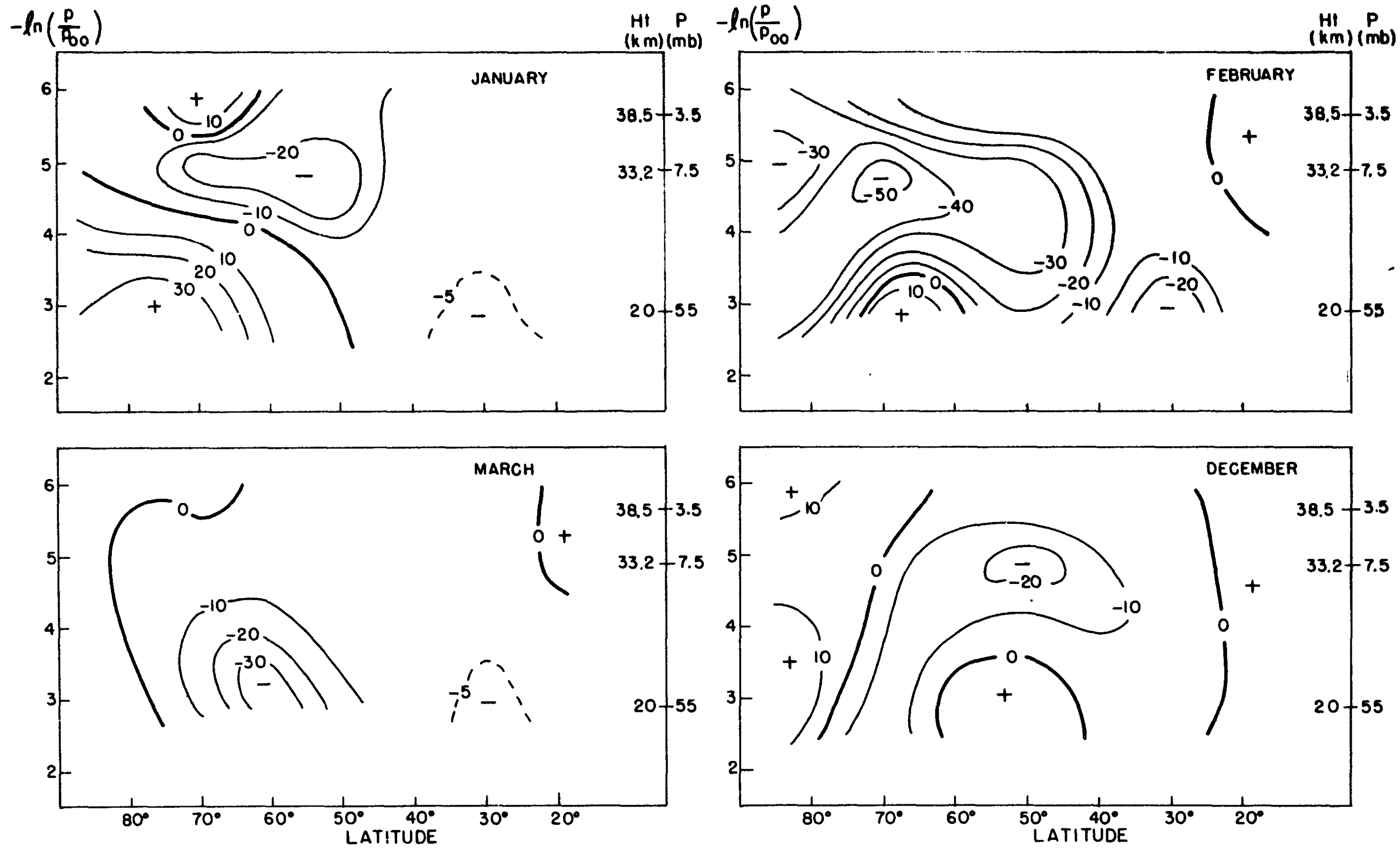

FIGURE 9. Meridional Cross-Sections of Total Energy Flux Divergence (positive numbers indicate divergence) for Selected Months. Units: 10^{-5} ergs cm^{-3} sec^{-1}.

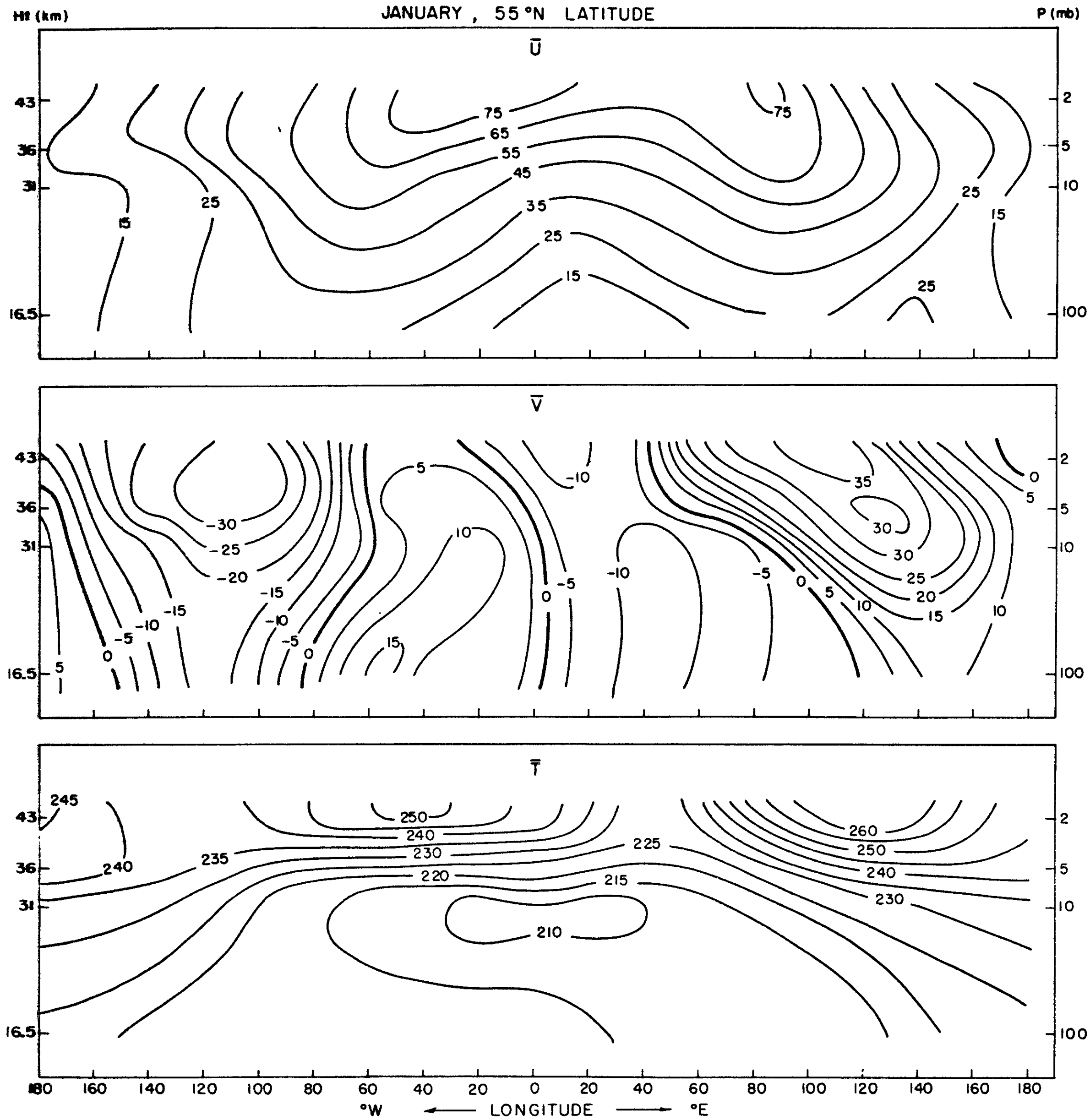

FIGURE 10. Zonal Cross-Sections of the Time Averaged Zonal Wind, $\bar{u}$ (top), Meridional Motion, $\bar{v}$ (middle), and Temperature, $\bar{T}$ (bottom) at 55°N, January 1972. Units: $\bar{u}$ and $\bar{v}$ in m sec^{-1}, and $\bar{T}$ in °K.

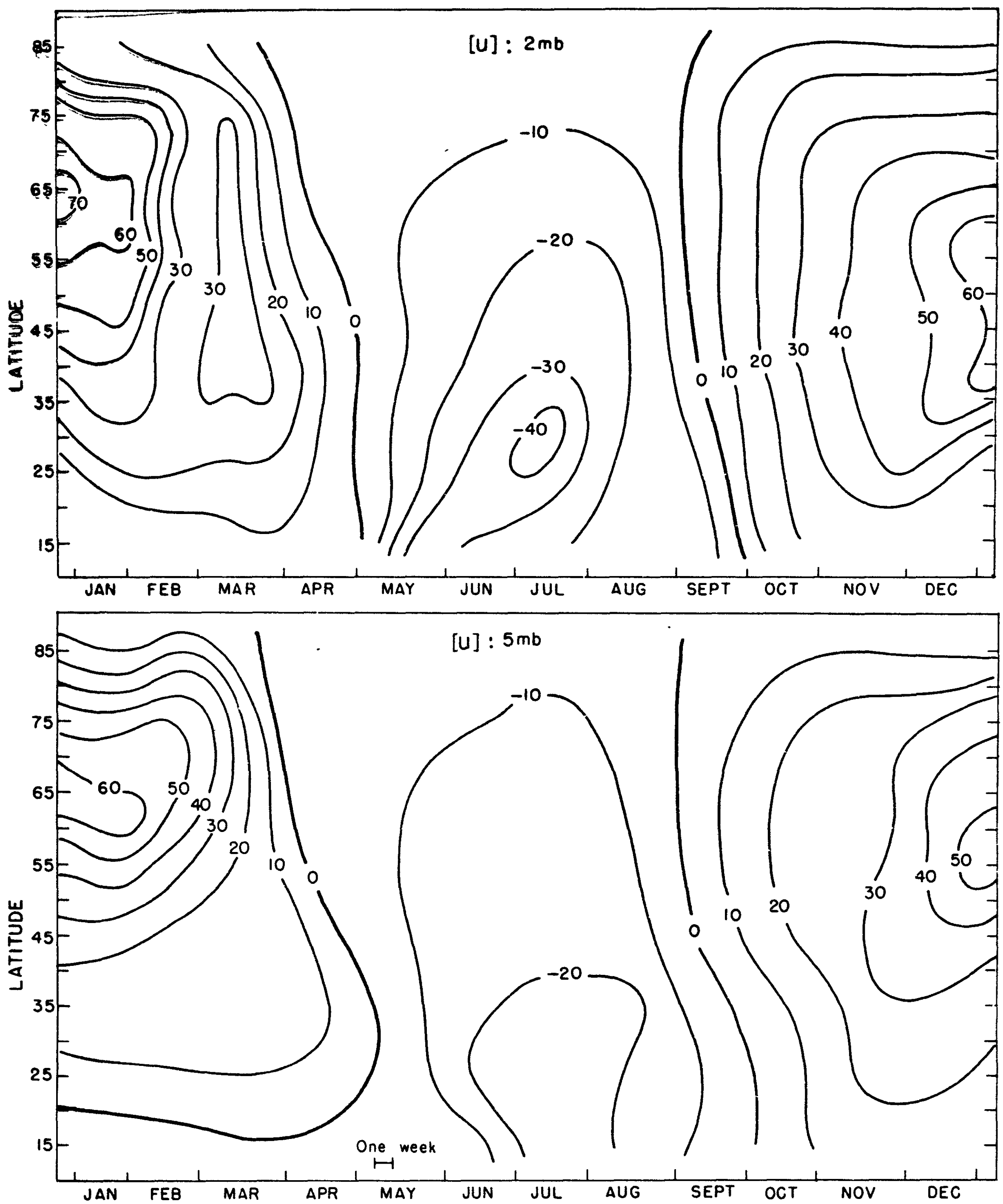

FIGURE 11. Weekly Pattern of Zonally Averaged Zonal Wind Component, [u], at the 2mb (top) and 5mb (bottom) levels. Units: m sec^{-1}.

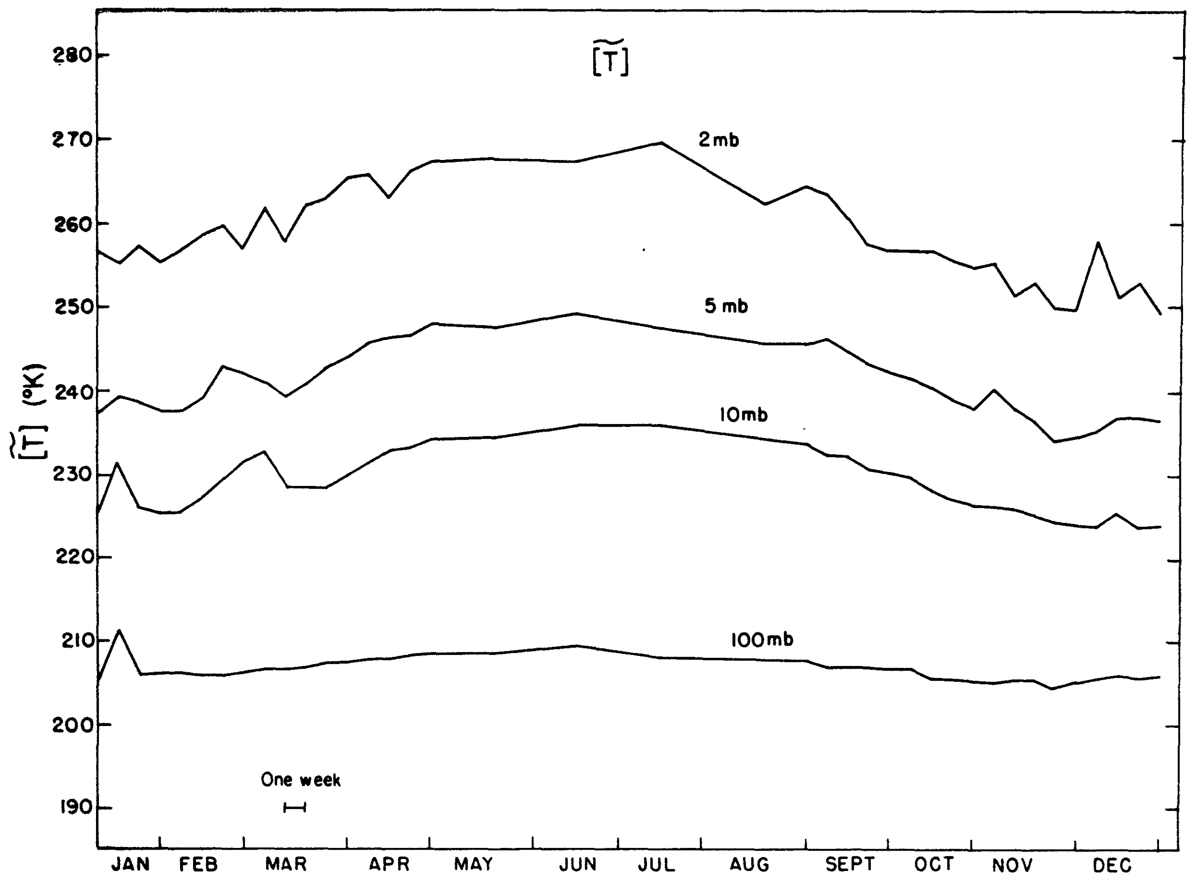

FIGURE 12. Weekly Pattern of Area Averaged Temperature, $\widetilde{[T]}$.

Units: °K.

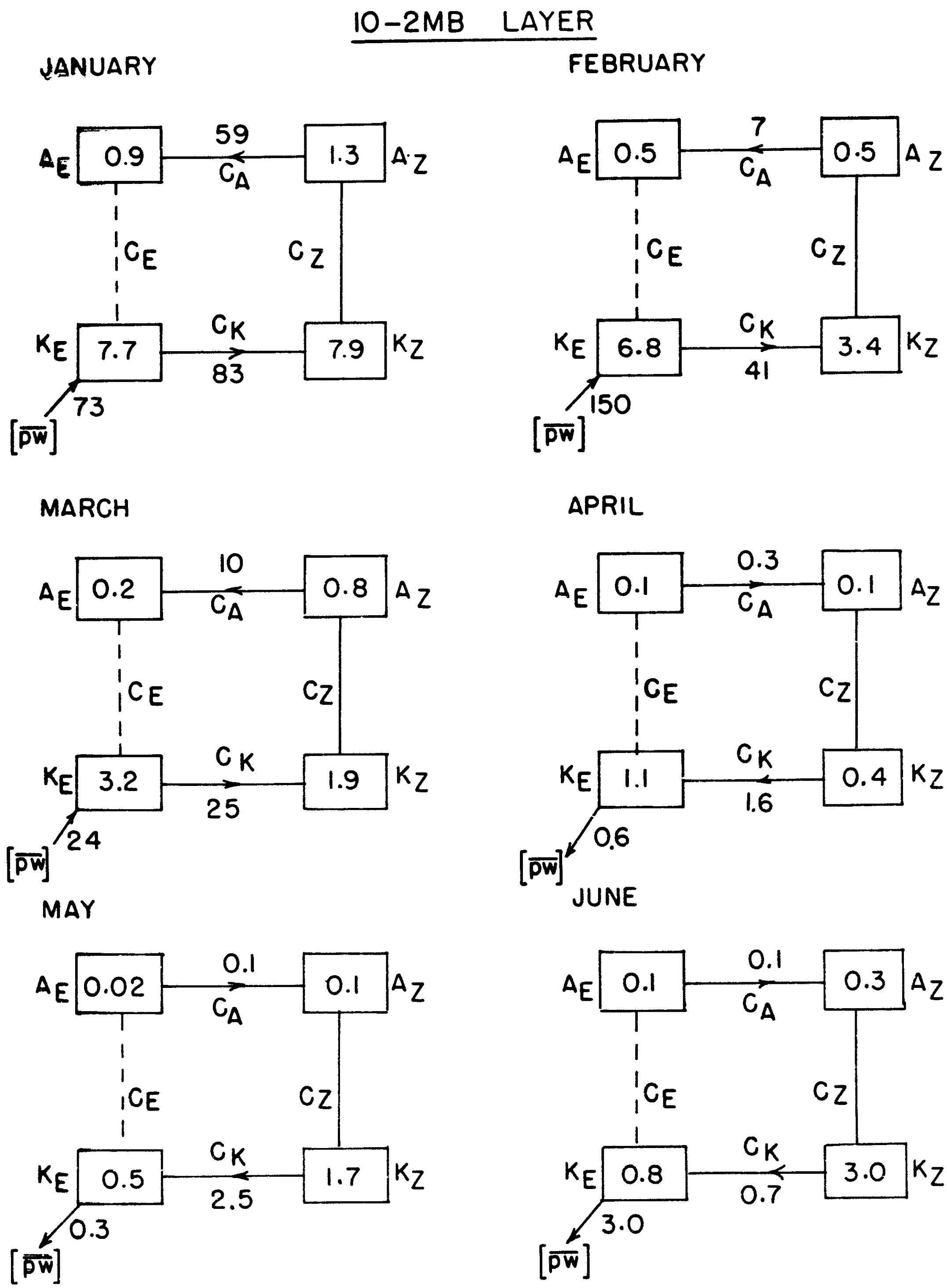

FIGURE 13. Energy Cycle for the Upper Stratosphere. Units: Contents in 10^{25} ergs, and Conversion Rates in 10^{18} ergs sec^{-1}.

10 – 2MB LAYER

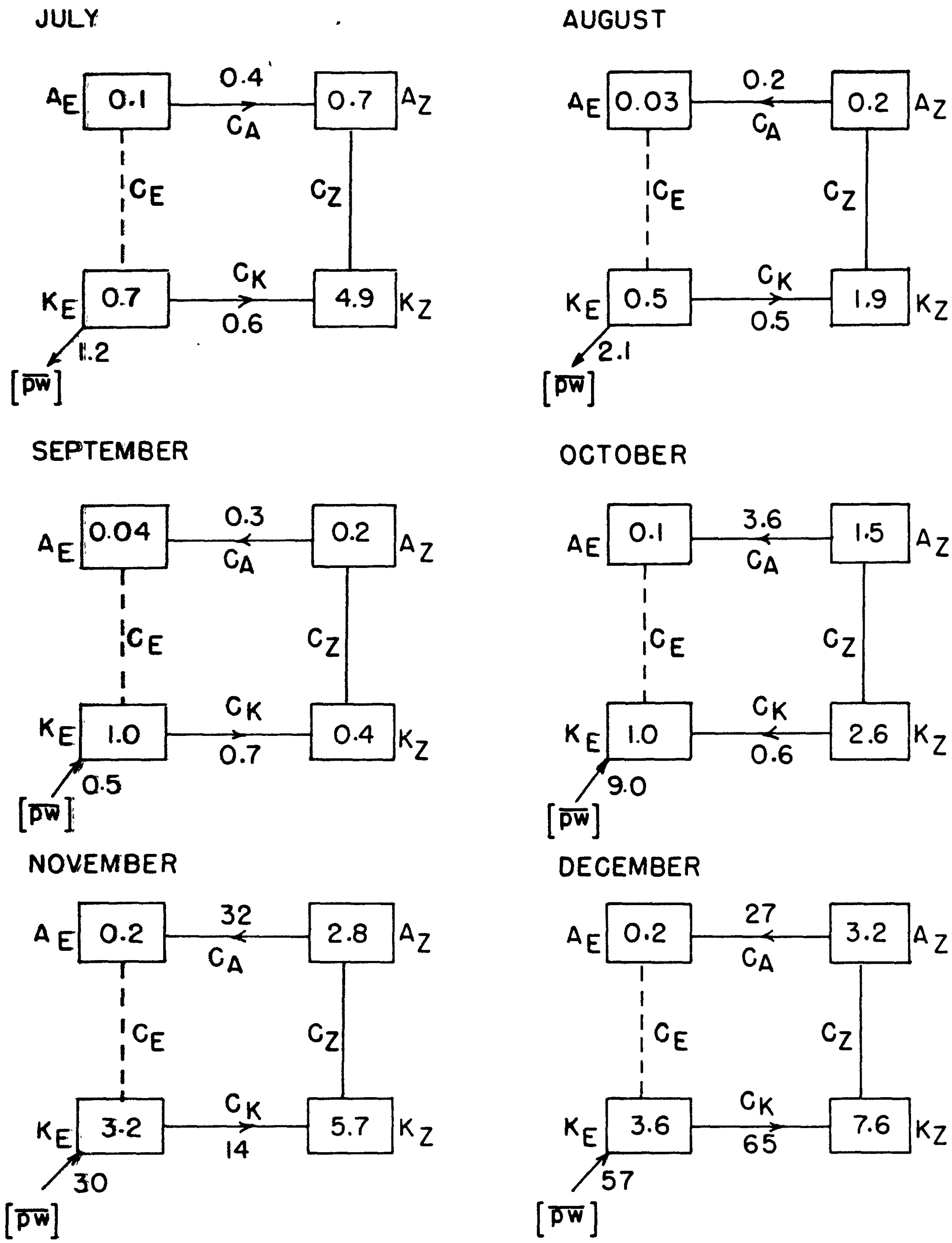

FIGURE 13 - Continued

BIBLIOGRAPHY

Barnes, A.A., Jr., 1962: Kinetic and potential energy between 100mb and 10mb during the first six months of the IGY. Final Rept., Planetary Circulations Project, Dept. of Meteorology, M.I.T., 131pp.

Eliassen, A., and E. Palm, 1961: On the transfer of energy in stationary mountain waves. Geof. Pub., XXII, 23pp.

Finger, F.G., H.M. Woolf, and C.E. Anderson, 1965: A method for objective analysis of stratospheric constant-pressure charts. Monthly Wea. Rev., 93, pp 619-638.

Groves, G.V., 1971: Atmospheric structure and its variations in the region from 25 to 125km. Air Force Cambridge Res. Labs., Report No. 71-0410, Bedford, Mass.

Kung, E.C., 1966: Kinetic energy generation and dissipation in the large-scale atmospheric circulation. Monthly Wea. Rev., 94, pp 67-82.

——, 1969: Further study of the kinetic energy balance. Monthly Wea. Rev., 97, pp 573-581.

——, 1972: A scheme for kinematic estimate of large-scale vertical motion with an upper-air network. Quart. J. Roy. Met. Soc., 98, pp 402-411.

Lorenz, E.N., 1955: Available potential energy and the maintenance of the general circulation. Tellus, 7, pp 157-167.

———, 1967: The Nature and Theory of the General Circulation of the Atmosphere. World Meteorological Organization, Geneva, 161 pp.

Miller, A.J., J.A. Brown, and K.A. Campana, 1972: A study of the energetics of an upper stratospheric warming (1969-1970). Quart. J. Roy. Met. Soc., 98, pp 730-744.

Newell, R.E., 1965: The energy and momentum budget of the atmosphere above the tropopause, in Problems of Atmospheric Circulation (Ed. by R.V. Garcia and T.F. Malone), Proceedings of the Sixth International Space Science Symposium, Spartan Books, Washington D.C., pp 106-126.

———, 1966: A review of studies of eddy fluxes in the stratosphere and mesosphere, in Les Problemes Meteorologiques de la Stratosphere et de la Mesosphere, C.N.E.S., Presses Universitaires de France, Paris, pp 81-129.

———, and M.E. Richards, 1969: Energy flux and convergence patterns in the lower and middle stratosphere during the IQSY. Quart. J. Roy. Met. Soc., 95, pp 310-328.

———, D.G. Vincent, T.G. Dopplick, D. Ferruzza, and J.W. Kidson, 1970: The energy balance of the global atmosphere, in The Global Circulation of the Atmosphere (Ed. by G.A. Corby), Royal Meteorological Society, London, pp 42-90.

———, J.W. Kidson, D.G. Vincent, and G.J. Boer, 1972: The General Circulation of the Tropical Atmosphere and Interactions with Extratropical Latitudes, Volume I. M.I.T. Press, Cambridge, Mass., 258 pp.

Oort, A.H., 1963: On the energy cycle in the lower stratosphere. Report No. 9, Planetary Circulations Project, Dept. of Meteor., M.I.T., 122 pp.

———, and E.M. Rasmusson, 1971: Atmospheric Circulation Statistics. Prof. Paper No. 5, N.O.A.A., U.S. Dept. of Commerce, Rockville, Md, 323 pp.

Oxford University, Dept. of Atmospheric Physics, 1972: Global Stratospheric Analyses. Oxford Press, Oxford, Eng., 109 pp.

Peixoto, J.P., 1965: On the role of water vapor in the energetics of the general circulation of the atmosphere. Portugaliae Physica, 4, p. 135.

Priestly, C.H.B., 1949: Heat transport and zonal stress between latitudes. Quart. J. Roy. Met. Soc., 75, p. 28.

Reed, R.J., J.L. Wolfe, and H. Nishimoto, 1963: A spectral analysis of the energetics of the stratospheric sudden warming of early 1957. J. Atmos. Sci., 20, p. 256.

Reynolds, O., 1894: On the dynamical theory of incompressible fluids and the determination of criterion. Phil. Trans. Roy. Soc., London (A), 136, p. 123.

Richards, M.E., 1967: The energy budget of the stratosphere during 1965. Report No. 21, Planetary Circulations Project, Dept. of Meteor., M.I.T., 171 pp.

Saltzman, B., 1957: Equations governing the energetics of the large scales of atmospheric turbulence in the domain of wave number. J. Meteor., 14, p. 513.

Staff, Upper Air Branch NMC, 1971: Weekly synoptic analyses 5-, 2-, and 0.4-millibar surfaces for 1968. NOAA Tech. Rep. NWS 14, U.S. Dept. of Commerce, Silver Spring, Md, 169 pp.

Starr, V.P., 1960: Questions concerning the energy of stratospheric motions. Archiv. fur Met., Geophys. und Biokl., A, 12, pp 1-7.

——, and R.M. White, 1952: Schemes for the study of hemispheric exchange processes. Quart. J. Roy. Met. Soc., 78, p. 407.

——, J.P. Peixoto, and N.E. Gaut, 1970: Momentum and zonal kinetic energy balance of the atmosphere from five years of hemispheric data. Tellus, 22, pp 251-274.

ACKNOWLEDGEMENTS

The author wishes to thank Professor Reginald E. Newell for his suggestion of the topic and for countless hours of discussion and counsel during the course of the investigation. The author is indebted to the Department of the Air Force who, through the Air Force Institute of Technology, provided the author with this educational opportunity. Thanks are due to Mrs. Susan Ary for many hours spent processing the data, Mrs. Mary Andresen, for putting the bulk of the data on computer cards, Miss Isabelle Kole, for drafting the figures, and Mrs. Jessica Makowski, for typing the tables. And last but not least, thanks are due to my wife Jeanne, whose patience and understanding helped make this study a reality.